Aus dem Zentrum für Innere Medizin der Universität zu Köln
Klinik und Poliklinik für Innere Medizin I
Direktor: Universitätsprofessor Dr. med. M. Hallek

Identifying mechanisms of resistance to BCL2 inhibitor venetoclax in acute myeloid leukemia (AML)

Inaugural-Dissertation zur Erlangung der Doktorwürde
der Medizinischen Fakultät
der Universität zu Köln

vorgelegt von
Leonie Breull-Wierschem
aus Bonn

promoviert am 26. September 2024

Gedruckt mit Genehmigung der Medizinischen Fakultät der Universität zu Köln

2024

Dekan: Universitätsprofessor Dr. med. G. R. Fink
1. Gutachter: Privatdozent Dr. med. L.-P. Frenzel
2. Gutachter: Universitätsprofessor Dr. rer. nat. H. Kashkar

Erklärung:

Ich erkläre hiermit, dass ich die vorliegende Dissertationsschrift ohne unzulässige Hilfe Dritter und ohne Benutzung anderer als der angegebenen Hilfsmittel angefertigt habe; die aus fremden Quellen direkt oder indirekt übernommenen Gedanken sind als solche kenntlich gemacht.

Bei der Auswahl und Auswertung des Materials sowie bei der Herstellung des Manuskriptes habe ich keine Unterstützungsleistungen erhalten.

Weitere Personen waren an der Erstellung der vorliegenden Arbeit nicht beteiligt. Insbesondere habe ich nicht die Hilfe einer Promotionsberaterin/ eines Promotionsberaters in Anspruch genommen. Dritte haben von mir weder unmittelbar noch mittelbar geldwerte Leistungen für Arbeiten erhalten, die im Zusammenhang mit dem Inhalt der vorgelegten Dissertationsschrift stehen.

Die Dissertationsschrift wurde von mir bisher weder im Inland noch im Ausland in gleicher oder ähnlicher Form einer anderen Prüfungsbehörde vorgelegt.

Die in dieser Arbeit angegeben Experimente sind mit Ausnahme des *whole exome sequencing, RNA sequencing* und *single cell RNA sequencing* von mir eigenständig durchgeführt worden. Die Sequenzierungen wurden von Dr. Janine Altmüller, Cologne Center for Genomics (CCG) durchgeführt. Die Auswertung der *whole exome sequencing*-Daten erfolgte durch Prof. Dr. Martin Peifer, Department of Translational Genomics, Universität zu Köln. Die Auswertung der *RNA sequencing*-Daten erfolgte durch Prerana Wagle, CECAD Bioinformatics Facility, Universitätsklinik Köln und Dr. Stuart Blakemore, AG Pallasch, CECAD/Universitätsklinik Köln. Die Auswertung der *single cell RNA sequencing*-Daten erfolgte durch Dr. Milos Nikolic, AG Peifer, Department of Translational Genomics und Dr. Stuart Blakemore, AG Pallasch, CECAD/Universitätsklinik Köln. Die Generierung eines Gen-Knockouts mit Hilfe der CRISPR/Cas9-Methode wurde vom medizinisch-technischen Assistenten Herrn Olaf Merkel mit meiner Unterstützung durchgeführt. Die initiale Testung der Sensitivität der parentalen AML-Zelllinien gegenüber Venetoclax erfolgte durch Dr. Laura Beckmann. Alle Experimente, die nicht von mir selbst durchgeführt wurden, sind im Ergebnisteil dieser Arbeit entsprechend gekennzeichnet.

Erklärung zur guten wissenschaftlichen Praxis:

Ich erkläre hiermit, dass ich die Ordnung zur Sicherung guter wissenschaftlicher Praxis und zum Umgang mit wissenschaftlichem Fehlverhalten (Amtliche Mitteilung der Universität zu Köln AM 132/2020) der Universität zu Köln gelesen habe und verpflichte mich hiermit, die dort genannten Vorgaben bei allen wissenschaftlichen Tätigkeiten zu beachten und umzusetzen.

Köln, den 18.10.2023

Leonie Breull-Wierschem

Acknowledgements

First and foremost, I would like to express my gratitude to Prof. Dr. Michael Hallek and PD Dr. Lukas Frenzel for entrusting me with this project. Thank you, Lukas, for encouraging me to think outside the box. Your support and confidence in my work mean a lot. Laura, thank you for introducing me to the lab and for staying on board throughout this project.

Everyone from AG Frenzel, AG Hallek, AG Pallasch and AG Krause made me feel at ease in the lab from day one – and I am very grateful for that. Thanks to all of you for creating such a welcoming atmosphere, which I have countless great memories of.

Olaf, thank you from the bottom of my heart for sharing your expertise and knowledge. Most importantly though, thanks for always making me laugh!

Stu, thank you for your commitment, your advice, and for patiently answering all of my questions. I appreciate it greatly and I am lucky to have you as a friend.

A very special thanks to my parents, whose unconditional support and confidence in my decisions allowed me to be where I am today.

Floyd, thank you so much for believing in me, especially when I don't. Thank you for always having my back and cheering me on. I can't wait to see what the future holds for us!

Table of content

Abbreviations

Abbreviation	Meaning
γH2A.x	*phosphorylated histone 2A family member X*
199R	*venetoclax-resistant*
7-AAD	*7-aminoactinomycin*
AF	*allelic fraction*
AML	*acute myeloid leukemia*
APAF-1	*apoptotic protease activating factor 1*
APL	*acute promyelocytic leukemia*
Ara-C	*cytarabine*
ASXL1	*additional sex combs L1/ putative polycomb group protein*
BAK	*Bcl-2-homologous antagonist killer*
BAX	*Bcl-2-associated X protein*
BBC-3	*Bcl-2-binding component 3*
BCL-xL	*B-cell lymphoma extra large*
BCL2	*B-cell lymphoma 2*
BID	*BH3 interacting domain death agonist*
BTD	*breakthrough therapy designation*
Cas9	*CRISPR-associated protein 9*
CBFB	*core-binding factor subunit beta*
CD	*cluster of differentiation*
CDK	*cyclin-dependent kinases*
CEBPA	*CCAAT/enhancer-binding protein alpha*
CLL	*chronic lymphocytic leukemia*
CR	*complete remission*
CRi	*complete remission with incomplete blood count recovery*
CRISPR	*clustered regularly interspaced short palindromic repeats*
CRTC2	*CREB regulated transcription coactivator 2*
CTG	*CellTiter-Glo®*
CTL	*cytotoxic T lymphocytes*
DCK	*deoxycytidine kinase*
DDR	*DNA damage response*
DLBCL	*diffuse large B cell lymphoma*
DMSO	*dimethylsulfoxid*
DNMT3A	*DNA (cytosine-5)-methyltransferase 3A*
DSMZ	*german collection of microorganisms and cell cultures*
ELN	*European LeukemiaNet*

EMA	*European Medicines Agency*
ER	*endoplasmic reticulum*
ERG	*ETS-related gene*
EZH2	*enhancer of zeste homolog 2*
FACS	*fluorescent activated cell sorting*
FADD	*Fas-associating death domain containing protein*
FBS	*fetal bovine serum*
FDA	*Food and Drug Administration*
FGFR1	*fibroblast growth factor receptor 1*
FISH	*fluorescence in situ hybridization*
FL	*follicular lymphoma*
FLT3	*FMS-like tyrosine kinase 3*
FOXC1	*forkhead box C1*
G-CSF	*granulocyte stimulating factor*
GATA1	*GATA-binding factor 1*
GO	*gemtuzumab ozogamicin*
GYP	*glycophorin*
HB	*hemoglobin*
HCT	*hematopoietic stem cell transplantation*
HDAC	*high dose Ara-C*
HES1	*hairy and enhancer of split-1*
HLA	*human leucocyte antigen*
HMA	*hypomethylating agents*
HUGO	*human genome organisation*
IC_{50}	*half maximal inhibitory concentration*
IL-3	*interleukin-3*
IDAC	*intermediate dose Ara-C*
IDH	*isocitrate dehydrogenase*
ITD	*internal tandem duplication*
KIT	*proto-oncogene receptor tyrosine kinase*
KMT2A	*histone-lysine N-methyltransferase 2A*
KRAS	*Kirsten rat sarcoma virus*
LDAC	*low dose Ara-C*
MAP2K	*mitogen-activated protein kinase kinase*
MCL-1	*myeloid cell leukemia 1*
MDM2	*mouse double minute 2*
MDS	*myelodysplastic syndrome*

MEK	*MAP2K*
MLL	*myeloid/lymphoid or mixed-lineage leukemia*
MM	*multiple myeloma*
MOM	*mitochondrial outer membrane*
MOMP	*mitochondrial outer membrane permeabilization*
MPO	*myeloperoxidase*
MRD	*minimal residual disease*
MRP	*mitochondrial ribosomal protein*
MRP	*mitochondrial ribosome protein*
mtDNA	*mitochondrial DNA*
MYH11	*myosin heavy chain 11*
NF1	*neurofibromin 1*
NF-κB	*nuclear factor kappa B*
NHL	*non-Hodgkin lymphoma*
NOTCH1	*neurogenic locus notch homolog protein 1*
NPM1	*nucleophosmin 1*
NRAS	*neuroblastoma RAS viral oncogene homolog*
OS	*overall survival*
OXPHOS	*oxidative phosphorylation*
PARP	*poly (ADP-ribose) polymerase*
PBS	*phosphate buffered saline*
PFS	*progression free survival*
PMAIP1	*Phorbol-12-Myristate-13-Acetate-Induced Protein 1*
PML	*promyelocytic leukemia*
PSDM4	*26S proteasome non-ATPase regulatory subunit 4*
PSTPIP2	*proline-serine-threonine phosphatase-interacting protein 2*
PTPN11	*tyrosine-protein phosphatase non-receptor type 11*
PUMA	*p53 upregulated modulator of apoptosis*
R/R	*refractory/relapsed*
RAF	*rapidly accelerated fibrosarcoma*
RARA	*retinoic acid receptor alpha*
RAS	*rat sarcoma virus*
RUNX1	*runt-related transcription factor 1*
RUNX1T1	*RUNX1 partner transcriptional co-repressor 1*
scRNA-seq	*single cell RNA sequencing*
SDS	*sodium dodecyl sulfate*
SDS-PAGE	*SDS polyacrylamide gel electrophoresis*

SNM	*single nucleotide mutation*
SRC	*single read counts*
SUCNR1	*succinate receptor 1*
TAE	*TRIS-acetate EDTA buffer*
TBE	*TRIS-borate EDTA buffer*
TBS	*Tris-buffered saline*
TCGA	*The Cancer Genome Atlas Project*
TDA	*transactivation domain*
TET2	*tet methylcytosine dioxygenase 2*
TKD	*tyrosine kinase domain*
TME	*tumor microenvironment*
TNF	*tumor necrosis factor*
TP53	*tumor suppressor gene 53*
TRADD	*TNF receptor type 1 associated death domain protein*
TRAIL	*TNF-related apoptosis inducing ligand*
UBQLN4	*ubiquilin 4*
UPS	*ubiquitin proteasome system*
USP18	*ubiquitin specific peptidase 18*
VPS	*vacuolar protein sorting-associated protein*
WES	*whole exome sequencing*
WHO	*world health organization*
wt	*wild type*

Zusammenfassung

Die akute myeloische Leukämie (AML) stellt die häufigste akute Leukämie im Erwachsenenalter dar. Mit einem Inzidenzgipfel von etwa 68 Jahren ist ein Großteil der Erkrankten aufgrund des fortgeschrittenen Alters und/oder Komorbiditäten nicht geeignet für die einzig kurative Behandlungsmöglichkeit mittels Hochdosis-Chemotherapie und allogener Stammzelltransplantation. Trotz intensiver Forschung hat sich das Überleben nach Diagnosestellung einer AML in den letztem Jahrzehnten nur geringfügig verbessert. Die Zulassung des BCL2-Inhibitors Venetoclax (ABT-199) in Kombination mit hypomethylierenden Substanzen oder niedrig-dosierter Chemotherapie, stellt einen der jüngsten Erfolge in der Behandlung der AML-Patienten, die nicht für eine intensive Therapie geeignet sind, dar. Im Vergleich zur konventionellen Therapie können höhere Remissions- und Überlebensraten erreicht werden. Allerdings treten bei Behandlung mit Venetoclax regelmäßig intrinsische oder erworbene Resistenzen auf. Da Venetoclax bereits früher für die Behandlung der chronisch lymphatischen Leukämie (CLL) zugelassen wurde, sind potenzielle Resistenzmechanismen in dieser Erkrankung bereits bekannt. Die Untersuchung von Venetoclax-Resistenz in AML ist Gegenstand dieser Arbeit.

Zunächst wurden durch kontinuierliche Exposition AML-Zelllinien mit Resistenz gegenüber Venetoclax generiert. Diese wurden anschließend auf DNA-, RNA- und Protein-Ebene untersucht. Wir konnten feststellen, dass eine Störung in der mitochondrialen Apoptose durch eine Imbalance der pro- und antiapoptotischen Bcl-2-Proteine die Resistenzbildung fördern kann. Zudem fanden wir genetische Mutationen, insbesondere im *TP53*-Gen, die sowohl die Resistenzentwicklung als auch das heterogene intrinsische Ansprechen auf Venetoclax erklären können. Eine Hochregulierung von tumorfördernden Signalwegen nach Venetoclax-Resistenz konnte ebenfalls festgestellt werden. Die Untersuchung von Patientenproben Venetoclax-resistenter AML-Patienten mittels *single cell RNA sequencing* zeigte ebenfalls die Deregulierung der mitochondrialen Bcl-2-Proteine und somit eine beeinträchtigte intrinsische Apoptose.

Im Anschluss wurden verschiedene Möglichkeiten, die Venetoclax-Resistenz in AML-Zelllinien zu überwinden, untersucht. Insbesondere der MCL1-Inhibitor S63846 stellte sich hierbei als sehr wirkungsvoll heraus. Zudem fanden wir ein heterogenes Ansprechen der Venetoclax-resistenten Zelllinien auf das Standard-Chemotherapeutikum der AML, Cytarabin, was darauf hinweist, dass eine Kreuzresistenz möglich ist.

Zusammenfassend konnten wir in dieser Arbeit Mechanismen der erworbenen und intrinsischen Resistenz gegenüber dem BCL2-Inhibitor Venetoclax identifizieren und Ansätze zur Überwindung der Resistenz aufzeigen.

1 Abstract

The BCL2 inhibitor venetoclax (ABT-199) has improved therapeutic options for acute myeloid leukemia (AML) patients ineligible for intensive treatment regimens. However, intrinsic and acquired resistance massively impedes drug efficacy.

Here, we aimed to elucidate mechanisms of venetoclax resistance in AML by characterizing a heterogeneous panel of venetoclax-resistant AML cell lines on DNA, RNA, and protein level. For this purpose, we generated AML cell lines with acquired resistance against venetoclax. We then identified driving forces of venetoclax resistance including impaired mitochondrial apoptosis, upregulation of tumor-promoting pathways and mutations of *TP53*. Single cell RNA sequencing results of AML patient samples pre and post venetoclax resistance emphasized the role of altered mitochondrial homeostasis in the emergence of resistance. Furthermore, we demonstrated that selectively targeting mitochondrial apoptosis, especially via MCL1 inhibition, circumvents venetoclax resistance in AML cell lines.

Taken together, these results improve understanding of intrinsic and acquired venetoclax resistance and identify potential therapeutic targets for the treatment of AML patients unfit for intensive therapy.

2 Introduction

2.1 Acute myeloid leukemia (AML)

2.1.1 Definition and Epidemiology

Acute myeloid leukemia (AML) is a neoplastic disease of the hematopoietic system. It is characterized by the proliferation and accumulation of mostly poorly differentiated myeloid progenitor cells [1]. AML is the most common acute leukemia in adults, with an incidence rate of approximately 3.7 per 100,000 persons [2,3]. Incidence drastically increases with age, resulting in an age-adjusted incidence rate of up to 40 cases per 100,000 population in male patients aged 85-89 [4] and an overall median age at diagnosis of 69 [5]. Elderly patients are typically not eligible for intensive treatment with high-dose chemotherapy, which highlights the need for less aggressive therapeutic options [1].

2.1.2 Diagnosis

To establish the diagnosis of AML, detection of one of the following AML-defining genetic abnormalities is required: *PML::RARA* fusion, *RUNX1::RUNX1T1* fusion, *CBFB::MYH11* fusion, *DEK::NUP214* fusion, *RBM15::MRFTA* fusion, *BCR::ABL1* fusion, *KMT2A* rearrangement, *MECOM* rearrangement, *NUP98* rearrangement, *NPM1* mutation, or *CEBPA* mutation [6]. Except for *BCR::ABL1* fusion and *CEBPA* mutation, which require an additional blast count of ≥20%, these mutations confirm the diagnosis of AML, irrespective of the blast count [6]. An important additional diagnostic procedure is immunophenotyping via flow cytometry. Quantifying the expression of AML blast-associated surface and cytoplasmic markers such as CD34, CD117 and HLA-DR (precursor markers), CD65 and MPO (myeloid markers) or CD14, CD36 and CD64 (monocytic markers) can facilitate diagnosis [7]. An additional characteristic feature of AML blasts is the cytoplasmic presence of needle-shaped inclusion bodies called Auer rods [8]. Moreover, cytogenetic and molecular genetic analysis are routinely conducted to detect both chromosomal and/or genetic aberrations [7]. In addition, fluorescence in situ hybridization (FISH) can be employed [7]. Testing for genomic aberrations is an essential step in the diagnosis of AML, since the results affect both prognosis and therapeutic options [9-12].

2.1.3 Pathophysiology

The origin of AML lies in the aberrant differentiation followed by excessive proliferation of clonal myeloid precursor cells [1]. As observed in other hematologic malignancies, high blast counts can lead to bone marrow overgrowth and therefore to suppressed physiological hematopoiesis

[1]. Consequently, common symptoms of AML can be attributed to bone marrow failure and include shortness of breath and fatigue (anemia), higher risk of infections and prolonged infections (leukopenia), as well as petechiae and prolonged bleeding (thrombocytopenia) [13].

AML genome analyses by The Cancer Genome Atlas (TCGA) research network have shown that, while containing fewer mutations than most other cancer genomes, almost all patients exhibit at least one mutation in one of the following categories: Signaling genes, DNA-methylation-related genes, chromatin-modifying genes, nucleophosmin gene, myeloid transcription factor genes, transcription-factor fusion genes, tumor-suppressor genes, spliceosome complex genes and cohesion complex genes (Table 1) [14]. Most frequently mutated genes include *FLT3* (containing either internal tandem duplication or tyrosine kinase mutation)*, NPM1, DNMT3A, IDH2, IDH1, TET2, RUNX1, TP53, NRAS* and *CEBPA,* the most frequent gene fusions are *PML::RARA, CBFB::MYH11* and *RUNX1::RUNX1T1* [14]. Although the exact pathomechanism underlying the emergence of AML is not fully understood, it is certain that chromosomal and genetic aberrations play a vital role. For example, *RUNX1-RUNX1T1* fusion gives rise to a chimeric protein with the ability to interfere with the differentiation process of myeloid progenitor cells [15].

The vast majority of AML cases occur in previously healthy individuals (*de novo)* [16]. However, in some cases, AML may arise as so called “secondary AML” either after treatment with cytotoxic agents and/or radiotherapy (t-AML), or as a result of a previously existing hematologic disease such as myelodysplastic syndrome (MDS) or myeloproliferative neoplasms (MPN) [17]. Rarely, exposure to certain chemicals like benzene and formaldehyde or high-dose radiation can provoke onset of AML [18-20].

Table 1: Most frequently mutated genes in AML and their respective functional class

Adapted from TCGA [14]

Functional class	**Example mutations**
Signaling and kinase pathway	*FLT3, KRAS, NRAS, KIT, PTPN11*
Epigenetic modifiers	*DNMT3A, IDH1, IDH2, ASXL1, EZH2, MLL/KMT2A*
Nucleophosmin	*NPM1*
Transcription factors	*CEBPA, RUNX1, GATA2*
Tumor suppressors	*TP53*
Spliceosome complex	*SRSF2, U2AF1, SF3B1*, *ZRSR2*
Cohesin complex	*RAD21, STAG1, STAG2, SMC1A*, *SMC3*

2.1.4 Classification

AML is a complex and heterogeneous disease. The current classification, published by the WHO in 2022, divides AML into two categories (Table 2) [6].

Table 2: WHO classification

Adapted from Khoury *et al*. [6]

AML with defining genetic abnormalities	Acute promyelocytic leukaemia with *PML::RARA* fusion
	AML with *RUNX1::RUNX1T1* fusion
	AML with *CBFB::MYH11* fusion
	AML with *DEK::NUP214* fusion
	AML with *RBM15::MRTFA* fusion
	AML with *BCR::ABL1* fusion
	AML with *KMT2A* rearrangement
	AML with *MECOM* rearrangement
	AML with *NUP98* rearrangement
	AML with *NPM1* mutation
	AML with *CEBPA* mutation
	AML, myelodysplasia-related
	AML with other defined genetic alterations
AML, defined by differentiation	AML with minimal differentiation
	AML without maturation
	AML with maturation
	Acute basophilic leukaemia
	Acute myelomonocytic leukaemia
	Acute monocytic leukaemia
	Acute erythroid leukaemia
	Acute megakaryoblastic leukaemia

2.1.5 Prognosis

Individual clinical features are essential to determine disease progression and ultimately patient prognosis. Overall survival (OS) and complete remission (CR) are significantly lower in patients with increased age, poor performance status and/or therapy-related disease [7,20-22]. Likewise, gender represents an independent prognostic factor as male patients have significantly lower OS [23]. However, the single most important prognostic factor remains genetic aberrations [12]. A multitude of studies have shown the extensive impact of cytogenetic and molecular abnormalities on patient survival. Chromosomal rearrangements t(8;21), inv(16) and t(15;17) are associated with a more favorable outcome [9]. The same is true for biallelic mutation and mutations within the bZIP domain of *CEBPA* [12]. However, patients exhibiting a complex karyotype, monosomy karyotype, *FLT3* internal tandem duplication (ITD) and mutations or further cytogenetic changes associated with MDS (such as *ASXL1* mutation, *RUNX1* mutation and/or *TP53* mutation) face poor outcome [9-12,24,25]. Mutated *TP53* is associated with a complex karyotype and thus confers a particularly dire prognosis [26,27]. According to the European LeukemiaNet (ELN), AML cases can be subdivided into three main risk categories depending on cytogenetic and molecular aberrations (Table 3) [7]. 5-year relative survival is 30.5% across all ages and individual clinical and genetic features, and approximately 7% in patients 65 years and above [5]. Acute promyelocytic leukemia (APL) is not included in this classification, as high rates of remission can typically be achieved [28,29].

Table 3: 2022 ELN risk stratification

Adapted from Döhner et al. [7]

Favorable	t(8;21)(q22;q22.1)/*RUNX1::RUNX1T1*
	inv(16)(p13.1q22) or t(16;16)(p13.1;q22)/*CBFB::MYH11*
	mutated *NPM1* without *FLT3*-ITD
	bZIP in-frame mutated *CEBPA*
Intermediate	mutated *NPM1* with *FLT3*-ITD
	wild-type *NPM1* with *FLT3*-ITD
	t(9;11)(p21.3;q23.3)/*MLLT3::KMT2A*
	cytogenetic and/or molectular abnormalities not classified as favorable or adverse
Adverse	t(6;9)(p23.3;q34.1)/*DEK::NUP214*
	t(v;11q23.3)/*KMT2A*-rearranged
	t(9;22)(q34.1;q11.2)/*BCR::ABL1*
	t(8;16)(p11.2;p13.3)/*KAT6A::CREBBP*
	inv(3)(q21.3q26.2) or t(3;3)(q21.3;q26.2)/*GATA2, MECOM(EVI1)*
	t(3q26.2;v)/*MECOM(EVI1)*-rearranged
	-5 or del(5q);-7;-17/abn(17p)
	complex karyotype, monosomal karyotype
	mutated *ASXL1, BCOR, EZH2, RUNX1, SF3B1, SRSF2, STAG2, U2AF1,* and/or *ZRSR2*
	mutated *TP53*

2.1.6 Therapy

Prior to treatment commencement, patients are individually assessed for general performance status, comorbidities, genetic profile of AML cells and individual therapy goals. Depending on the results, patients are considered either fit or unfit for intensive therapy [7]. Advanced age alone should not be a reason to exclude patients from intensive therapy, as better long-term survival could be observed in older patients receiving intensive therapy, even if they had significant comorbidities [30]. Regardless of the chosen treatment regimen, induction therapy is the first therapeutic measure and aims at achieving complete remission (CR) [7].

Again, APL is excluded in the following as it requires a different treatment regimen comprising all-trans-retinoic acid and arsenic trioxide [28,29].

2.1.6.1 Patients fit for intensive chemotherapy

For patients eligible for intensive chemotherapy, the treatment regimen of induction therapy has not changed much over the past decades. It comprises the antimetabolic agent cytarabine and a DNA-intercalating anthracycline (e.g., daunorubicine, idarubicine), known as the "7+3" scheme due to the administration pattern [7]. The standard of care is a continuous infusion of 100-200 mg/m^2 cytarabine over seven days plus three days of anthracycline (at least 60 mg/m^2 daunorubicin, 12 mg/m^2 idarubicin or 12 mg/m^2 mitoxantrone) infusion [7]. The addition of nucleoside analogs like fludarabine or cladribine has been shown to increase CR rate and enhance OS in some cases, and therefore is suggested by the MD Anderson Cancer Center for frontline AML therapy in younger adults [31-33]. According to the individual genetic profile, intensive induction chemotherapy can be supplemented with targeted therapies. *FLT3* ITD and tyrosine kinase domain (TKD) mutation are directly targetable with *FLT3* tyrosine kinase inhibitor midostaurin, which prolongs event-free survival (EFS) and OS [34-36]. Clinical trials evaluating the impact of even more *FLT3* inhibitors like gilteritinib and quizartinib for induction therapy in combination with conventional chemotherapy are ongoing (HOVON 156ML; NCT04027309, QUANTUM-First, NCT02668653). Another therapeutic option is gemtuzumab ozogamicin, a CD33 monoclonal antibody [37]. After conflicting results and previous withdrawal, it has been re-approved for CD33-positive *CBF*-AML, CD33-positive AML with *NPM1* mutation and *FLT3*-wt, and CD33-positive AML with biallelic *CEBPA* mutation at low doses [37,38]. Patients with secondary AML receive dual-drug liposomal cytarabine and daunorubicin as this has been shown to significantly prolong survival rates [39]. Moreover, *IDH1* inhibitor ivosidenib and *IDH2* inhibitor enasidenib are currently being investigated for induction therapy in combination with intensive chemotherapy for *IDH1 or IDH2* mutated AML [40] (HOVON150AML).

Induction therapy should always be followed by post-remission/consolidation therapy in order to minimize the risk of relapse due to minimal residual disease (MRD) [16]. Risk of relapse is largely based on cytogenetic and molecular genetic risk profile, the existence of secondary

AML and clinical patient features such as age [7,22,41-43]. According to an individual risk and benefit assessment, consolidation therapy for fit patients consists of either high-dose chemotherapy or allogeneic hematopoietic stem cell transplantation (allo-HCT). For patients with a low risk of relapse or in case allo-HCT is not considered an option, the administration of up to four cycles of intermediate-dose cytarabine (1000-1500 mg/m^2) is the consolidation standard of care [7]. However, patients with a high risk of relapse should undergo allo-HCT as consolidation therapy [7]. Although it reduces the overall risk of relapse, allo-HCT is associated with a higher risk of non-relapse mortality (NRM) [44]. Therefore, careful evaluation of the risk-benefit ratio for each patient is crucial. Several tools have been developed for this purpose [45,46]. If allo-HCT is technically required but impossible, for example due to a lack of donor or a disproportionately high risk of NRM, chemo-consolidation should be followed by maintenance therapy with oral hypomethylating agent azacitidine [47]. Patients with *FLT3* mutated AML may additionally receive midostaurin as consolidation therapy and possibly for maintenance therapy in case the drug was used for induction therapy previously [36].

2.1.6.2 Patients unfit for intensive chemotherapy

Elder AML patients are more likely to present severe comorbidities (diabetes, hypertension, organ dysfunction like renal, liver or heart failure), or poor performance status in general. Since advanced age also correlates with adverse genetic risk profile (i.e., complex karyotype, monosomal karyotype and/or *TP53* mutation) and higher incidence of antecedent hematologic diseases (secondary AML), chances of cure are very low [7,26,48]. Therefore, such patients are considered unfit for intensive chemotherapy and receive a different, lower-intensity treatment regimen [26,31,49].

Low dose cytarabine (LDAC, 20 mg s.c. twice daily for ten days) has been shown to significantly elevate CR rates and prolong OS when compared to palliative/best supportive care [50]. Subsequent clinical trials showed that the application of hypomethylating agents (HMA) such as azacitidine or decitabine further improved response rates in comparison to standard therapies like intensive chemotherapy, LDAC or best supportive care [51-54]. Simultaneously, HMA and LDAC treatment regimens are associated with significantly lower early mortality rates and fewer therapy-associated complications [52], and thus have been established as therapeutic options in patients not considered candidates for intensive chemotherapy. However, the addition of the BCL2 inhibitor venetoclax (Chapter 1.3) significantly improves CR rates in combination with either LDAC or HMA, and OS in combination with HMA [55-59]. These results led to the FDA approval of venetoclax in combination with either HMA or LDAC as first line therapy in patients unfit for intensive chemotherapy. In 2021, EMA approval for venetoclax in combination with HMA for the same indication followed. Second line treatment consists of either HMA monotherapy or LDAC + glasdegib, a hedgehog pathway inhibitor which has

shown to improve CR and OS compared to third line LDAC monotherapy [60]. Ivosidenib has been approved by the EMA for unfit patients with *IDH1* mutation in combination with hypomethylating agents [61].

Patients not eligible for any antileukemic therapy or patients who do not want any therapy should be treated with best supportive care including hydroxyurea for cytoreduction [7].

2.1.6.3 Salvage therapy

Treating refractory or relapsed (R/R) AML remains a challenge due to the heterogeneous background of patients. Despite thorough investigation, no specific induction treatment regimen is in place and therefore individual evaluation of disease characteristics, patient features and wishes, previous therapies and duration of response is mandatory [31,62,63].

In order to reestablish CR, reinduction therapy should include intermediate or high dose cytarabine (IDAC or HDAC, respectively). An effective approach has been the combination of fludarabine, IDAC, idarubicin and G-CSF (FLAG-IDA) [64,65] or the combination of mitoxantrone, etoposide and IDAC (MEC) [66]. In recent years, numerous trials were carried out that assessed the application of targeted therapies in R/R AML. For example, combining FLAG-IDA with venetoclax showed promising results [67]. Furthermore, in *FLT3* mutated AML, monotherapy with gilteritinib is a well-established therapeutic option, as it prolongs OS and achieves higher rates of CR compared with salvage chemotherapy [68]. Likewise, IDH inhibitors ivosidenib and enasidenib are FDA approved for *IDH1* or *IDH2* mutated AML, respectively [69,70]. GO monotherapy can be used carefully in $CD33^+$ AML [63]. Additional therapeutic options include combination of venetoclax with HMA or chemotherapy [71-73].

If possible, patients should receive follow-up allo-HCT after second remission as it represents the only change of long-term cure [74]. However, this is only an option for few patients. Especially relapse after previous allo-HCT is a poor prognostic factor [75].

2.2 The role of Bcl-2 family proteins in mitochondrial apoptosis

2.2.1 Apoptosis

The physiological process of programmed cell death is called apoptosis. It describes the essential regulatory part for maintaining homeostasis of cell turnover and is therefore subject to strict control mechanisms. The term “apoptosis” was coined by Kerr, Wyllie and Currie in 1972 [76]. Not only is apoptosis vital for the removal of potentially harmful cells, but it also plays an important role in the formation of structures during embryogenesis [77,78]. Morphological characteristics of apoptosis comprise cell shrinkage and pyknosis through chromatin condensation, followed by karyorrhexis (chromatin fragmentation) and cell separation into apoptotic bodies [76,79]. As opposed to necrosis, apoptosis does not cause inflammation, as all cell components including organelles and cytoplasm are still encased within the plasma membrane [80]. Subsequently, apoptotic bodies are engulfed and incorporated by phagocytic cells such as macrophages [81]. A crucial step in the process of apoptosis is caspase activation. Caspases are cysteine proteases characteristically cleaving proteins at aspartic acid residues (cysteine-dependent aspartate-directed proteases) [82,83]. Usually, they reside within the cytosol as inactive procaspases, but are activated by apoptotic stimulation. Mutual activation of procaspases causes a proteolytic cascade, resulting in the amplification of apoptotic signaling and ultimately in cell death [84]. Other biochemical features of apoptosis include DNA fragmentation through endonucleases [85] and the exposure of cell surface markers that facilitate detection by phagocytes [86]. Apoptosis-triggering signals include both extra- and intracellular events. Therefore, apoptosis can be divided into two main cell death signaling pathways: extrinsic and intrinsic apoptosis, both converging in the joint execution pathway [87]. In addition, T cells are able to mediate apoptosis via the perforin/granzyme pathway [79].

2.2.1.1 Extrinsic apoptosis

Extrinsic apoptosis is triggered by extracellular signals, which require transmembrane receptor-mediated signaling [88]. These so called “death receptors” (e.g., Fas/CD95 or TRAIL) belong to the tumor necrosis factor (TNF) receptor family [88-90]. Receptor ligands (“death factors”) include TNF and cytokines [90]. Upon stimulation, adapter proteins like FADD and TRADD are recruited to the cytoplasmatic receptor domain called “death domain”, where they bind with their own death domains [91,92]. Following this, procaspase 8 is activated to initiator caspase 8. This results in the formation of death-inducing signaling complex (DISC) comprised of death receptor, adapter protein and caspase 8 [93]. Caspase 8 in turn activates effector caspases 3, 6 and 7, initiating the execution phase of apoptosis (Chapter 1.2.1.4) [84]. Of note, caspase 8 is also capable of cleaving Bcl-2 protein BID, thus leading to mitochondrial

cytochrome c release. This way, an extrinsic stimulus may stimulate intrinsic/mitochondrial apoptosis [94].

2.2.1.2 Perforin/Granzyme B cascade

$CD8^+$ lymphocytes, also called cytotoxic T lymphocytes (CTL), are capable of inducing apoptosis via secretion of perforin and granzyme. Upon recognition of a virus-infected or pathologically transformed cell, CTL will release the pore-inducing molecule perforin followed by serine proteases, mostly granzyme A and B [95]. Granzyme B cleaves proteins at aspartic acid residues. This way, procaspases 3 and 10 become activated and trigger the caspase cascade, which eventually sets off the apoptotic execution phase [96,97]. Granzyme A on the other hand induces DNA fragmentation via DNase activation [98].

2.2.1.3 Intrinsic/mitochondrial apoptosis

The intrinsic pathway of apoptosis is initiated inside mitochondria and triggered by intracellular signals. These stimuli can be either negative, like the lack of growth factors or cytokines, or positive, like DNA damage or hypoxia [79]. Intrinsic apoptosis is subject to strict regulations by Bcl-2 family proteins (Chapter 1.2.2) [99]. Apoptotic stimuli result in the activation of p53 and proapoptotic members of the Bcl-2 family, which then allow mitochondrial outer membrane permeabilization (MOMP) [100]. Subsequently, molecules residing within the mitochondrial intermembrane space like cytochrome c, endonuclease g, Omi/HtrA2, AIF and DIABLO are released into the cytosol [101-105]. DIABLO and HtrA2 are inhibitors of IAP (inhibitors of apoptosis proteins) and thereby promote apoptosis [102], while AIF and endonuclease g cause DNA fragmentation in later stages of apoptosis [101,106]. Cytochrome c binds to procaspase 9 and APAF-1, which are activated thereupon and thus form the so called “apoptosome” [107,108]. This crucial step in the process of intrinsic apoptosis leads to cascade-like activation of effector caspases 3, 6 and 7 and sets off the execution phase of apoptosis [84].

2.2.1.4 Execution phase

The activation of effector caspases 3, 6 and 7 causing irreversible cascade-like caspase activation marks the final phase of apoptosis [84]. Substrates of the most important execution caspase 3 are numerous and include poly(ADP-ribosome)-polymerase (PARP), inhibitor of caspase-activated DNase (ICAD), endonucleases and cytokeratins [109,110]. Caspase-activated DNase (CAD), freed from its inhibitor ICAD by caspase 3 activity, induces chromosomal DNA degradation [97]. PARP is a polymerase involved in DNA damage response (DDR). PARP cleavage is detectable via immunoblotting or immunohistochemistry, which is a widely used technique for validation of apoptosis [111-113]. Additionally, membrane disintegration takes place during apoptotic execution phase, thereby exposing molecules on the cell surface for

phagocyte recognition [79]. A well-known example is phosphatidylserine, which is usually located at the inner leaflet of a cell's lipid bilayer, but undergoes translocation to the outer leaflet during apoptosis [114]. Here, it is not only recognized by phagocytic cells, but also by binding protein Annexin V. Therefore, detection of Annexin V via flow cytometry or immunofluorescence microscopy serves as an analytic marker for apoptosis and has become a well-established research method [115].

2.2.2 Bcl-2 family proteins

As mentioned above, Bcl-2 family proteins play a decisive role in mitochondrial apoptosis. Tsujimoto et al. first discovered the BCL2 protein and its overexpression through chromosomal translocation in B cell lymphoma cells [116-118]. The fact that BCL2 exerts its oncogenic potential through apoptosis evasion was described in the following years [119]. Due to these findings, the whole family was named after the BCL2 protein and nowadays comprises more than 15 proteins [120].

Bcl-2 family proteins can be divided into proapoptotic (anti-survival) and antiapoptotic (pro-survival) proteins. However, despite their divergent functionality, they share similar composition and structure, and continuously interact with each other [121]. All members contain up to four Bcl-2 homology (BH) domains (BH1, BH2, BH3, BH4) and one C-terminal transmembrane (TM) domain, which enables protein anchoring in mitochondrial outer membrane (MOM) or endoplasmic reticulum (ER) membrane [121]. Antiapoptotic proteins typically consist of all four domains, while proapoptotic proteins contain either three/four domains ("multi-domain"), or only the BH3 domain ("BH3-only") [121-123]. Multi-domain proapoptotic and all antiapoptotic proteins additionally share the same 3D structure comprised of two central hydrophobic α-helices within six or seven amphipathic α-helices [124]. This structure forms a hydrophobic binding groove, which can hold the amphipathic α-helix of the BH3 domain of an interacting Bcl-2 protein partner in a receptor/ligand-like fashion. Therefore, the hydrophobic groove is the basis of interaction between Bcl-2 family proteins [124]. Equilibrium of pro- and antiapoptotic Bcl-2 family protein interaction is a crucial part of cell turnover and thus organism health. Imbalances can result in disorders like autoimmune diseases, neurodegenerative diseases, and cancer [125,126].

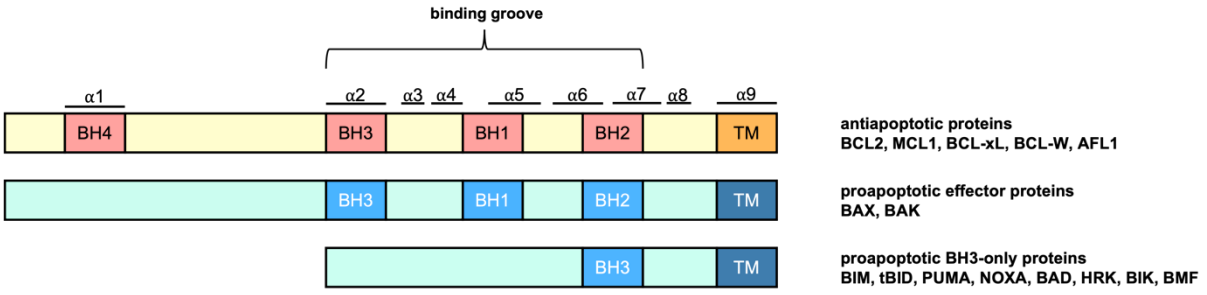

Figure 1: BH domains of Bcl-2 family proteins

2.2.2.1 Antiapoptotic proteins

Antiapoptotic Bcl-2 family proteins include B cell lymphoma 2 (BCL2), BCL2 like protein/B cell lymphoma extra-large (*BCL2L1*/BCL-xL), myeloid cell lymphoma 1 (MCL1), BCL2 like protein 2 (*BCL2L2*/BCL-W) and BCL2 related protein A1 (*BCL2A1*/BFL1). They exert their pro-survival potential through sequestration and thereby inhibition of all proapoptotic proteins [127].

During organism development, antiapoptotic Bcl-2 family proteins are essential for the formation of healthy cells. *In vivo* and *in vitro* studies showed that hematopoietic stem cells (HSC) rely on BCL2, MCL1 and BCL-xL during early hematopoiesis [128-130]. Bcl-2 protein dependence of B cell development has been studied in particular, providing evidence that BCL-xL is necessary for survival of immature B cells, BCL2 promotes mature B cell survival and MCL1 is required throughout the entire B cell development [131,132].

Resisting cell death has been described as one of the hallmarks of cancer by Hanahan and Weinberg [133,134]. Unsurprisingly, upregulation of antiapoptotic Bcl-2 family proteins is a common finding in cancers including hematologic malignancies, melanoma, nasopharyngeal cancer, Burkitt lymphoma or prostate cancer and can be attributed to various mechanisms [135-138]. For example, MCL1 is necessary for development and growth in AML and its overexpression was found to be associated with resistance to chemotherapy [139-143]. Several studies have found translocation of the *BCL2* gene to the immunoglobulin heavy locus (IGH) called t(14;18) to be one of the main causes for overexpression of BCL2 and cell survival in follicular lymphoma (FL) and diffuse large b cell lymphoma (DLBCL) [116,144-146]. Additionally, chromosomal amplification was found to be another driving force for BCL2 overexpression in DLBCL [147,148]. Amplification of *MCL1* and *BCL-xL* was also found in solid tumors [149,150]. In fact, the genetic region containing the *MCL1* gene is one of the most commonly amplified regions in human cancers [151]. In summary, translocations, amplifications, and epigenetic modifications seem to play a major role in driving overexpression and upregulation of antiapoptotic Bcl-2 family genes and proteins, respectively.

2.2.2.2 Proapoptotic proteins

As discussed above, proapoptotic members of the Bcl-2 family are subclassified into “BH3-only” and “multi domain” proapoptotic proteins. BH3-only proteins include BCL2-interacting mediator of cell death (BIM), BH3-interacting domain death agonist (BID), BCL2 binding component 3/p53 upregulated modulator of apoptosis (*BBC3*/PUMA), phorbol-12-myristate-13-acetate-induced protein 1 (*PMAIP1*/NOXA), BCL2-associated antagonist of cell death (BAD), BCL2 modifying factor (BMF), Harakiri (HRK) and BCL2 interacting killer (BIK) [99]. Multi-domain proteins are also called effector proteins and are comprised of Bcl2-associated X protein (BAX), Bcl2 homologous antagonist killer (BAK) and BCL2-related ovarian killer protein (BOK) [120,152]. Upon activation, effector proteins BAK and BAX are both located at the

mitochondrial outer membrane and undergo conformational changes that allow homodimerization of the two proteins. The resulting homodimers become interlinked into oligomers, which eventually form ring-like structures in the MOM [153-156]. The process of MOMP, as described in chapter 1.2.1.3, results in the effusion of molecules from the mitochondrial intermembrane space into the cytosol, which then initiate further apoptotic steps [105]. Oligomerization of BAK/BAX is induced when the homeostasis of Bcl-2 proteins tilts in favor of proapoptotic proteins either through activation via BH3-only proteins and/or the absence of antiapoptotic proteins [157-159]. In vital cells, antiapoptotic proteins inhibit BAX and BAK, thereby keeping effector-mediated apoptosis initiation in check [160].

BH3-only proteins BIM, tBID, and PUMA are called “activators” as they directly interact with BAX and BAK, thereby triggering MOMP [158]. BH3-only proteins NOXA, BAD, BMF, HRK, and BIK act as “sensitizers” and bind to antiapoptotic proteins, thus liberating BH3-activator proteins, which had been unavailable before [158]. Of note, activator proteins can also adopt sensitizing function by inhibiting antiapoptotic proteins [161]. PUMA, NOXA and BID expression levels are regulated by transcription factor p53 and therefore affected by cytotoxic stimuli [162,163]. However, p53 also accounts for the transcription of effector protein BAX, which highlights its far-reaching impact [164]. BID establishes a connection to death-receptor-mediated/extrinsic apoptosis, as it is cleaved and thereupon activated by caspase 8 in the event of extracellular cell death stimulation. Truncated BID (tBID) then relocates from its usual cytosolic location to mitochondria, inducing apoptosis via BAX/BAK activation [165].

BH3-only and antiapoptotic proteins exhibit varying affinities for each other. Therefore, only some protein pairs interact. While BIM and PUMA bind to any antiapoptotic protein, BAD preferably binds to BCL2, BCL-xL and BCL-W, and NOXA only associates with MCL1 and BFL1 [160]. The principle of affinity-based interaction also holds true for the interaction between antiapoptotic proteins and proapoptotic effector proteins. MCL1 and BCL-xL both inhibit BAK [166], while BAX is primarily inhibited by BCL-xL [167].

In vivo and *in vitro* studies have shown that BAX and BAK are essential for healthy organism development. For example, mice lacking both BAX and BAK exhibit developmental defects like preserved interdigital webs. However, lack of only one protein does not impair physiological processes and growth [168,169]. Homozygous deletion and inactivating mutations of *BAX* can account for loss of apoptotic signaling in colon cancer and hematologic malignancies [170,171]. Other than that, deletion of PUMA-encoding gene *BBC3* has been found in a variety of cancer types [149].

2.3 BCL2 inhibitor venetoclax (ABT-199)

2.3.1 History of BCL2 inhibition

The discovery of Bcl-2 family protein importance in cell death combined with detailed knowledge on Bcl-2 protein interactions has spurred efforts to capitalize on these targetable molecules for therapeutic purposes. Consequently, so called “BH3 mimetics”, small molecule drugs specifically targeting the binding groove of antiapoptotic proteins, were developed, providing a *target therapy* concept. They are designed to imitate the inhibitory effect of BH3-only proteins on antiapoptotic proteins. First attempts of inhibiting antiapoptotic proteins in *in vitro* and *in vivo* models were carried out in the late 2000s [172-175]. One of the more promising early BH3 mimetics was ABT-737 and its orally available analogue ABT-263 (Navitoclax), which targets antiapoptotic proteins BCL2, BCL-xL and BCL-W. Impressive on-target effects of Navitoclax were outweighed by dose-limiting thrombocytopenia, which derives from platelet dependence on BCL-xL [176,177].

2.3.2 Venetoclax

Further investigation led to the development of ABT-199/venetoclax, which is a highly selective BCL2 inhibitor with low affinity to BCL-xL, thus preventing thrombocytopenia [178]. Owing to successful clinical trials conducted in patients with R/R CLL and non-Hodgkin lymphoma (NHL), venetoclax received breakthrough therapy designation (BTD) status by the Food and Drug Administration (FDA) in 2015 [179-181]. Emerging evidence on the efficacy of venetoclax in preclinical AML models prompted clinical trials using venetoclax monotherapy in high-risk R/R AML patients ineligible for intensive chemotherapy [182,183]. These single-agent trials provided evidence for safety and efficacy of venetoclax. However, responses were short-lived and left patients in need for better therapeutic options [183]. More durable remissions and longer OS were achieved in promising phase 1b studies combining venetoclax with HMA azacitidine or decitabine, or venetoclax with LDAC in treatment-naïve AML patients [57,184,185]. Following phase 3 clinical trials eventually led to BTD by the FDA for venetoclax first line combination therapy with either HMA azacitidine and decitabine or LDAC in AML patients ineligible for intensive chemotherapy [55,58,71]. Venetoclax plus HMA/LDAC currently represents the standard of care for unfit AML patients. Other venetoclax-based therapies for elder patients include combination with cladribine and LDAC alternating with HMA, or combination with FLAG-IDA [67,186]. However, investigations on venetoclax combination treatment in younger patients and/or patients with R/R AML are ongoing [67] (e.g., NCT03709758: combination with intensive chemotherapy, NCT04070768: combination with GO, NCT03625505: combination with gilteritinib). The most recent success of venetoclax is its FDA approval for patients with higher risk MDS in combination with azacitidine [187].

To this date, venetoclax obtained breakthrough status by the FDA for the following indications:

1. Patients with R/R CLL with 17p deletion
2. Patients with R/R CLL in combination with rituximab
3. Treatment-naïve patients with AML ineligible for intensive chemo in combination with HMA
4. Treatment-naïve patients with AML ineligible for intensive chemo in combination with LDAC
5. Treatment-naïve CLL patients in combination with obinutuzumab for chemotherapy-free treatment regimens
6. Treatment-naïve patients with higher risk MDS in combination with azacitidine

2.3.3 Resistance to BCL2 inhibition

Despite all efforts and recent treatment advances, most patients eventually relapse under continuous BCL2 inhibition [188]. This stresses the importance of understanding resistance mechanisms in order to circumvent treatment failure. Previous studies on venetoclax resistance in B cell malignancies uncovered main mechanisms underlying resistance including upregulation of antiapoptotic Bcl-2 family proteins [188-190] and acquisition of genetic mutations. For example, genetic mutations in or loss of proapoptotic proteins like NOXA and BAX, dysfunction of *TP53*, complex karyotype and recurrent genetic mutations in cancer-associated genes like *BRAF, NOTCH1, BTG1* and *TP53* were found to promote venetoclax resistance [188,191-193]. Of special interest, genetic mutations in the gene encoding BCL2 have been found as well. In CLL, acquired *BCL2* mutation G101V, D103 (E/Y/V), A113G and more were found in venetoclax-resistant patients. These mutations may lead to reduced venetoclax-BCL2 binding and thus render tumor cells resistant to the drug [194-200]. Furthermore, mutations in other Bcl-2 family genes like *NOXA, BAX* and *BAD* have been found in CLL patients who relapsed under venetoclax treatment [199]. Recently, our group could demonstrate that B-cell lymphoma cell lines with acquired resistance to venetoclax exhibited increased MCL1 as well as reduced BAX and PUMA protein levels [201].

These results spurred numerous studies investigating mechanisms of venetoclax resistance in AML. In preclinical models and in AML patients, upregulation of antiapoptotic proteins MCL1 and BCL-xL and downregulation of the proapoptotic protein BAK were associated with acquired resistance to venetoclax [183,202-204]. Various attempts to explain the exact regulatory mechanism behind deregulation of Bcl-2 proteins following venetoclax resistance in AML exist. A recent publication suggests that MCL1/BCL-xL upregulation is mediated by increased RAS/MAPK signaling [205]. Another possible explanation is increased MCL1 protein stability [202]. Other than that, preclinical data attribute venetoclax resistance to loss of *BAX, TP53* and

PMAIP1 (NOXA) [206]. In patients receiving frontline venetoclax-based therapy, genomic analyses reveal that acquisition or enrichment of *FLT3* ITD*, RAS* and *TP53* mutations give rise to activated kinase signaling and *TP53* perturbation, respectively [207]. These mechanisms are considered the main causes for both adaptive and primary resistance to venetoclax-based therapy [207]. Contrary to CLL, no mutations hindering inhibitor-protein-interaction have been found in the *BCL2* gene following venetoclax resistance to this date. In fact, it is suggested that not acquisition, but expansion of dominant mutations like *FLT3* ITD promote venetoclax resistance in AML [208,209]. Other publications consider altered mitochondrial metabolism and epigenetic modifications possible driving forces behind the development of venetoclax resistance [204,209-211].

Although the main reason for acquired venetoclax resistance remains unknown, strategies to overcome or forestall resistance are already in place. A variety of MCL1 inhibitors have shown efficacy in preclinical models either as a single agent or in combination with venetoclax [212-216], and therefore are currently being investigated phase 1 clinical trials (MIK665 in R/R lymphoma and MM: NCT02992483, S64315 in AML/MDS: NCT02979366, AMG 176 in R/R MM and R/R AML: NCT02675452, S64315 alone or in combination with venetoclax in AML: NCT03672695, AZD5991 alone or in combination with venetoclax: in R/R hematologic malignancies: NCT03218683). However, multiple studies are suspended or placed on clinical hold due to the high toxicity of the drug leading to potential safety risks. Inhibition of BCL-xL demonstrated efficacy in preclinical models [217] and therefore provided rationale for clinical testing as well (DT2216 in R/R malignancies: NCT04886622). Additional strategies to circumvent venetoclax resistance include MDM2 inhibition, MEK inhibition and CDK9 inhibition [218-220].

2.4 Hypotheses/ Aims

AML is a highly lethal disease. The advent of BCL2 inhibition via venetoclax has augmented therapeutic options, but survival has only improved marginally, and resistance remains a problem. Attempts have already been made to uncover the exact mechanisms underlying primary and adapted venetoclax resistance, but more investigation is needed. We aim to further elucidate venetoclax resistance by providing an in-depth characterization of multiple venetoclax-resistant AML cell lines including extensive DNA, RNA and protein analysis regarding mitochondrial apoptosis and Bcl-2 family interactions. Additionally, we present single cell RNA sequencing data of venetoclax-resistant AML patients. Based on these considerations we have formulated two hypotheses:

1. Venetoclax resistance emerges from impaired mitochondrial apoptosis. This is mediated by altered protein and mRNA level, and/or genetic mutations.
2. Venetoclax resistance can be overcome by manipulating members of the Bcl-2 family in order to reestablish efficient mitochondrial apoptosis.

3 Materials and Methods

3.1 Materials

3.1.1 Cell lines

Table 4: Collection of AML cell lines

Cell line	Supplier
HL-60	Leibniz-Institute DSMZ, Braunschweig
KASUMI-1	Leibniz-Institute DSMZ, Braunschweig
ML-2	Leibniz-Institute DSMZ, Braunschweig
MOLM-13	Leibniz-Institute DSMZ, Braunschweig
MOLM-16	Leibniz-Institute DSMZ, Braunschweig
NOMO-1	Leibniz-Institute DSMZ, Braunschweig
OCI AML-2	Leibniz-Institute DSMZ, Braunschweig
PL-21	Leibniz-Institute DSMZ, Braunschweig
SIG-M5	Leibniz-Institute DSMZ, Braunschweig
PUMA knockout of OCI AML-2	

3.1.2 Equipment

Table 5: List of technical equipment

Product	Supplier
CO_2 incubator CB170	Binder, Tuttlingen
CoolCell LX freezing container #432003	Corning, NY, USA
Eppendorf Centrifuge 5427 R	Eppendorf, Hamburg
Eppendorf Centrifuge 5810 R	Eppendorf, Hamburg
Eppendorf Thermomixer comfort	Eppendorf, Hamburg
FLUOstar OPTIMA Microplate Reader	BMG Labtech, Ortenberg

Gel DocTM XR+	Bio-Rad Laboratories, CA, USA
Heidolph Duomax 1030 Orbital Shaker	Heidolph Instruments, Schwabach
Laminar flow cabinet Scanlaf MARS 1200	LaboGene, Lillerød, Dänemark
Light microscopes	Zeiss, Oberkochen
MACSQuant VYB Flow Cytometer	Miltenyi Biotech, Bergisch Gladbach
MACSQuant X Flow Cytometer	Miltenyi Biotech, Bergisch Gladbach
Micropipettes	Eppendorf, Hamburg
Nanodrop 1000 Spectrophotometer	Peqlab/VWR, PA, USA
Odyssey CLx Imaging System	Li-Cor, Nebraska, USA
Pipetting aid	Hirschmann, Eberstadt
ZOE microscope	Bio-Rad Laboratories, CA, USA

3.1.3 Consumables

Consumables not listed below were exclusively purchased from Sarstedt, Nümbrecht.

Table 6: List of consumables

Product	**Supplier**
96 well plates NUNC U bottom	Thermo Fisher Scientific, MA, USA
96 well plates NUNC white flat bottom	Thermo Fisher Scientific, MA, USA
Chromatography Paper 3mm Whatman	GE Healthcare Life Sciences, IL, USA
Nitrocellulose Blotting Membrane Amersham Protran Premium 0,45µM	GE Healthcare Life Sciences, IL, USA
NuPAGE 4-12% Bis-Tris Gel 10 well	Thermo Fisher Scientific, MA, USA
NuPAGE 4-12% Bis-Tris Gel 12 well	Thermo Fisher Scientific, MA, USA

3.1.4 Compounds

Table 7: List of compounds

Product	Target	Supplier
ABT-199 (venetoclax)	BCL2	AbbVie, IL, USA Selleckchem, München
Cytarabine	DNA	Selleckchem, München
MCL1-inhibitor S63845	MCL-1	ApexBIO Technology, TX, USA
Puromycin	ribosome	InvivoGen, CA, USA

3.1.5 Reagents

Table 8: List of reagents

Product	Supplier
10x TBE	Invitrogen, MA, USA
7-AAD Viability Staining	Thermo Fisher Scientific, MA, USA
Agarose	Sigma Life Science, MO, USA
Albumin Fraction V (BSA)	PanReac AppliChem, Darmstadt
Albumin Fraction V (pH 7.0)	PanReac AppliChem, Darmstadt
Annexin V Binding Buffer	BD Pharmingen, Hamburg
Annexinv V Fluoresceinisothiocyanat (FITC)	ImmunoTools, Friesoythe
BsmB1	New England Biolabs, MA, USA
Cell Titer Glo (CTG)	Promega, WI, USA
Chloroform	Merck, Darmstadt
Dialyzed Fetal Calf Serum (dFCS)	Thermo Fisher Scientific, MA, USA
Dimethylsulfoxid (DMSO)	Sigma Life Science, MO, USA
DMEM	Thermo Fisher Scientific, MA, USA
DNA Gel Loading Dye 6X	Thermo Fisher Scientific, MA, USA

Ethanol 70%	PanReac AppliChem, Darmstadt
Fetal Bovine Serum (FBS)	Thermo Fisher Scientific, MA, USA
GelRed® Nucleic Acid Gel Stain	Biotium, CA, USA
GeneRuler 100bp Plus DNA Ladder	Thermo Fisher Scientific, MA, USA
IMDM	Thermo Fisher Scientific, MA, USA
Isopropanol/2-Propanol	PanReac AppliChem, Darmstadt
LDS Sample Buffer	Thermo Fisher Scientific, MA, USA
lentiCRISPR v2 transfer plasmid	AddGene, MA, USA
LentiX concentrator solution	Takara Bio, Shiga, Japan
MACS Quant Running Buffer	Miltenyi Biotech, Bergisch Gladbach
MACS Quant Washing Solution	Miltenyi Biotech, Bergisch Gladbach
MEMalpha	Thermo Fisher Scientific, MA, USA
Natriumchlorid (NaCl) >99,9%	Carl Roth, Karlsruhe
NuPAGE Novex MES SDS Running Buffer	Life Technologies, CA, USA
Odyssey Blocking Buffer TBS/PBS	Li-Cor, Bad Homburg
Page Ruler^{TM} Prestained Protein Ladder	Thermo Fisher Scientific, MA, USA
Penicillin Streptomycin	Thermo Fisher Scientific, MA, USA
peqGOLD TriFast	VWR, PA, USA
Phosphate-Buffered Saline (PBS)	Thermo Fisher Scientific, MA, USA
PhosSTOP EASYpack	Roche, Basel, Schweiz
pMD2.G envelope plasmid	AddGene, MA, USA
Protease Inhibitor Cocktail	Sigma Life Science, MO, USA
psPAX2 packaging plasmid	AddGene, MA, USA
RiboRuler High Range RNA Ladder	Thermo Fisher Scientific, MA, USA
RPMI-1640	Thermo Fisher Scientific, MA, USA
Sample Reducing Agent	Thermo Fisher Scientific, MA, USA
Sodium Butyrate	Sigma Life Science, MO, USA
Sodium dodecyl sulfat (SDS)	Sigma Life Science, MO, USA

Tris Buffer	Carl Roth, Karlsruhe
Tween 20	PanReac AppliChem, Darmstadt
UltraPure Destilled Water	Thermo Fisher Scientific, MA, USA
UltraPure RNase DNase free H_2O	Thermo Fisher Scientific, MA, USA
UltraPure TBE Buffer 10X	Invitrogen, MA, USA
Whatman Puradisc FP 30 mm Cellulose Acetate Syringe Filter, 0,45µm	Whatman, GE Healthcare Life Sciences

3.1.6 Buffers

Table 9: List of buffers

Product	Composition	Usage
5% BSA in TBS-T	2,5 g BSA 50 ml TBS-T	Blocking of nitrocellulose membrane
50X TAE	242g Tris 57mL acetic acid 100% 100mL EDTA (0.5M) 1L H_2O	DNA gel electrophoresis
Blot-Buffer	25 mM Tris 192 mM Glycin	Immunoblotting
RIPA Lysis Buffer	25mM Tris HCl pH 7,6 150mM NaCl 1% NP-40 1% Sodium deoxycholate 0,1% SDS	Cell lysis
TBS (pH 7,5)	10 mM Tris 150 mM NaCl	Washing of nitrocellulose membrane
TBS-T	TBS Tween20	Washing of nitrocellulose membrane

3.1.7 Kits

Table 10: List of kits

Kit	Usage	Supplier
DNeasy Blood & Tissue Kit	Extraction of genomic DNA	Qiagen, Hilden
Pierce™ BCA Protein Assay Kit	Determination of protein concentration	Thermo Fisher Scientific, MA, USA

3.1.8 Antibodies

Table 11: List of antibodies

Primary Antibody	Species	Supplier
Anti γH2A.x No. 9718	rabbit	Cell Signaling, MA, USA
Anti Actin MAB1501 clone 4	mouse	Merck Millipore, MA, USA
Anti BAK No. 6947	rabbit	Cell Signaling, MA, USA
Anti BAX No. 5023	rabbit	Cell Signaling, MA, USA
Anti Bcl-2 No. 05-729	mouse	Merck, Darmstadt
Anti Bcl-2 No. 3498	rabbit	Cell Signaling, MA, USA
Anti BCL-X_L No. 2764	rabbit	Cell Signaling, MA, USA
Anti cleaved caspase 3 No. 9661	rabbit	Cell Signaling, MA, USA
Anti GAPDH CB1001 6C5	mouse	Merck Millipore, MA, USA
Anti MCL-1 No. 4572	rabbit	Cell Signaling, MA, USA
Anti PARP No. 9542	rabbit	Cell Signaling, MA, USA
Anti PUMA No. 4976	rabbit	Cell Signaling, MA, USA

Secondary Antibody	Species	Supplier
IRDye 680LT Donkey anti-mouse	donkey	Li-Cor, Nebraska, USA
IRDye 800CW Donkey anti-rabbit	donkey	Li-Cor, Nebraska, USA

3.2 Methods

3.2.1 Cell culture

All cell culture work was carefully performed in laminar flow cabinets. Cells were incubated in a 37 °C humidified atmosphere containing 5% CO_2 and passaged according to the recommendations of DSMZ. For this, cells were centrifuged at 300 * g followed by one or more washing steps using PBS. After washing, cells were resuspended in their respective complete medium. Cell lines were cultivated in either RPMI (HL-60, MOLM-13, MOLM-16, KASUMI-1, NOMO-1, PL-21, ML-2), MEMα (OCI AML-2) or IMDM (SIG-M5) medium, each supplemented with 20% fetal bovine serum (FBS) and 1% penicillin-streptomycin (PS). Prior to use, FBS was heat inactivated for 30 minutes at 65°C.To avoid contamination and to monitor viability and growth, cells were frequently examined under a light microscope. For cryopreservation, 5x10^6 cells were resuspended in freezing medium containing 90% FBS and 10% dimethylsulfoxide (DMSO) and transferred into cryovials. Cells were frozen at 1°C/min in a -80°C freezer. All cells were checked for mycoplasma presence.

3.2.2 Generation of venetoclax-resistant (199R) cell lines

Parental AML cell lines were cultivated in the presence of low doses of venetoclax, starting at a concentration of 1nM. Using a light microscope, cells were thoroughly monitored in the process. As soon as treated cells showed similar growth rate and viability as the parental equivalent cultivated without the drug, doses of venetoclax were increased exponentially. All cell lines were eventually treated with a maintenance dose of 2µM of venetoclax. To ensure stable resistance and comparable results, cells were cultivated at the maintenance dose for several months, while simultaneously parental cells were cultivated without venetoclax.
In order to differentiate between parental and venetoclax-resistant cell line, parental cells were named *Cell Line* S, whereas cells with acquired resistance to venetoclax were named *Cell Line* 199R.

3.2.3 CellTiter-Glo® Luminescent Cell Viability Assay

CellTiter-Glo® Luminescent Cell Viability Assay (CTG) is a metabolic assay which determines the number of viable cells by measuring the amount of ATP present, utilizing the nucleotide as a marker for metabolically active and therefore viable cells. ATP is a necessary component to convert luciferin to oxyluciferin. Thereby, a luminescent signal is generated, which can be detected by a luminometer. In our case, FLUOstar OPTIMA microplate reader was used for readout of the luminescent signal. A high signal mirrors high amounts of ATP and therefore high numbers of viable cells.

1x10^5 cells in 100µL per well were plated out into a white Nunc 96 well plate, treated with different concentrations of inhibitor and incubated for 48 hours. After incubation, plates were left for about 15 minutes at room temperature to achieve temperature equilibration. CTG reagent was then used according to the supplier's protocol to measure cell viability. CellTiter-Glo® Luminescent cell viability assay was used in order to determine IC_{50} of venetoclax for each cell line, to validate resistance to venetoclax in 199R (199R) cell lines and to measure differences in cell viability between S and 199R cell lines when treated with cytarabine.

3.2.4 Flow Cytometry

In addition to CTG, flow cytometric measurement of Annexin V and 7AAD was employed to determine cell viability. Annexin V binds to phosphatidylserine, a molecule that, whenever a cell undergoes apoptosis, is flipped from the inner to the outer leaflet of the membrane, where it then can be detected by Annexin V, thereby functioning as an early apoptotic marker. 7-Aminoactinomycin (7-AAD) is a peptide which binds to DNA via intercalation between cytosine and guanine. Due to their disrupted membranes, 7-AAD can enter dead cells and thus serves as a marker for dead cells. Viable cells appear negative for both stains when measured via flow cytometry.

For our experiments using flow cytometric measurements, 1x10^5 cells in 100µL per well were plated out into a 96 well plate, treated with different concentrations of a variable compound and incubated for 24, 48 or 72 hours. After washing with PBS, cells were stained with 1% Annexin V and 7AAD in Annexin V Binding Buffer for 15-20 minutes while kept in a dark and cold place. After staining, cell viability was determined using fluorescent activated cell sorting (FACS).

3.2.5 Gel electrophoresis and Western Blotting

A maximum of 10^7 cells were used for Western Blotting analysis. After washing with PBS, a total amount of approximately 10-20µL per 1x10^6 cells RIPA lysis buffer containing protease and phosphatase inhibitors was added to the cell pellet. After incubating on ice for 30 minutes, the sample was centrifuged and the lysate-containing supernatant was obtained. Protein concentration was then assessed using Pierce™ BCA Protein Assay Kit according to the supplier's protocol. LDS sample buffer and sample reducing agent were added. The mixture was either stored at -20°C for future use, or heated at 70°C for 10 minutes for protein denaturation. For protein separation, 10-15 µL of the mixture were then applied to a 4-12% gradient polyacrylamide gel, which allows for protein segregation according to size via SDS-polyacrylamide gel electrophoresis. The gel was run in running buffer at 200 V for approximately 45-55 minutes, or until the migration front was at the bottom end of the gel. Following this, all protein was transferred from the polyacrylamide gel to a nitrocellulose

membrane via wet transfer in blot buffer at 180 V for 120 min. Once the transfer was finished, the membrane was blocked for one hour at room temperature using 5% BSA in TBS-T. After three washing steps with TBS-T, the membrane was incubated in TBS containing 0.1% Tween, 5% BSA and primary antibodies overnight at 4°C, then washed three times, and then incubated with secondaries antibody in a 1:1 mixture of either TBS or PBS, and Li-Cor Odyssey blocking buffer for one hour at room temperature. After three more washes, protein signal was detected using the Odyssey CLx Imaging System by Li-Cor. Hereafter, densitometric measurement in Image Studio Lite was performed to quantify the findings, followed by a normalization to the loading control.

3.2.6 CRISPR-Cas9 knockout

CRISPR-Cas9 is a relatively new technique of genome editing and can be utilized to modify the genome efficiently. This method exploits a natural defense mechanism of bacteria against viruses including CRISPR (clustered regularly interspaced short palindromic repeats) and the endonuclease Cas9 (CRISPR-associated protein 9). CRISPR are specific DNA sequences that represent parts of bacteriophagic DNA and have been incorporated into the cells own genome during previous viral infections. Upon reinfection with similar viruses, the corresponding viral DNA can easily be detected and then cut by Cas9. Based on this mechanism it is possible to cut, delete or even insert DNA sequences at a given location. In scientific research, the equivalent to the bacteria's CRISPR is called sgRNA (single guide RNA). The sgRNA guides Cas9 and allows cutting at the desired genomic sequence. This method is used to generate gene knockouts [221].

AML cell line OCI AML-2 was selected for genetic knockout of proapoptotic Bcl-2 family protein PUMA. Employing CRISPR-Cas9 to knock out *BBC3*, which encodes PUMA, we selected a 20-nt DNA sequence (Table 12) of the *BBC3* locus for the sgRNA using the public website CHOPCHOP [222].

Table 12: *BBC3* DNA sequence for CRISPR-Cas9

Sequence	Target Site
5'-CACCGGCACCGCCCCTCACCCTGGA-3'	Exon 4

PUMA/*BBC3* knockout was mainly performed by Olaf Merkel. For the generation of a plasmid vector containing all necessary genetic information, AddGene's lentiviral transfer plasmid lentiCRISPR v2 was used [223]. Apart from an sgRNA cassette for the respective oligonucleotide and a Cas9 cassette containing genetic information for the endonuclease, this lentiviral vector also contains selection genes which render cells resistant to various substances such as

ampicillin or puromycin. This facilitates selection of successfully transformed bacteria and transduced cells.

As a first step, the oligonucleotide (Table 12) was cloned into the sgRNA scaffold of the empty lentiviral vector with the aid of digesting enzyme *BsmBI.* The complete vector was then transformed into *Stbl3* bacteria, which were plated out onto ampicillin-containing plates. Due to the vector containing an ampicillin selection gene, only successfully transformed bacteria were able to survive and grow. After incubation overnight, the growing clones were selected and amplified. The construct was then analyzed to confirm successful cloning. Following this, bacteria were lysed and plasmid DNA was prepared. For the production of a high quantity of lentiviral particles, the lentiviral plasmid was co-transfected with a packaging and envelope plasmid into HEK293T cells. Viral harvest was performed three times every 24 hours. To infect OCI AML-2 cells, 10^7 cells were incubated in viral supernatant for 24 hours, washed and eventually cultured in regular medium. After four to five days, cells were selected using puromycin. Successful transduction and knockout were reviewed by immunoblotting for PUMA. Furthermore, single cell clones were established by serial dilution and checked regularly for the successful knockout by immunoblotting.

3.2.7 DNA isolation

Extraction of genomic DNA was performed using DNeasy Blood and Tissue Kit by Qiagen. For this purpose, 5x10^6 cells were used for DNA isolation, which was performed according to the supplier's protocol. DNA was then eluted in 100 µL UltraPure RNase/DNase free H_2O by Thermo Fisher. DNA quality and concentration were determined using the Nanodrop 1000 Spectrophotometer by Peqlab. Quantity and purity were examined by running the DNA on a 0.7% agarose gel. A final concentration of 50-100 ng/µL genomic DNA in at least 20 µL was used for sequencing analyses.

3.2.8 Whole exome sequencing

Whole exome sequencing (WES) is a genomic technique for high throughput analysis of protein-coding regions in the genome (exons). This method facilitates efficient identification of relevant genetic variants. WES detects the exact location of a mutation on DNA and protein level and the mutation type like single nucleotide mutation (SNM), which result in missense, nonsense or splice mutations, or short deletions and insertions, which can result in a frameshift. WES was carried out by Dr. Janine Altmüller, Cologne Center for Genomics. Data was analyzed by Prof. Dr. Martin Peifer, Department of Translational Genomics.

3.2.9 RNA isolation

Extraction of RNA was performed using peqGOLD TriFast by vwr according to the supplier's protocol. 5x10^6 cells were used for RNA isolation. As a final step, RNA was resuspended in 30 µL UltraPure RNase/DNase free H_2O by Thermo Fisher. Quality and concentration were again determined using the Nanodrop 1000 Spectrophotometer by Peqlab. Quantity and purity were examined by running the RNA on a 1.5% agarose gel. A final concentration of 50-200 ng/µL total RNA in a minimum of 10 µL volume was used for further analysis.

3.2.10 RNA sequencing

RNA sequencing is a genomic technique for high throughput analysis of RNA. It allows quantification of gene expression and provides an insight into posttranscriptional modification and the emergence of fusion genes. RNA seq is based on next generation sequencing (NGS), which is why RNA first must be translated into cDNA. RNA sequencing was performed by Dr. Janine Altmüller, Cologne Center for Genomics. Data analysis was conducted by Prerana Wagle, CECAD Bioinformatics Facility, University Hospital Cologne and Dr. Stuart Blakemore, AG Pallasch, CECAD/University Hospital Cologne.

3.2.11 Single cell RNA sequencing

Single cell RNA sequencing (scRNA-seq) marks one of the major advances of RNA sequencing. While conventional, "bulk" RNA sequencing analyzes RNA levels from large numbers of cells, this technique identifies RNA profiles of individual cells. Based on this, cells can by characterized regarding type and condition, which promotes better understanding of a cell's specific role in its individual context. Moreover, scRNA-seq provides insight into clonal evolution of subpopulations. Bone marrow samples were collected from two patients treated in the City of Hope Comprehensive Cancer Center in Duarte, CA, USA, under the direction of Vinod Pullarkat, MD. Samples were obtained just before venetoclax treatment started (pre-treatment) and after relapse (post-resistance). After samples were transferred to Cologne, they were sequenced by Dr. Janine Altmüller, Cologne Center for Genomics, pre-analyzed by Dr. Milos Nikolic, AG Peifer, Department of Translational Genomics and further analyzed by Dr. Stuart Blakemore, AG Pallasch, CECAD/University Hospital Cologne. A total of 10,000 cells were individually analyzed regarding gene expression level.

3.3 Software and statistics

Statistical analyses were performed using Microsoft Excel, GraphPad Prism 7 and RStudio. To determine the significance of difference between parental and resistant cell lines in cytotoxicity assays and Western Blots, GraphPad Prism was used. Due to the heterogeneity of cell lines after acquisition of venetoclax resistance, parental and resistant cell lines were regarded as independent samples. After testing for normal distribution through Shapiro-Wilks test, normally distributed data was further examined using independent samples t-test (cytotoxicity assays) or one sample t-test (protein expression ratio in Western Blots). Prior to an independent t-test, data was examined for equality of variance. In case of equal variances, independent samples t-test was used to determine significance. In case of unequal variances, an adjusted t-test (Welsh test) was used to determine significance. For non-normally distributed data, Mann-Whitney-U test was used. IC_{50} was determined via nonlinear regression algorithm in GraphPad Prism. Kaluza software (Beckman Coulter) was used for the analysis of flow cytometric data. For densitometric measurement and analysis of Western Blots, Image Studio Lite (Li-Cor) was used. RStudio and Microsoft PowerPoint were used for data visualization (ggplot2 package, H. Wickham, 2016).

4 Results

Part I: Generation of venetoclax-resistant (199R) AML cell lines

4.1 AML cell line characterization

Ten AML cell lines were selected from the German Collection of Microorganisms and Cell Cultures GmbH (DSMZ) as potential candidates for our study: OCI AML-2, HL-60, SIG-M5, MOLM-13, MOLM-16, KASUMI-1, NOMO-1, PL-21 and ML-2 and ME-1. The cell lines were then screened for venetoclax susceptibility and characterized regarding background and genetic profile.

4.1.1 Viability after venetoclax treatment

Initial response to venetoclax treatment was assessed in a dose-dependent manner.

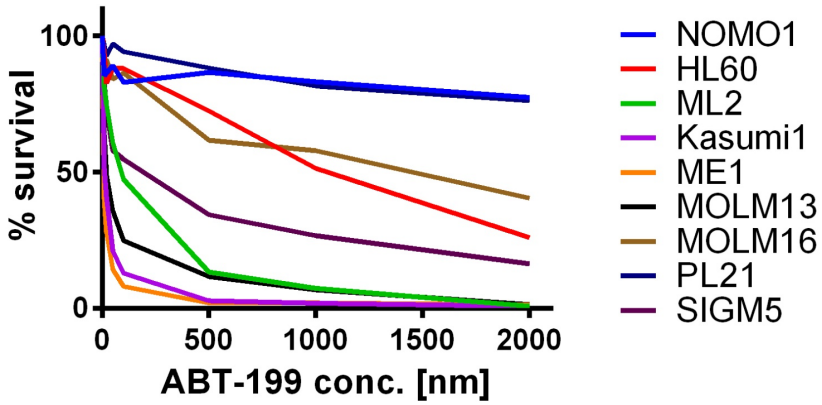

Figure 2: Sensitivity of AML cell lines to venetoclax

Nine out of ten cell lines were treated with different concentrations of venetoclax (ABT-199) for 48 h before read-out via CellTiter-Glo® Luminescent Cell Viability Assay. This experiment (n=1) was performed and analyzed by Dr. Laura Beckmann.

To obtain a large and heterogeneous set of cell lines representing acute myeloid leukemia, nine out of the ten initial cell lines were selected for additional experiments: OCI AML-2 (not shown in Figure 2), HL-60, SIG-M5, MOLM-13, MOLM-16, KASUMI-1, NOMO-1, PL-21, and ML-2. Cell line ME1 was not used as cells were too susceptible in order to establish a stable resistance towards venetoclax.

4.1.2 Cell line profile according to literature

Since immortalized cell lines are highly heterogeneous regarding heritage and genetics, Table 13 gives an overview of all the cell lines used in this study. It includes information about the initial patient who had donated cells for immortalization according to the Deutsche Sammlung von Mikroorganismen und Zellkulturen (DSMZ), as well as selected genetic characteristics like oncogenic mutations or chromosomal aberrations according to cBioPortal. Based on this information, cell lines were assigned to relevant AML classifications (WHO and ELN).

cBioPortal is an open-source platform that provides easily accessible cancer genomics data sets including cell line genomics [150]. From this data, a selection of the following genomic alterations is presented: relevant genetic mutations, copy number alterations (amplifications, deletions) and fusion genes. These sequencing results provide evidence of the many oncogenic mutations found in cancers including AML, such as *TP53, KRAS, BRAF, FLT3, DNMT3A, NRAS, PIK3CA, ASXL1, NOTCH1,* and *KIT* [14].

Oncogenic mutations and/or aberrations were reported for all cell lines. HL-60, KASUMI-1, MOLM-16, and NOMO-1 reportedly exhibited mutated *TP53* amongst many other mutations and were therefore assigned to the adverse risk category. Furthermore, *KMT2A* rearrangement was found in OCI AML-2, ML-2, and MOLM-13, which falls into the adverse or intermediate risk category, depending on the rearrangement. PL-21 was reported to contain mutated *ASXL1* and was therefore assigned to the adverse risk category as well. SIG-M5 did not harbor abnormalities classifiable as either favorable or adverse, and was thus allocated to the intermediate ELN risk category. Cell lines were established from a variety of primary patients aged seven to 77, either suffering from *de novo* AML (n=6) or secondary AML (n=3). In summary, although cell line heritage and genetic background varied a lot, most cell lines had an adverse genetic risk according to the literature.

Table 13: Genetic profile of each AML cell line based on literature

Cell Line	**DSMZ**	**cBioPortal**	**WHO classification**	**ELN risk stratification**
OCI AML-2	65 y/o, *MUT*: DNMT3A, retinoic acid receptor gene	*MUT:* SPEN, KMT2A, FLT3 *AMP:* MDM4, IKBKE, AKT3 *DEL:* TNFRSF14, ERRFI1, MSH2, MSH6 *FUSION:* KMT2A-MLLT4, MBNL1-RAF1	AML with defining genetic abnormalities: AML with *KMT2A* rearrangement	adverse: t(v;11q23.3)/*KMT2A*-rearranged
HL-60	35 y/o, *AMP:* MYC	*MUT:* CEBPA, TP53, NRAS, CDKN2A *AMP:* MYC *DEL:* TP53, CDKN2A, MAP3K1, PIK3R1, MSH3, APC	AML with defining genetic abnormalities: AML with *CEBPA* mutation	adverse: mutated *TP53*
SIG-M5	63 y/o, monocytic origin	*MUT:* BRAF; DNMT3A, KMT2D (2), TET (2) *AMP:* NOTCH1 *DEL:* AIRID5B	AML, defined by differentiation: Acute monocytic leukaemia	intermediate: abnormalities not classified as favorable or adverse
MOLM-16	77 y/o, relapse after failed chemo, former FAB M0	*MUT:* TP53 (2) *AMP:* JAK2, PDL1, PDL2 *DEL:* CREBBP, ARID3A, ERCC4	AML, defined by differentiation: AML without maturation	adverse: mutated *TP53*
KASUMI-1	7 y/o, 2nd relapse after stem cell transplantation, *FUSION:* t(8;21) = RUNX1-RUNX1T1, *MUT:* KIT	*MUT:* TP53, KIT *AMP:* PIK3CA, KIT *DEL:* TP53, CDKN2A, BRCA2, CREBBP *FUSION:* RUNX1-RUNX1T1, BRAF-SRPK2, ARID1B-WDR27	AML with defining genetic abnormalities: AML with *RUNX1::RUNX1T1* fusion	adverse: mutated *TP53*
NOMO-1	31 y/o, 2nd relapse, *FUSION:* t(9;11)(p22;q23) = KMT2A-MLLT3	*MUT:* CEBPA, ASXL1, TP53, KRAS *AMP:* RICTOR, CDK6 *DEL:* CDKN2A, CDKN2B, KMT2A *FUSION:* KMT2A-MLLT3	AML with defining genetic abnormalities: AML with *KMT2A* rearrangement	adverse: mutated *TP53*
MOLM-13	20 y/o, relapse after initial MDS, *MUT:* FLT3 ITD, CBL	*MUT:* BCBL, MLH1, ARID4B, PML *AMP:* PIK3CA, MYC, FGFR1 *DEL:* CDKN2A, CDKN2B, KMT2A *FUSION:* KMT2A-MLLT3	AML with defining genetic abnormalities: AML, myelodysplasia-related	intermediate: t(9;11)(p21.3;q23.3)/ *MLLT3::KMT2A*
PL-21	24 y/o, refractory APL after granulocytic sarcoma, no *PML::RARA* fusion, but monocytic origin, *MUT:* FLT3 ITD	*MUT:* ASXL1, KRAS, MYC *AMP:* RAF1, PML *DEL:* GATA3	AML, defined by differentiation: Acute monocytic leukaemia	adverse: mutated *ASXL1*
ML-2	26 y/o, after T-NHL and T-ALL, *FUSION:* t(6;11)(q27;q23) = KMT2A-AFDN	*MUT:* KRAS, NOTCH1, CREBBP	AML with defining genetic abnormalities: AML with *KMT2A* rearrangement	adverse: t(v;11q23.3)/*KMT2A*-rearranged

4.2 Validation of acquired venetoclax resistance

As described in Chapter 3.2.2, each parental AML cell line was divided into two groups. Parental cells (*Cell Line* – S) were cultivated according to the DSMZ instructions, while prospective venetoclax-resistant cells (*Cell Line* – 199R) were continuously exposed to increasing doses of venetoclax and eventually kept at a maintenance dose for several months. As all additional experiments relied on the generation of stable resistance to venetoclax, we then verified induced resistance to high doses of venetoclax (>5 µM) using the following methods.

4.2.1 Measurement of cell viability

To assess sensitivity of parental and 199R cells to venetoclax in a dose-dependent fashion, cell viability assays were performed using CTG (Figure 3). While venetoclax had a strong effect on most parental cell lines, some showed no decreased viability after treatment. Depending on the absolute half maximal inhibitory concentration (IC_{50}), parental cell lines were divided into three categories: High susceptibility, low susceptibility, and no susceptibility/ intrinsic resistance to venetoclax (Table 14). Especially OCI AML-2, KASUMI-1 and MOLM-13 showed low cell survival even at low doses (<100 nM). On the contrary, MOLM-16 and NOMO-1 were the only cell lines not affected by venetoclax treatment, even at high doses. No 199R cell line showed impaired survival after venetoclax treatment. The difference in viability was significant for all cell lines except MOLM-16 and NOMO-1.

Cell Line	IC_{50} S (nM)	IC_{50} 199R (nM)
MOLM-13	25,76	>5000
KASUMI-1	44,7	>5000
OCI AML-2	86,52	>5000
ML-2	198,9	>5000
HL-60	2698	>5000
SIGM-5	3920	>5000
PL21	~5000	>5000
MOLM-16	>5000	>5000
NOMO-1	>5000	>5000

Table 14: IC_{50} values for venetoclax in S and 199R AML cell lines

Cell lines are ordered by the parental cells' IC_{50}. Parental cell lines highlighted in green show high susceptibility to venetoclax treatment (IC_{50} S <200nM). Parental cells color-coded in yellow and orange are less susceptible to venetoclax, but can still be targeted with higher doses (IC_{50} S <5000nM). Parental cells highlighted in red show primary/intrinsic resistance to venetoclax as an IC_{50} could not be determined in our experimental setup. For all 199R cell lines in red, no IC_{50} was achieved.

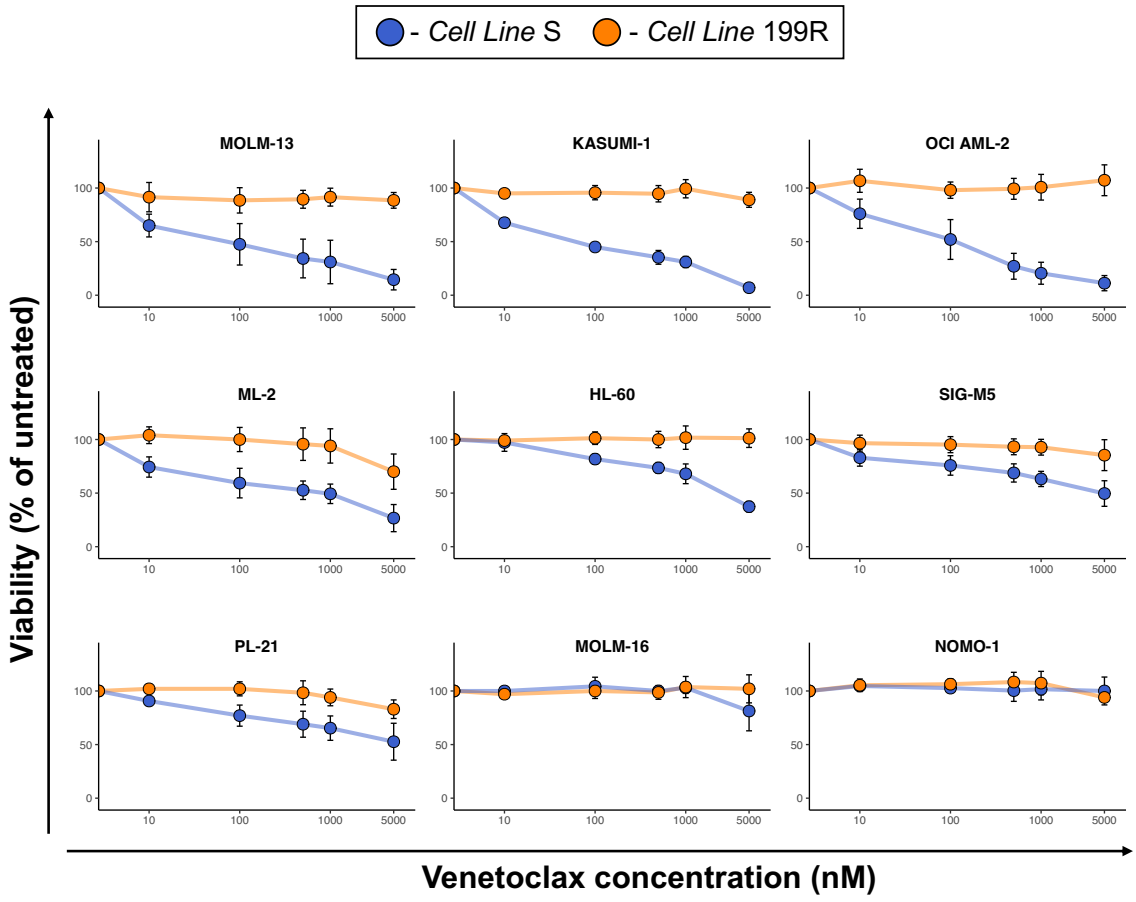

Figure 3: Cell viability of AML cell lines S and 199R treated with venetoclax

Experimental setup: In a 96-well plate, 1x10^5 cells per well were incubated in 100 µL medium containing 0, 10, 100, 500, 1000 and 5000 nM venetoclax. Plates were incubated for 48 h before read-out via CellTiter-Glo® Luminescent Cell Viability Assay. DMSO was used as a vehicle control. Results show mean and standard deviation of three to four independent experiments.

4.2.2 Detection of cell death markers

In a next step, we intended to validate venetoclax resistance with a different method and gain further insight into cellular mechanisms underlying the resistance. We selected AML cell lines OCI AML-2 and HL-60 and performed immunoblot analysis of proteins related to cell death. Cleavage of PARP, cleavage of caspase 3 and expression of γH2A.x was examined to check whether cells were undergoing apoptosis upon venetoclax treatment (Figure 4).

Induction of PARP cleavage, caspase 3 cleavage and expression of γH2A.x was observed in OCI AML-2 and HL-60 S after four hours of venetoclax treatment. On the contrary, neither definite cleavage of PARP and caspase 3, nor expression of γH2A.x was found in OCI AML-2 and HL-60 199R treated with venetoclax. Hence, venetoclax induced apoptosis in parental cells only.

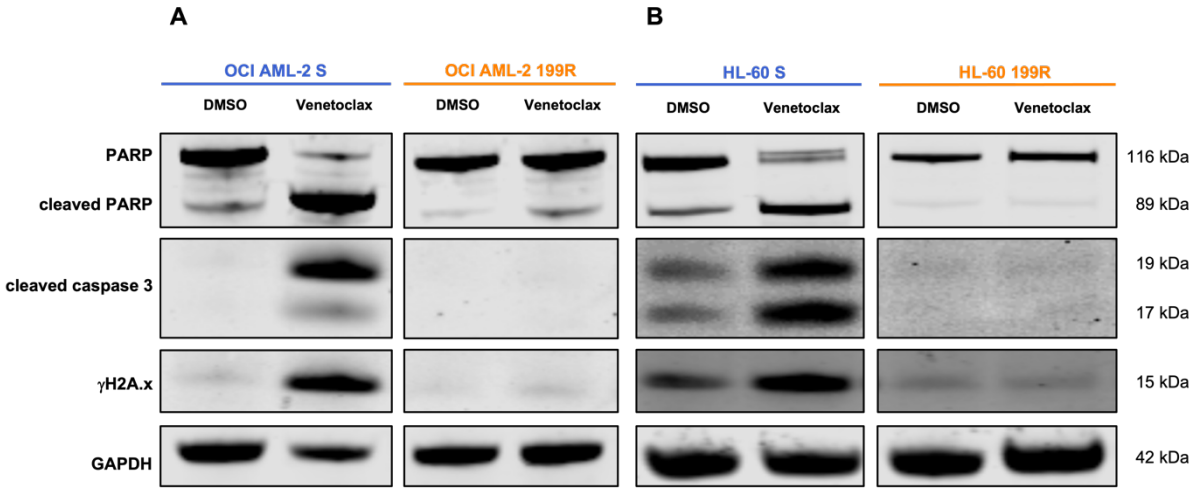

Figure 4: Western Blot analysis of cell death related proteins after venetoclax treatment

A: OCI AML-2 S and OCI AML-2 199R treated with venetoclax. **B:** HL-60 S and HL-60 199R treated with venetoclax. Experimental setup: 3x10^6 cells were incubated with 2 µM venetoclax and DMSO as a vehicle control for 4 h. GAPDH was used as loading control. This Western Blot is representative for three independent experiments.

Part II: Characterization of 199R cell lines on DNA, RNA and protein level

4.3 Analysis of genetic aberrations in 199R cell lines

A common cause for the selection and growth of treatment-refractory cancer cells is the emergence of genetic mutations.

To investigate the altered genetic profile of 199R AML cell lines, whole exome sequencing (WES) was performed on parental and resistant cell lines. We thereby aimed to pinpoint possible resistance-inducing mutations, e.g., via oncogenic signaling or deregulation of mitochondrial apoptosis. WES was performed by Dr. Janine Altmüller, Cologne Center for Genomics. WES results were analysed by Prof. Dr. Martin Peifer, Department of Translational Genomics, University of Cologne.

4.3.1 Newly acquired mutations

First, newly acquired genetic mutations (Δ mutations) that only occurred in 199R cell lines, but not in the respective parental counterparts, were analyzed. Table 15 shows the number of Δ mutations for each cell line. AML cell line HL-60 acquired the most mutations (168), while MOLM-16 acquired the fewest (22).

Table 15: Number of Δ mutations for each AML cell line

Cell Line	MOLM-13	KASUMI-1	OCI AML-2	ML-2	HL-60	SIG-M5	PL-21	MOLM-16	NOMO-1
No. of Δ mut. (without silent mut.)	47 (36)	45 (40)	110 (84)	51 (40)	168 (112)	67 (45)	28 (22)	22 (19)	51 (43)

In the following, all silent mutations were excluded from our analysis.

Recent studies have put increasing emphasis on the Allelic Fraction (AF), also called “mutation dose”, which is the number of mutation reads divided by total read number. It allows for a rough estimate of the cell proportion carrying the mutation. Therefore, it can be used to track driver genes and evolving clones within a tumor [224,225]. For our data, a cutoff of 0.2 AF (20%) was set in order to filter for relevant mutations that were present in a larger proportion of cells. Table 16 lists all newly acquired mutations with an AF ≥0.2 in 199R cell lines.

Table 16: Genes containing newly acquired mutations with an Allelic Fraction ≥ 0,2 for each cell line

One table for each respective cell line containing gene name (according to HUGO), chromosome number, mutation type (missense, nonsense, splice, frameshift, deletion, insertion), change within DNA, change within protein and allelic fraction of 199R cell lines. Color-coding is according to parental performance upon venetoclax treatment (IC_{50} S, see Table 14).

MOLM-13

Gene	Chr.	Type	change DNA	change protein	AF 199R
VPS50	7	splice	c.540_splice	e7+2	0.5
PRLHR	10	missense	c.367G>A	p.E123K	0.490463
LDB2	14	missense	c.196A>G	p.T66A	0.47541
SOWAHA	5	in_frame_ins	c.9_10insGCCGCCGCC	p.L3_A4insAAA	0.473684
IGFN1	1	missense	c.10381C>A	p.L3461I	0.472924
CLSTN3	12	missense	c.2100G>C	p.E700D	0.464286
ACTA1	1	missense	c.779C>A	p.P260Q	0.44
ZGPAT	20	missense	c.350G>T	p.G117V	0.427273
UBR4	1	frame_shift_del	c.11426delA	p.N3809fs	0.407895
MUC19	12	missense	c.10141G>T	p.A3381S	0.399445
ACOT4	14	missense	c.356T>C	p.L119P	0.398876
HNRNPH3	10	missense	c.201G>T	p.K67N	0.396226
LAMB3	1	missense	c.1792C>T	p.R598C	0.391753
PCDH10	4	missense	c.2633C>A	p.T878N	0.377778
C3orf14	3	missense	c.149C>A	p.A50D	0.357143
PPL	16	missense	c.568C>A	p.Q190K	0.325444
ARHGAP29	1	missense	c.1262G>T	p.C421F	0.323529
ZNF699	19	missense	c.1456C>T	p.R486C	0.291209
OR5V1	6	missense	c.831G>T	p.L277F	0.265537
ZNF99	19	missense	c.126C>A	p.F42L	0.222222
ZNF85	19	nonsense	c.103G>T	p.E35*	0.221154

KASUMI-1

Gene	Chr.	Type	change DNA	change protein	AF 199R
IQCA1	2	missense	c.1498G>T	p.D500Y	0.825
MAGEB6	X	missense	c.564G>T	p.K188N	0.811189
ZFR	5	missense	c.2810C>T	p.P937L	0.44086
ATXN7L2	1	missense	c.1913C>T	p.T638I	0.436782
SLFN5	17	nonsense	c.895G>T	p.E299*	0.417526
CCT8L2	22	missense	c.277G>T	p.A93S	0.416185
FAM50B	6	missense	c.837C>A	p.D279E	0.395034
MASP1	3	missense	c.1814T>C	p.I605T	0.390558
PTPRZ1	7	missense	c.5830A>G	p.I1944V	0.390244
MOV10	1	missense	c.368G>A	p.G123D	0.384615
NPAS4	11	missense	c.98C>A	p.A33D	0.373134
MTDH	8	missense	c.1606G>C	p.V536L	0.368421
TBX15	1	missense	c.580C>T	p.P194S	0.356436
NCK2	2	missense	c.623C>T	p.S208L	0.353383
FGF20	8	missense	c.565C>A	p.H189N	0.347561
STXBP2	19	nonsense	c.1736C>G	p.S579*	0.333333
LRIG3	12	missense	c.2262T>G	p.I754M	0.318996
TBX5	12	missense	c.1226G>T	p.S409I	0.29661
ATG16L2	11	missense	c.685G>T	p.A229S	0.267606
ANXA7	10	missense	c.280G>A	p.G94R	0.238636
BCAS3	17	missense	c.584G>A	p.R195Q	0.238636

ML-2

Gene	Chr.	Type	change DNA	change protein	AF 199R
ATP13A2	1	missense	c.538C>A	p.Q180K	0.386364
AQP10	1	missense	c.755G>A	p.G252E	0.254902
ZNF202	11	missense	c.466C>G	p.P156A	0.252174
CDH11	16	nonsense	c.1912G>T	p.E638*	0.236364
COL5A1	9	missense	c.1601C>A	p.S534Y	0.234568
FSTL5	4	missense	c.1061C>A	p.P354H	0.225806
LRP1B	2	missense	c.1862G>A	p.R621K	0.202381

OCI AML-2

Gene	Chr.	Type	change DNA	change protein	AF 199R
NRXN3	14	missense	c.4575G>T	p.E1525D	1
CDH19	18	splice	c.196_splice	e3-3	1
TP53	17	missense	c.659A>G	p.Y220C	0.988636
ACOXL	2	missense	c.537G>T	p.M179I	0.6
QTRT2	3	splice	c.16_splice	e2-1	0.588235
ZFP28	19	missense	c.34C>T	p.P12S	0.571429
TBX2	17	nonsense	c.1541C>A	p.S514*	0.549296
EIF2AK3	2	missense	c.2426A>T	p.E809V	0.537736
CAGE1	6	nonsense	c.1960A>T	p.K654*	0.535714
SMG8	17	nonsense	c.808C>T	p.Q270*	0.527473
CELSR2	1	missense	c.8743G>A	p.E2915K	0.524823
RAB18	10	missense	c.431T>C	p.I144T	0.522388
TGFBR2	3	missense	c.1666G>T	p.A556S	0.520124
KCNG4	16	missense	c.980C>A	p.S327Y	0.507003
CFD	19	missense	c.743T>A	p.V248E	0.502008
TFCP2	12	missense	c.907C>T	p.L303F	0.5
CREBBP	16	splice	c.5172_splice	e31+1	0.5
TTN	2	missense	c.33664G>T	p.V11222L	0.492537
HECW2	2	missense	c.4365A>T	p.E1455D	0.491228
MAP2K4	17	missense	c.1205C>T	p.T402I	0.491071
RHPN1	8	missense	c.673A>G	p.T225A	0.490476
OR6C65	12	missense	c.667A>G	p.I223V	0.488
SPPL2B	19	missense	c.1301T>C	p.F434S	0.486486
CER1	9	missense	c.395A>G	p.K132R	0.484979
LTBP3	11	nonsense	c.3631G>T	p.E1211*	0.484127
DPY19L2	12	missense	c.1945C>A	p.L649M	0.483871
ZNF841	19	nonsense	c.1143C>A	p.C381*	0.480392
MUC17	7	missense	c.6926C>A	p.P2309H	0.475806
40422	2	nonsense	c.1498A>T	p.K500*	0.473684
TPSB2	16	missense	c.788A>G	p.Y263C	0.473684
KANK1	9	missense	c.2957A>G	p.D986G	0.471338
MADD	11	missense	c.573G>C	p.E191D	0.470356
TMEM176A	7	nonsense	c.644G>A	p.W215*	0.464174
OR10G8	11	frame_shift_del	c.163_169delACCACCA	p.T55fs	0.463415
ANTXRL	10	missense	c.336G>A	p.M112I	0.463303
RREB1	6	missense	c.3216C>G	p.I1072M	0.459227
GABRG3	15	missense	c.270G>C	p.M90I	0.457143
DUSP12	1	missense	c.544T>A	p.Y182N	0.451923
BARHL2	1	frame_shift_del	c.428delT	p.L143fs	0.45
NUTM2G	9	missense	c.1636G>A	p.G546R	0.448029
PCDHGA6	5	missense	c.2429G>C	p.S810T	0.433824
CH25H	10	missense	c.2T>C	p.M1T	0.428571
ATOX1	5	missense	c.136C>G	p.H46D	0.423256
HNRNPH3	10	missense	c.580G>A	p.G194S	0.420213
SIK1	21	missense	c.424G>A	p.D142N	0.417722
POLD1	19	splice	c.202_splice	e1+2	0.416667
HYDIN	16	missense	c.949C>G	p.R317G	0.40625
PALMD	1	missense	c.791A>C	p.N264T	0.401869
ACAD11	3	missense	c.299C>A	p.P100H	0.4
RUVBL2	19	missense	c.817C>T	p.R273C	0.396476
MSI2	17	missense	c.79G>A	p.G27R	0.386364
SLC16A9	10	missense	c.334G>T	p.V112F	0.384615
ITGAV	2	missense	c.2075C>T	p.A692V	0.382022
ADCY9	16	missense	c.3G>T	p.M1I	0.37931
NUDT9	4	missense	c.655C>T	p.P219S	0.375
FNDC1	6	missense	c.523G>A	p.V175I	0.353414
PKHD1	6	missense	c.4882C>A	p.P1628T	0.345646
SLC2A12	6	nonsense	c.456T>A	p.C152*	0.338462
SLC2A12	6	missense	c.1459C>A	p.L487I	0.328
PLCH1	3	nonsense	c.4099G>T	p.E1367*	0.325103
CDC42BPA	1	missense	c.4768G>A	p.E1590K	0.310484
SLC26A9	1	frame_shift_ins	c.1025_1026insT	p.I342fs	0.310174
NRROS	3	missense	c.1651T>C	p.F551L	0.309524
PCYT1A	3	missense	c.58G>A	p.G20R	0.302326
ENPP2	8	splice	c.972_splice	e12+1	0.3
OR11H2	14	missense	c.74A>C	p.N25T	0.3

HL-60

Gene	Chr.	Type	change DNA	change protein	AF 199R
UTP15	5	missense	c.1160T>C	p.I387T	0.787879
OR51A2	11	missense	c.221G>T	p.G74V	0.628571
ARSH	X	missense	c.1003G>T	p.V335F	0.586207
ZNF544	19	missense	c.923C>T	p.S308F	0.484375
SCAF1	19	missense	c.694C>T	p.H232Y	0.401316
SACS	13	missense	c.254G>A	p.G85E	0.4
PEX19	1	missense	c.337G>A	p.G113R	0.394366
SYTL4	X	missense	c.1651G>T	p.V551F	0.384615
CEP350	1	missense	c.3379G>A	p.E1127K	0.367347
RNF213	17	missense	c.14090C>T	p.P4697L	0.358209
NAV3	12	missense	c.494G>T	p.R165I	0.340426
MYPN	10	missense	c.1657C>A	p.L553M	0.31875
PDE10A	6	missense	c.1142C>A	p.P381H	0.311828
ALS2	2	missense	c.4495C>T	p.R1499C	0.302632
PLEKHG3	14	nonsense	c.1231G>T	p.E411*	0.302521
KLHL14	18	missense	c.535G>A	p.D179N	0.301339
GRIN2B	12	missense	c.1559C>T	p.S520L	0.294521
CNTNAP2	7	missense	c.439C>T	p.R147W	0.294118
OR52A1	11	missense	c.14A>G	p.N5S	0.288732
ASTN2	9	nonsense	c.1932C>A	p.Y644*	0.288194
SFRP4	7	frame_shift_del	c.162delC	p.A54fs	0.283951
ZFP90	16	missense	c.916G>A	p.G306R	0.283688
CACHD1	1	missense	c.2182G>A	p.V728I	0.282828
FCRL3	1	splice	c.1811_splice	e11-3_-4	0.28135
USH2A	1	missense	c.1247C>T	p.A416V	0.28125
SPATA31C2	9	missense	c.731C>A	p.S244Y	0.279793
NOB1	16	missense	c.380G>T	p.G127V	0.278689
TLR5	1	missense	c.466C>A	p.Q156K	0.266667
MYH15	3	missense	c.4472C>A	p.T1491K	0.26601
GRN	17	missense	c.151A>G	p.T51A	0.264822
PIGB	15	frame_shift_ins	c.1027_1028insT	p.V343fs	0.263158
OR2A12	7	missense	c.422C>A	p.T141N	0.257669
SDF4	1	missense	c.1015C>T	p.P339S	0.251748
SYN2	3	missense	c.332G>C	p.R111T	0.25
ANO6	12	missense	c.1792G>A	p.V598I	0.25
U2SURP	3	frame_shift_ins	c.2870_2871insAGAA	p.S957fs	0.25
LRGUK	7	missense	c.140G>T	p.G47V	0.247525
DPCR1	6	missense	c.3025G>T	p.A1009S	0.240741
KIF2C	1	missense	c.1367G>A	p.R456K	0.239617
SPOCD1	1	missense	c.2418C>A	p.F806L	0.238596
DNAJC6	1	missense	c.382T>C	p.S128P	0.236842
FBLN1	22	missense	c.115G>T	p.D39Y	0.236364
SSUH2	3	missense	c.686G>C	p.C229S	0.232673
RNASEH1	2	missense	c.49C>T	p.P17S	0.229885
ADGRB3	6	missense	c.3020A>G	p.Y1007C	0.22807
RGS13	1	missense	c.347C>A	p.P116H	0.227273
KRT7	12	missense	c.643G>A	p.V215M	0.226994
COL8A2	1	missense	c.1865T>A	p.F622Y	0.226481
DSP	6	splice	c.2298_splice	e17-2	0.226087
MRI1	19	missense	c.745C>T	p.R249C	0.224189
WDPCP	2	splice	c.634_splice	e10-1	0.222222
ABCA12	2	missense	c.1746G>C	p.K582N	0.219512
TUBB4A	19	missense	c.1459G>A	p.E487K	0.211429
ZNF177	19	missense	c.832C>T	p.H278Y	0.208333
MAP2	2	missense	c.4466C>A	p.P1489H	0.207317
MAGI1	3	missense	c.895_896delinsAA	p.L299K	0.206558
HIST1H4J	6	missense	c.208G>A	p.A70T	0.204255
HECW2	2	missense	c.1092C>G	p.S364R	0.2

SIG-M5

Gene	Chr.	Type	change DNA	change protein	AF 199R
LEPR	1	missense	c.1099G>T	p.V367F	0.363636
SLC35E1	19	missense	c.973G>A	p.A325T	0.344
PTGFR	1	missense	c.563A>G	p.Y188C	0.328
FBN3	19	splice	c.541_splice	e6+2	0.326241
FADS1	11	missense	c.178C>A	p.P60T	0.326087
SEL1L2	20	missense	c.1028T>A	p.M343K	0.308642
FRMD6	14	missense	c.670G>T	p.V224F	0.303279
ZBBX	3	frame_shift_del	c.1692delC	p.S564fs	0.296296
NCAPD3	11	splice	c.3868_splice	e31-3	0.285714
PCSK5	9	frame_shift_del	c.5339delA	p.E1780fs	0.282353
OPRD1	1	missense	c.964G>C	p.D322H	0.277108
PHLPP2	16	missense	c.935G>T	p.G312V	0.268657
TRIM61	4	missense	c.218G>A	p.S73N	0.265823
OR2F2	7	missense	c.398C>T	p.S133L	0.262009
TRAK1	3	missense	c.843A>C	p.Q281H	0.260274
ZBTB22	6	missense	c.1692G>T	p.E564D	0.245935
FSIP2	2	missense	c.5818T>G	p.F1940V	0.237113
LRRN3	7	missense	c.577C>G	p.L193V	0.227273
ABCA13	7	missense	c.5276_5277delinsTG	p.G1759V	0.224371
GRM1	6	missense	c.3489C>G	p.S1163R	0.217742
IGF2BP1	17	missense	c.68C>A	p.A23E	0.204124
VIP	6	nonsense	c.446C>A	p.S149*	0.2

PL-21

Gene	Chr.	Type	change DNA	change protein	AF 199R
ARMCX3	X	missense	c.223T>C	p.W75R	0.476923
CSPG4	15	nonsense	c.4266G>A	p.W1422*	0.4375
VCL	10	nonsense	c.2179G>T	p.E727*	0.320442
ARHGEF17	11	nonsense	c.2623G>T	p.E875*	0.310345
FSIP2	2	missense	c.3557C>A	p.S1186Y	0.301587
MUC16	19	nonsense	c.36120C>A	p.Y12040*	0.290323
BROX	1	missense	c.1208A>C	p.Q403P	0.285714
KMT2D	12	missense	c.8G>T	p.S3I	0.270073
GALK1	17	missense	c.40G>T	p.A14S	0.262295
SRRM2	16	missense	c.1850C>A	p.S617Y	0.257545
ZNF577	19	missense	c.827G>T	p.G276V	0.247788
COL9A3	20	missense	c.1423G>T	p.G475C	0.236364
TRIM42	3	nonsense	c.1007C>A	p.S336*	0.222798
TMEM150B	19	splice	c.197_splice	e5-3	0.220149
NISCH	3	missense	c.2976C>A	p.F992L	0.216129

MOLM-16

Gene	Chr.	Type	change DNA	change protein	AF 199R
ZNF462	9	frame_shift_del	c.7295_7296delAT	p.H2432fs	0.352941
TSNARE1	8	missense	c.1115A>T	p.Q372L	0.325
EXD3	9	missense	c.1984C>T	p.R662C	0.290698
DCHS1	11	missense	c.326G>A	p.R109H	0.272727
URGCP	7	missense	c.1880A>G	p.E627G	0.271605
CHST6	16	missense	c.614G>A	p.R205Q	0.269076
ALKBH8	11	missense	c.1762A>T	p.T588S	0.261468
BPIFB2	20	missense	c.1190T>G	p.I397S	0.221106
PRPF6	20	missense	c.2005C>T	p.R669W	0.211921
CD44	11	missense	c.1967C>A	p.S656Y	0.208861
MYH1	17	missense	c.1326G>C	p.M442I	0.201258

NOMO-1

Gene	Chr.	Type	change DNA	change protein	AF 199R
NUP50	22	missense	c.520C>A	p.H174N	0.537313
INPP5F	10	missense	c.601C>A	p.L201I	0.494505
INSC	11	missense	c.499G>A	p.E167K	0.46087
TTN	2	missense	c.11212G>A	p.D3738N	0.445946
GDAP2	1	missense	c.953A>C	p.N318T	0.42953
NSD1	5	missense	c.2275T>C	p.S759P	0.407407
EPPK1	8	missense	c.1193A>T	p.Q398L	0.392523
SOX9	17	missense	c.696G>T	p.Q232H	0.325714
SCN7A	2	missense	c.4690C>G	p.L1564V	0.315068
GPLD1	6	missense	c.2334G>T	p.W778C	0.314286
EPHA7	6	missense	c.2756C>T	p.T919I	0.269841
ITM2B	13	missense	c.238G>A	p.A80T	0.205882

To get a general idea about the carcinogenic nature of the newly acquired mutations, we compared all Δ mutations with an AF ≥0.2 with a dataset containing genes involved in the hallmarks of cancer [226]. These hallmarks describe biological capabilities and processes, which are acquired during tumorigenesis and tumor growth. Hanahan and Weinberg originally established six hallmarks, and since updated the concept to ten hallmarks, which are displayed in Figure 5 [133,227]. Most mutations were found in genes which are associated with the hallmarks "activating invasion and metastasis", "sustaining proliferative signaling" and "resisting cell death" (21, 19 and 16, respectively).

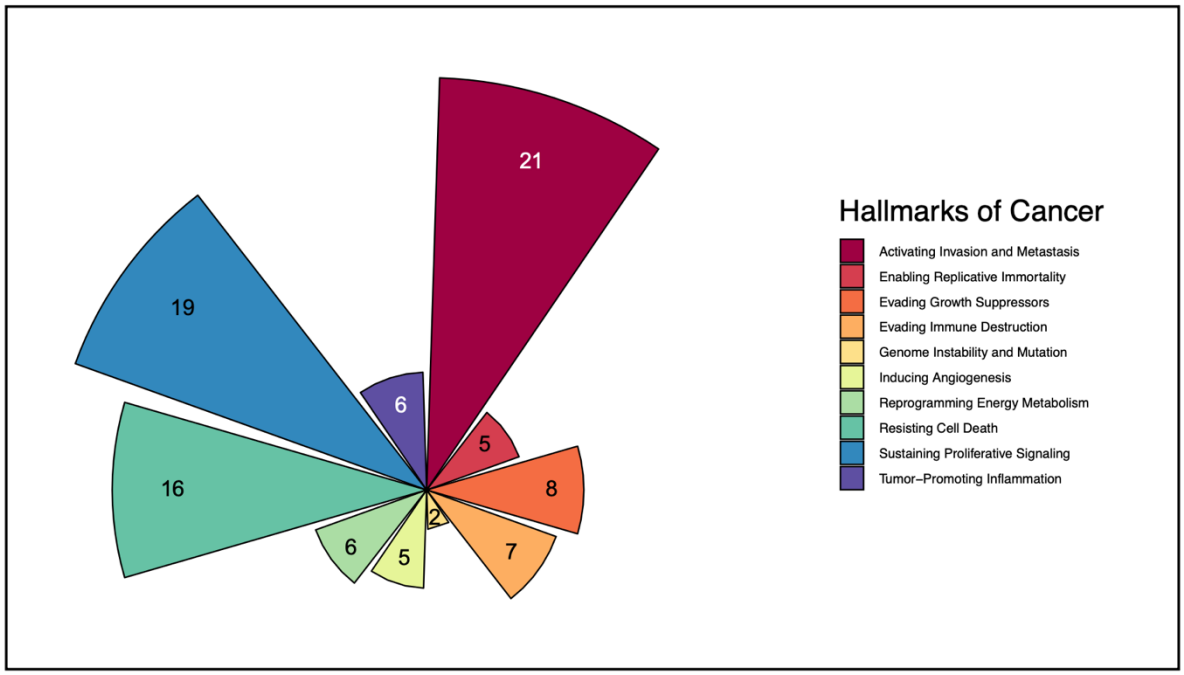

Figure 5: Δ mutations found in hallmarks of cancers genes

Analysis of all mutations with an AF >0.2 which occurred in venetoclax resistant cell lines, but not in parental cell lines.

Lastly, we examined Δ mutations of genes that were recurrently mutated following venetoclax resistance across all cell lines. More specifically, these included genes with at least two mutations across cell lines. In total, 13 genes were found as summarized in Table 17. Two genes were mutated in three 199R cell lines: *TTN* and *MUC16* (in OCI AML-2, HL-60, NOMO-1 and SIG-M5, PL-21, ML-2, respectively). The *USH2A* gene acquired two mutations within 199R cell line HL-60 and another mutation in SIG-M5 199R. The remaining ten genes were found to be mutated in two cell lines.

Table 17: Recurrently mutated genes with ≥2 Δ mutations across all 199R cell lines

The table contains gene name (according to the human genome organization HUGO), cell line acquiring the mutation, chromosome number, mutation type (missense, nonsense, splice, frameshift, deletion, insertion), change within DNA, change within protein and allelic fraction.

Cell Line	Gene	Chr.	Type	change DNA	change Protein	Allelic Fraction
OCI AML-2	**TTN**	2	missense	c.33664G>T	p.V11222L	0.492537
HL-60				c.46059G>T	p.K15353N	0.0397351
NOMO-1				c.11212G>A	p.D3738N	0.445946
SIG-M5	**MUC16**	19	nonsense	c.8920G>T	p.E2974*	0.0707395
PL-21			nonsense	c.36120C>A	p.Y12040*	0.290323
ML-2			missense	c.8239G>T	p.A2747S	0.0803571
HL-60	**USH2A**	1	missense	c.6943G>T	p.A2315S	0.0568182
				c.1247C>T	p.A416V	0.28125
SIG-M5				c.3759A>T	p.K1253N	0.0257235
OCI AML-2	**HECW2**	2	missense	c.4365A>T	p.E1455D	0.491228
HL-60				c.1092C>G	p.S364R	0.2
OCI AML-2	**HNRNPH3**	10	missense	c.580G>A	p.G194S	0.420213
MOLM-13				c.201G>T	p.K67N	0.396226
OCI AML-2	**DNAH9**	17	missense	c.1002G>T	p.Q334H	0.0263158
NOMO-1				c.12374G>T	p.R4125I	0.0869565
HL-60	**FLG2**	1	missense	c.7043G>T	p.S2348I	0.0882658
NOMO-1				c.5340T>A	p.H1780Q	0.0897571
SIG-M5	**FSIP2**	2	missense	c.5818T>G	p.F1940V	0.237113
PL-21				c.3557C>A	p.S1186Y	0.301587
HL-60	**NHSL1**	6	missense	c.643G>T	p.D215Y	0.0697674
PL-21				c.4193C>G	p.P1398R	0.116505
HL-60	**ASTN2**	9	nonsense	c.1932C>A	p.Y644*	0.288194
KASUMI-1			missense	c.2782G>C	p.E928Q	0.0452675
HL-60	**COL5A1**	9	missense	c.715C>A	p.H239N	0.198529
ML-2				c.1601C>A	p.S534Y	0.234568
HL-60	**KLHL1**	13	missense	c.394G>T	p.G132C	0.0292135
ML-2				c.464C>T	p.S155F	0.0330789
ML-2	**PTPRZ1**	7	missense	c.2563C>A	p.P855T	0.146067
KASUMI-1				c.5830A>G	p.I1944V	0.390244

4.3.2 Enriched mutations (AF ≥ 0.2)

Next, we examined genetic mutations which already existed in parental cells but were present in a larger AF in 199R cells (enriched mutations). Table 18 lists all enriched mutations with an AF enrichment ≥0.2 in 199R cell lines.

Table 18: Gene mutations with an Allelic Fraction enrichment ≥ 0.2 from S to 199R for each cell line

One table for each respective cell line containing gene name (according to HUGO), chromosome number, mutation type (missense, nonsense, splice, frameshift, deletion, insertion), change within DNA, change within protein and allelic fraction. Color-coding is according to parental performance upon venetoclax treatment (IC_{50} S, see Table 14).

MOLM-13

Gene	Chr.	Type	change DNA	change Protein	AF enrichment
ZNF107	7	nonsense	c.1117G>T	p.E373*	0,505882
FLG	1	missense	c.2509G>A	p.G837S	0,427687
HRNR	1	missense	c.2528G>A	p.R843Q	0,417771
SCN2A	2	missense	c.1571G>A	p.R524Q	0,286325
HRNR	1	missense	c.7537G>A	p.G2513S	0,211463
KIF7	15	missense	c.2364G>C	p.R788S	0,204866
SH3D19	4	missense	c.1394A>G	p.H465R	0,201705
EML4	2	missense	c.1319G>A	p.G440D	0,2

KASUMI-1

Gene	Chr.	Type	change DNA	change Protein	AF enrichment
LOXHD1	18	missense	c.6290T>C	p.I2097T	0,348073
C18orf63	18	nonsense	c.1393C>T	p.Q465*	0,32163
ZNF236	18	missense	c.4006A>G	p.I1336V	0,315982
CEP104	1	missense	c.701A>G	p.K234R	0,308864
PHLPP1	18	missense	c.1864A>G	p.T622A	0,291776
SIGLEC15	18	missense	c.523G>A	p.V175M	0,272936
CCDC150	2	missense	c.1531C>T	p.H511Y	0,271099
CCER2	19	missense	c.695A>C	p.E232A	0,26194
CNDP1	18	insertion	c.43_44insTGC	p.V15delinsVL	0,251726
HIP1R	12	missense	c.2828A>G	p.N943S	0,246994
ARMC3	10	missense	c.2107C>T	p.P703S	0,207131

OCI AML-2

Gene	Chr.	Type	change DNA	change Protein	AF enrichment
ZMYM5	13	missense	c.247A>G	p.I83V	0,687075
DSEL	18	missense	c.3381_3382delinsTA	p.LL1127_1128FM	0,532895
DOCK9	13	missense	c.5737G>A	p.E1913K	0,53
WNK1	12	insertion	c.2172_2173insC	p.P725fs	0,526599
FLG2	1	missense	c.3185C>T	p.S1062F	0,438835
FLT3	13	missense	c.2039C>T	p.A680V	0,411765
ALPK2	18	deletion	c.4164_4166delCTT	p.F1388del	0,39942
NBPF11	1	missense	c.664G>A	p.E222K	0,397432
RAX	18	missense	c.863C>A	p.P288Q	0,391304
SACS	13	missense	c.10033G>A	p.V3345I	0,378947
SEC14L2	22	deletion	c.791delT	p.I264fs	0,365272
TRIM67	1	missense	c.1382A>C	p.D461A	0,308696
TMEM9	1	missense	c.481C>T	p.R161C	0,29108
C1orf131	1	missense	c.746G>C	p.R249T	0,278261
CDC42BPA	1	missense	c.3970C>G	p.Q1324E	0,226667
FAM110A	20	missense	c.43G>A	p.A15T	0,206719
ABCC2	10	missense	c.1585C>T	p.R529W	0,206667
MAN2A1	5	missense	c.2213A>G	p.N738S	0,203898

ML-2

Gene	Chr.	Type	change DNA	change Protein	AF enrichment
SELENOT	3	missense	c.443C>T	p.A148V	0,244444
ACOT4	14	insertion	c.563_564insTCAA	p.L188fs	0,21375
ACOT4	14	deletion	c.566_569delCTTA	p.A189fs	0,206864

HL-60

Gene	Chr.	Type	change DNA	change Protein	AF enrichment
CAT	11	missense	c.751G>A	p.A251T	0,369871
HLA-DRB5	6	missense	c.790C>T	p.L264F	0,357692
IRF2BP2	1	deletion	c.465_472delCATCCTGG	p.G155fs	0,34375
NOP14	4	missense	c.2089C>T	p.R697C	0,325136
SH2B3	12	missense	c.1696C>T	p.R566W	0,310458
MYOM1	18	missense	c.4895C>T	p.T1632I	0,295794
TRMT112	11	missense	c.70C>T	p.R24C	0,29339
ZMIZ2	7	missense	c.367G>A	p.G123R	0,29089
KRT24	17	missense	c.1547T>A	p.V516D	0,286017
CCDC88B	11	missense	c.2632G>A	p.V878M	0,285948
SLC33A1	3	missense	c.1525G>A	p.G509S	0,277778
METTL12	11	nonsense	c.571C>T	p.Q191*	0,277072
ZCCHC2	18	missense	c.2837C>T	p.A946V	0,270519
DCPS	11	missense	c.647T>C	p.L216S	0,262336
NOX4	11	missense	c.334A>G	p.S112G	0,258242
FOXP2	7	nonsense	c.1267G>T	p.E423*	0,255795
TMPRSS5	11	missense	c.1144G>A	p.G382R	0,251473
SH3BP2	4	nonstop	c.1857A>G	p.*619W	0,249231
KIRREL3	11	missense	c.908T>C	p.V303A	0,243344
BEND4	4	missense	c.1543G>A	p.D515N	0,243077
C2CD3	11	missense	c.2859G>A	p.M953I	0,236985
LRRC36	16	missense	c.61G>A	p.E21K	0,233333
OR6K2	1	deletion	c.671_672delCT	p.A224fs	0,231866
PRKG1	10	missense	c.1592G>T	p.W531L	0,23052
AKAP9	7	missense	c.6176A>G	p.E2059G	0,228985
DNAH5	5	missense	c.4510G>C	p.G1504R	0,225767
WWTR1	3	missense	c.768G>T	p.R256S	0,22509
NPVF	7	deletion	c.212_214delTTA	p.I71del	0,223982
ARHGEF7	13	missense	c.1025C>A	p.T342K	0,218582
MIA3	1	missense	c.2500A>G	p.I834V	0,217471
OR5M1	11	deletion	c.429_432delTCTG	p.C143fs	0,209463
CCDC168	13	missense	c.19809G>T	p.L6603F	0,207954
FOXP1	3	missense	c.179A>G	p.Q60R	0,206911
OAS2	12	missense	c.1504G>A	p.V502I	0,204546

SIG-M5

Gene	Chr.	Type	change DNA	change Protein	AF enrichment
SBNO1	12	missense	c.2305A>G	p.N769D	0,298449
OCA2	15	missense	c.1594T>C	p.W532R	0,278619
BRAF	7	missense	c.1799T>A	p.V600E	0,264214
APBA2	15	missense	c.1126T>C	p.Y376H	0,247567
LOR	1	insertion	c.110_111insCGG	p.F37delinsFG	0,244014
ARL6IP4	12	missense	c.821C>T	p.S274F	0,226303
NPVF	7	deletion	c.212_214delTTA	p.I71del	0,216861
LTK	15	missense	c.1127G>C	p.R376P	0,216791
CAPN3	15	missense	c.2393C>A	p.A798E	0,21328
MORN3	12	missense	c.457C>T	p.R153C	0,21039
ESYT1	12	missense	c.198A>G	p.I66M	0,206742
MYH15	3	missense	c.409G>C	p.G137R	0,204907

PL-21

Gene	Chr.	Type	change DNA	change Protein	AF enrichment
ABCC9	12	missense	c.1160T>C	p.L387P	0,373447
RGPD3	2	missense	c.1771A>C	p.N591H	0,309716
KIF21A	12	nonsense	c.3893C>A	p.S1298*	0,308621
EVX2	2	missense	c.1322C>T	p.A441V	0,292506
NDUFS1	2	missense	c.1838C>T	p.T613I	0,279635
MPHOSPH10	2	missense	c.1973T>C	p.I658T	0,27913
ITSN2	2	missense	c.2438T>C	p.V813A	0,276119
INTU	4	missense	c.712G>A	p.D238N	0,2695763
BEND4	4	missense	c.772C>G	p.L258V	0,2613768
PCDH11X	X	missense	c.2150G>A	p.G717E	0,26044
IFNA14	9	missense	c.167G>T	p.R56I	0,2588551
MDS2	1	insertion	c.278_279insAAG	p.V93delinsVR	0,258797
40787	4	missense	c.835G>A	p.D279N	0,2563831
PAX2	10	missense	c.91C>T	p.P31S	0,255881
CCDC66	3	insertion	c.1816_1817insCTC	p.S606delinsSP	0,25471
FGGY	1	missense	c.1489G>A	p.G497S	0,253084
TAF1L	9	missense	c.3359G>T	p.G1120V	0,2492366
KRTAP9-4	17	missense	c.161C>A	p.P54Q	0,2485683
ADGRA3	4	missense	c.3527G>T	p.S1176I	0,2484083
CRYBA2	2	missense	c.295C>T	p.L99F	0,242653
GPR1	2	missense	c.193T>C	p.F65L	0,240676
TENM4	11	missense	c.7916G>A	p.R2639Q	0,239882
CWC22	2	missense	c.2434T>G	p.L812V	0,238032
ARL16	17	missense	c.38C>A	p.A13D	0,2348389
EXO5	1	deletion	c.792_793delTG	p.S264fs	0,233527
TNIK	3	missense	c.415C>T	p.R139W	0,231373
MUC5B	11	missense	c.674G>A	p.R225K	0,2307689
POLN	4	deletion	c.2509delC	p.Q837fs	0,230159
QTRT1	19	splice	c.972_splice	e9-3	0,2269933
NPC1L1	7	missense	c.1327G>A	p.E443K	0,2243921
RERE	1	deletion	c.30_35delCAAAGA	p.D10_K11del	0,221804
ZMYM4	1	missense	c.3761C>T	p.A1254V	0,216792
CHMP4A	14	missense	c.262C>A	p.Q88K	0,2167699
PTPN13	4	missense	c.1082C>T	p.P361L	0,215779
TRIM51	11	splice	c.859_splice	e5+3	0,215054
MRFAP1L1	4	missense	c.62A>G	p.E21G	0,209896
DDX54	12	missense	c.2596G>T	p.A866S	0,20915
GCKR	2	missense	c.273G>C	p.Q91H	0,206373
KRT76	12	missense	c.1087G>A	p.E363K	0,202302
CAPN14	2	missense	c.1120T>C	p.F374L	0,201295
FRMD8	11	splice	c.253_splice	e2+3	0,200926

MOLM-16

Gene	Chr.	Type	change DNA	change Protein	AF enrichment
MTX1	1	missense	c.820A>C	p.K274Q	0,549145
FAM47C	X	missense	c.2016G>T	p.E672D	0,513799
AIM2	1	missense	c.245A>G	p.Q82R	0,479727
HIST2H2AC	1	missense	c.32C>T	p.A11V	0,458402
ZNF350	19	missense	c.111G>A	p.M37I	0,373696
GPR50	X	deletion	c.1503_1514delCACCACTGGCCA	p.P501_H505delinsP	0,366114
ELMSAN1	14	missense	c.700C>G	p.P234A	0,364931
PCNX1	14	missense	c.1043A>G	p.N348S	0,347619
ATP12A	13	missense	c.2705G>A	p.R902H	0,34249
GUCY2F	X	nonsense	c.1912C>T	p.Q638*	0,322581
TCEAL8	X	missense	c.199G>A	p.V67I	0,315087
ZNF432	19	missense	c.1181C>A	p.T394N	0,308081
MTMR6	13	splice	c.727_splice	e8-2_-7	0,303406
MAP3K15	X	splice	c.1591_splice	e12-1	0,3008
SHANK1	19	missense	c.5954G>A	p.G1985D	0,298011
ARHGEF3	3	missense	c.38A>G	p.K13R	0,286637
ALDH16A1	19	missense	c.532T>C	p.S178P	0,263551
GRAMD1A	19	deletion	c.251_252delAG	p.Q84fs	0,258037
PDHX	11	missense	c.541C>T	p.R181W	0,256808
KLC3	19	deletion	c.1294_1295delCT	p.L432fs	0,256692
CYP2F1	19	insertion	c.14_15insC	p.S5fs	0,252849
ZNF852	3	missense	c.1241A>G	p.N414S	0,248254
SHROOM4	X	missense	c.2165G>A	p.R722H	0,245784
WDR87	19	missense	c.7343C>T	p.P2448L	0,238337
ATG2B	14	missense	c.320G>A	p.R107H	0,237472
DNAAF3	19	missense	c.1132A>G	p.T378A	0,234037
HMGCS1	5	missense	c.878G>C	p.S293T	0,222619
CNOT3	19	missense	c.827A>C	p.N276T	0,217773
ZNF814	19	missense	c.2200C>T	p.H734Y	0,211763
ZNF135	19	missense	c.283G>A	p.V95M	0,21095
CDC42BPA	1	missense	c.4813A>G	p.T1605A	0,204841
PCDH11X	X	missense	c.3370G>C	p.A1124P	0,204681
NLRP2	19	missense	c.292A>G	p.K98E	0,203983

NOMO-1

Gene	Chr.	Type	change DNA	change Protein	AF enrichment
FMO4	1	missense	c.667C>T	p.R223C	0,372541
CD48	1	deletion	c.725delG	p.G242fs	0,30703
HHAT	1	missense	c.1417G>A	p.V473I	0,304922
PRG4	1	deletion	c.1433_1435delCTC	p.T478_P479delinsT	0,28551
NID1	1	missense	c.3442G>A	p.E1148K	0,279777
OR2L8	1	missense	c.619G>A	p.V207M	0,269917
PRDM13	6	missense	c.1310C>T	p.P437L	0,267904
MED17	11	missense	c.653A>G	p.H218R	0,25
FLG	1	missense	c.2509G>A	p.G837S	0,242966
KRT10	17	deletion	c.1521_1535delAAGCTCCGGCGGCGG	p.G507_G511del	0,242857
RPS2	16	missense	c.844G>A	p.V282M	0,235633
PRELP	1	missense	c.29C>T	p.P10L	0,224444
COPA	1	missense	c.2405A>G	p.K802R	0,216356
MAP10	1	missense	c.1259A>G	p.N420S	0,205757
NBEAL1	2	missense	c.2588A>T	p.D863V	0,203557

Again, we compared all enriched mutations to the hallmarks of cancer dataset[226] (Figure 6). Most mutations occurred in genes which are associated with the hallmarks “resisting cell death”, “activating invasion and metastasis” and “evading immune destruction” (6, 5 and 5, respectively). No mutations were found in genes belonging to the hallmarks “enabling replicative immortality” and “genome instability and mutation”.

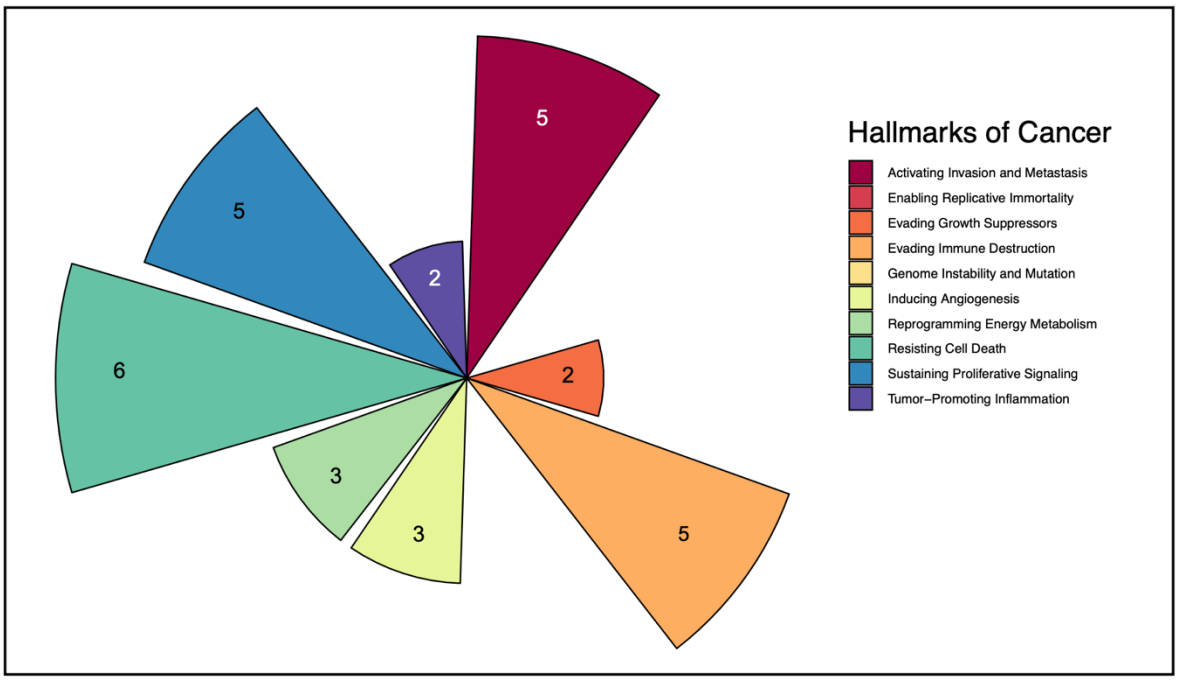

Figure 6: Enriched mutations found in hallmarks of cancers genes

Analysis of all mutations which had enriched AF (>0.2) in venetoclax resistant cell lines compared to parental cell lines.

4.3.3 Cancer/ apoptosis-associated mutations

In an effort to harmonize our findings and create a comprehensive overview of relevant mutations, we selected a variety of highly oncogenic mutated genes found across both hallmarks of cancer analyses (chapter 4.3.1 and 4.3.2). Additionally, we looked for commonly mutated genes in AML (i.e., *NPM1, DNMT3A, IDH2 or RUNX1*), and all apoptosis-related genes (with a focus on Bcl-2 family genes), which were either newly acquired or enriched (AF or AF enrichment >0.2) in 199R cell lines.

While no Bcl-2 family gene mutations were found, several other cancer-related mutations occurred in 199R cells. The majority of relevant mutations occurred in OCI AML-2 199R. Of note, OCI AML-2 cells both gained a new *TP53* mutation and showed an enrichment in *FLT3* mutation. Strong enrichment was also found in *BRAF* mutation of SIG-M5.

Table 19: Cancer/ apoptosis-associated mutations

∆ mutations with an Allelic Fraction ≥0.2 and enriched mutations with an Allelic Fraction enrichment of ≥0.2

Cell Line	**Gene**	**Chr.**	**Type**	**change DNA**	**change Protein**	**Allelic Fraction S**	**Allelic Fraction 199R**
MOLM-13	**SCN2A**	2	missense	c.1571G>A	p.R524Q	0.444444	0.730769
KASUMI-1	**HIP1R**	12	missense	c.2828A>G	p.N943S	0.645514	0.892508
OCI AML-2	**EIF2AK3**	2	missense	c.2426A>T	p.E809V	-	0.537736
	ITGAV	2	missense	c.2075C>T	p.A692V	-	0.382022
	TGFBR2	3	missense	c.1666G>T	p.A556S	-	0.520124
	TP53	17	missense	c.659A>G	p.Y220C	-	0.988636
	FLT3	13	missense	c.2039C>T	p.A680V	0.588235	1
	CREBBP	16	splice	c.5172_splice	e31+1	-	0.5
	MAP2K4	17	missense	c.1205C>T	p.T402I	-	0.491071
SIG-M5	**BRAF**	7	missense	c.1799T>A	p.V600E	0.543478	0.807692
MOLM-16	**CD44**	11	missense	c.1967C>A	p.S656Y	-	0.208861

4.3.3.1 TP53 mutations

TP53, the so called “guardian of the genome”, is the single most mutated gene across all types of cancer [228] and therefore requires to be addressed individually. As presented in chapter 4.3.3, OCI AML-2 acquired a new *TP53* mutation with venetoclax resistance. Parental OCI AML-2 cells also exhibited a missense *TP53* mutation, namely c.820G>C/p.V274L at an AF of approximately 0.35. However, this mutation disappeared in 199R cells. The newly acquired mutation is located at c.659A>G/p.Y220C.

Table 20: TP53 mutations in OCI AML-2 pre and post venetoclax resistance

Cell Line	**Gene**	**Chr.**	**Type**	**change DNA**	**change Protein**	**Allelic Fraction S**	**Allelic Fraction 199R**
OCI AML-2	**TP53**	17	missense	c.820G>C	p.V274L	0.354167	-
				c.659A>G	p.Y220C	-	0.988636

Apart from OCI AML-2 199R, four more 199R AML cell lines showed *TP53* mutation: KASUMI-1, PL-21, MOLM-16, and NOMO-1. However, these mutations were already preexistent in the parental equivalent (Table 21). Prior to venetoclax treatment, the entirety of cells within KASUMI-1, PL-21 and NOMO-1 already contained *TP53* mutation (AF S 1, 0.95 and 0.97, respectively). This did not change with venetoclax resistance (AF 199R 0.99, 0.98 and 0.98, respectively). MOLM-16 (S and 199R) harbored two mutations, both affecting the DNA binding domain, but at different loci. Both mutations were mildly enriched after venetoclax resistance (0.46 to 0.51 and 0.45 to 0.5, respectively). An overview of the p53 protein domains can be seen in Figure 7. *TP53* mutations in 743G>A (KASUMI-1), 713G>C (MOLM-16), 517G>A (MOLM-16) and *TP53 deletion* in 723delC (NOMO-1) affect the p53 DNA binding domain. Deletion in PL-21 is located at the transactivation domain (TAD) of p53.

Table 21: Preexisting *TP53* mutations in four AML cell lines

Cell Line	**Gene**	**Chr.**	**Type**	**change DNA**	**change Protein**	**Allelic Fraction S**	**Allelic Fraction 199R**
KASUMI-1	**TP53**	17	missense	c.743G>A	p.R248Q	1	0.993421
PL21			deletion	c.107delC	p.P36fs	0.952381	0.97619
MOLM-16			missense	c.713G>C	p.C238S	0.461333	0.511873
			missense	c.517G>A	p.V173M	0.448276	0.5
NOMO-1			deletion	c.723delC	p.S241fs	0.9701	0.97541

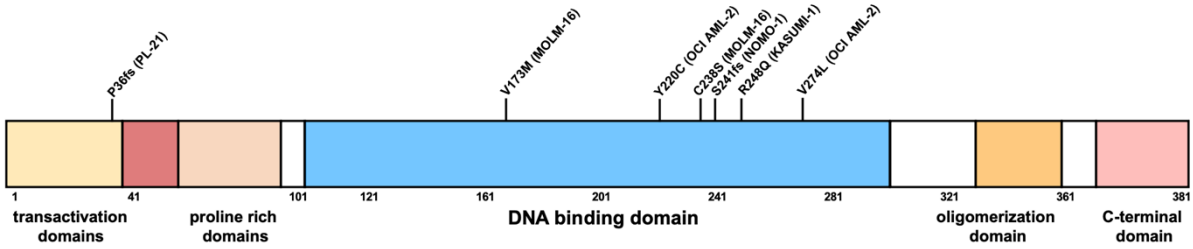

Figure 7: p53 protein domains including the most frequent mutation sites

4.4 Analysis of mRNA levels in parental 199R cell lines

Another potential mechanism which can render cells resistant to treatment is regulation of gene expression. As described above, mitochondrial Bcl-2 family proteins are frequently involved in the emergence of resistance to venetoclax. Measurement of mRNA levels via 3´RNA sequencing of parental and 199R cell lines was performed to explore underlying causes of resistance to venetoclax on gene expression level. Dr. Janine Altmüller, Cologne Center for Genomics, performed the RNA sequencing. Sequencing results were then analyzed by Prerana Wagle, CECAD Bioinformatics Facility, University Hospital Cologne, and Dr. Stuart Blakemore, AG Pallasch, CECAD/University Hospital Cologne.

4.4.1 Differential gene expression based on pooled data of all cell lines

Based on the Single Read Counts (SRC) for each mRNA and each cell line, an analysis of all nine cell lines taken together (pooled analysis) was conducted (n=9). Figure 8 shows significantly up- and downregulated mRNA in all 199R AML cell lines at a glance. More mRNAs were found to be significantly upregulated than downregulated, i.e., proteasome complex PSMD4, VPS72 as well as mitochondrial ribosome proteins MRPL9 and MRPS21. Of note, FOXC1 was the single most significantly upregulated finding (Log2 FC 2,48, *p* value 0.0298). MCL1 mRNA was among the most upregulated in our analysis (Log2 FC 1,69, *p* value <0.001). However, no other Bcl-2 family proteins were found to be deregulated in this analysis.

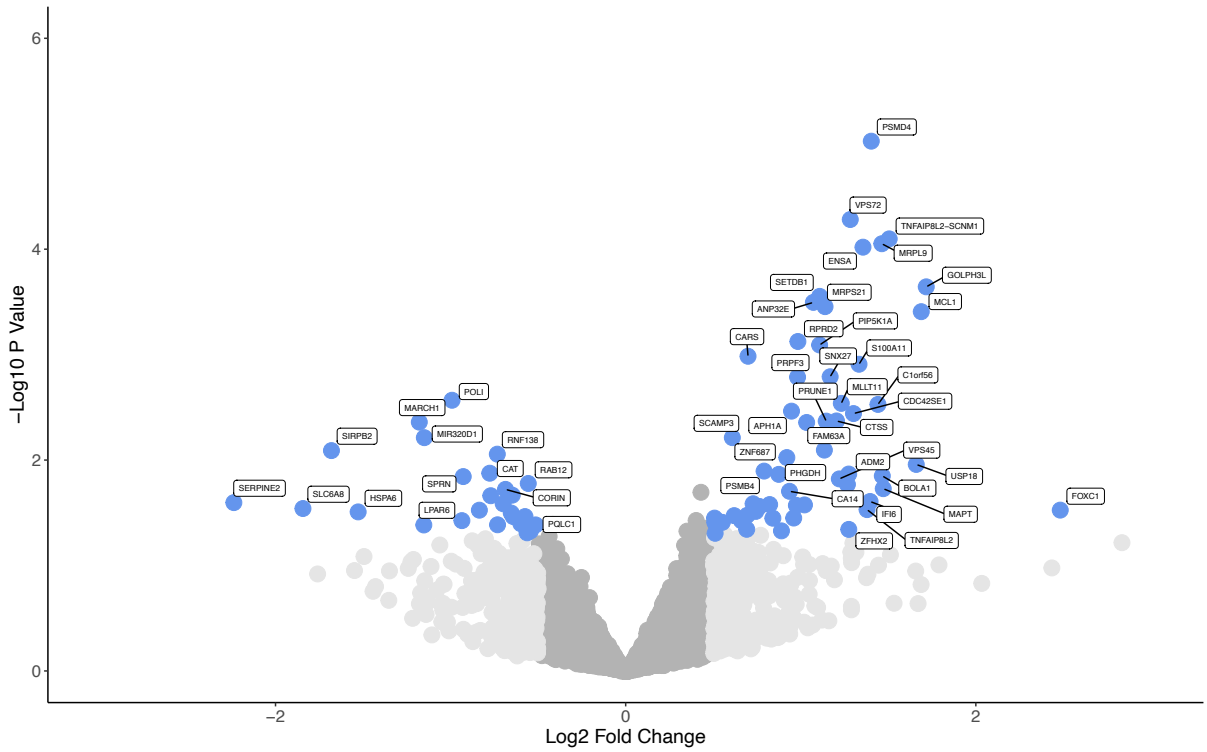

Figure 8: Volcano Plot of RNA sequencing results based on pooled data of all cell lines

p value on the y axis represents level of significance, Log2 Fold Change on the x axis pictures change in expression level (>0 = upregulation, <0 = downregulation). Blue dots show significant genes (*p* value <0.05) with a Log2 Fold Change of ≥ 0.5 or ≤ -0.5.

4.4.2 Differential gene expression based on intrinsic susceptibility to venetoclax

Due to the parental cell line's heterogeneous susceptibility to venetoclax, an additional analysis based on the cell lines' intrinsic susceptibility was performed. For this, the cell lines were subdivided into two groups based on their initial IC_{50} as presented in chapter 4.2.1. The first group (group 1, high intrinsic susceptibility) comprises highly susceptible cell lines MOLM-13, KASUMI-1, OCI AML-2, and ML-2 (n = 4). The second group (group 2, intrinsic resistance) consists of cell lines HL-60, SIG-M5, PL-21, MOLM-16, and NOMO-1 (n = 5), which were only susceptible to high doses of venetoclax (>3 µM) or showed no susceptibility towards the drug at all.

Figure 9A shows a summary of significantly up- and downregulated mRNA in group 1. Several significantly deregulated mRNAs correspond with hits from Figure 8 such as upregulation of PSMD4, VPS72, MCL1, MRPS21, MRPL9. However, the majority of significant hits including all downregulated and several upregulated mRNAs are exclusively altered in group 1 as highlighted in dark blue. FCN1 stands out as the single most upregulated mRNA (Log2 FC 3.76, *p* value 0.009). Other relevant findings include upregulation of HES1 (Log2 FC 2.36, *p* value 0.012) and VPS45 (Log2 FC 1.59, *p* value 0.002). On the other hand, PSTPIP2 (Log2 FC -2.27, *p* value 0.002) and SUCNR1 (Log2 FC -2.57, *p* value 0.031) represent the most downregulated mRNAs. MCL1 was, again, found to be strongly upregulated (Log2 FC 1.58, *p* value 0.003). However, it was not exclusively upregulated in intrinsically sensitive AML cell lines, because upregulation could also be found in intrinsically resistant AML cell lines.

An overview of significantly deregulated mRNAs within group 2 can be seen in Figure 9B. Evidently, most hits coincide with our findings from the pooled RNA sequencing analysis and some with findings from group 1. However, it is noteworthy that a few significantly downregulated mRNAs, especially the second most downregulated hit, CRTC2 (Log2 FC -2.04, *p* value 0.002), can only be found in group 2.

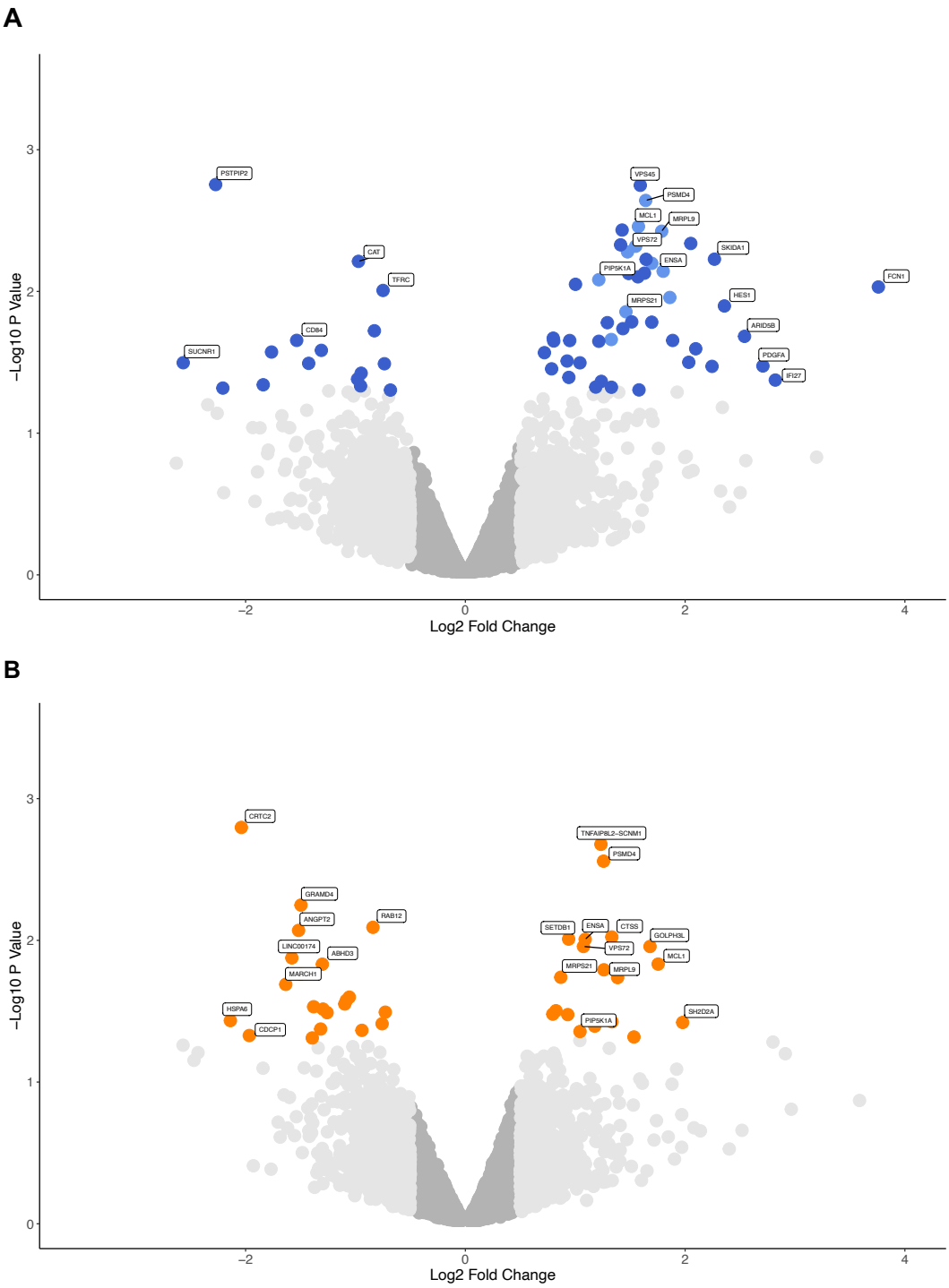

Figure 9: Volcano Plots of RNA sequencing results based on intrinsically sensitive (A) and intrinsically resistant (B) AML cell lines

P Value on the y axis shows level of significance, Log2 Fold Change on the x axis pictures change in expression level (>0 = upregulation, <0 = downregulation). A: Deregulated mRNA in **intrinsically sensitive** cell lines MOLM-13, KASUMI-1, OCI AML-2 and MOLM-13. Blue dots show significant genes (P Value <0.05) with a Log2 Fold Change of ≥ 0.5 or ≤ -0.5. Dots in dark blue mark deregulated proteins that are exclusive to Group 1. **B**: Deregulated mRNA in **intrinsically resistant** cell lines HL-60, SIG-M5, PL-21, MOLM-16 and NOMO-1. Orange dots show significant genes (P Value <0.05) with a Log2 Fold Change of ≥ 0.5 or ≤ -0.5.

4.4.3 Single Read Count Analysis of Bcl-2 family mRNA

Since MCL1 was the only significantly deregulated BCL2 family protein in the previous analyses, we took a closer look at the SRC of several relevant BCL2 family members: MCL1, BCL2, BCL-xL and BCL-W as antiapoptotic, as well as BAK, BAX, PUMA, NOXA, BIM and BID as proapoptotic. A heat map displaying gene expression changes, arranged according to the respective expression profile, can be seen in Figure 10. MCL1 showed the strongest overexpression of all proteins, especially in AML cell lines HL-60 and OCI AML-2. It was found to be upregulated in all cell lines except NOMO-1. BIM, BAK and BCL-xL were overexpressed in most 199R cell lines, while BCL2, NOXA and BCL-W showed lower expression levels in most 199R cell lines. PUMA was upregulated in HL-60, PL-21, MOLM-16 and SIG-M5, while it was downregulated in OCI AML-2, ML-2, and KASUMI-1.

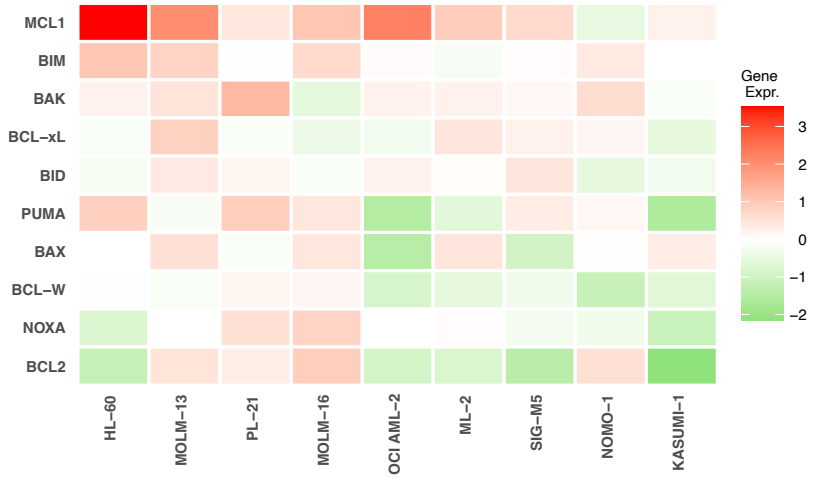

Figure 10: Bcl-2 family gene expression changes in 199R cell lines based on SRC

Gene expression change of pro- and antiapoptotic Bcl-2 family members after venetoclax resistance calculated by Log2 Fold Change. Upregulation colored in red, downregulation in green.

4.5 Analysis of mRNA levels in venetoclax-resistant patients

As venetoclax resistance is known to occur in AML patients [207], we investigated changes in mRNA levels following acquired venetoclax resistance in AML patient samples next. This allowed us to explore similarities and differences between *in vitro* and *in vivo* venetoclax resistance. Including this real-world data set also added another layer of clinical relevance to our laboratory findings. For this purpose, bone marrow samples of two patients pre-venetoclax-treatment and post-venetoclax-resistance were analyzed using single cell RNA sequencing (scRNA-seq). scRNA-seq was performed by Dr. Janine Altmüller, Cologne Center for Genomics. Analysis of results was performed by Dr. Milos Nikolic, AG Peifer, Department of Translational Genomics, and Dr. Stuart Blakemore, AG Pallasch, CECAD/University Hospital Cologne.

Based on the expression profile of genes specific for cell type, pre-treatment and post-resistance cells were clustered into three groups including two tumor cell clusters and several tumor microenvironment (TME) clusters (Figure 11). This way, cells sharing similar gene expression profile, i.e., cells of the same type, can be distinguished from other cell types.

We defined a pre-treatment cluster (“Majority Pre Cluster”) containing the majority of tumor cells prior to treatment, a post-resistance cluster (“Majority Post Cluster”) containing the majority of tumor cells after relapse during venetoclax treatment. Gene expression changes were then analyzed by comparing these two timepoints (i.e., cells pre-treatment and post-resistance) within the “Majority Pre Cluster” (condition 1), within the “Majority Post Cluster” (condition 2) and from “Majority Pre Cluster” to “Majority Post Cluster” (condition 3).

Analysis results based on the median of all three conditions are presented in Figure 12. The volcano plot contains information on the respective extent of up- or downregulation, level of significance, and number of conditions a hit was significantly deregulated in (1, 2 or 3 according to dot size). Some of the most downregulated hits include hemoglobin- or erythrocyte-associated mRNAs such as HBG1, HBM, HBB, HBA1, HBG2, HBD, GATA1, GYPB and GYPA. BCL2L1/BCL-xL, highlighted in red, was also found to be downregulated (Median Log2 FC -4.55, Q Value 0.023). The strongest upregulation was found in CITED4, FGFR1, SLC2A5, NOTCH1, and ERG. Additionally, BCL2, highlighted in red, was upregulated (Median Log2 FC 3.58, Q Value <.001).

Figure 13 illustrates the respective analysis for conditions 1 and 3 with an emphasis on Bcl-2 family members. No significant Bcl-2 family member alterations were detectable in condition 2. Post-resistance cells within the “Majority Pre Cluster” had elevated levels of BCL2, BID and MCL1, and decreased levels of BCL2L1/BCL-xL, BCL2L11/BIM and BBC3/PUMA compared to pre-treatment cells within the “Majority Pre Cluster” (A). Post-resistance cells within the “Majority Post Cluster” had elevated levels of BCL2 and diminished levels of BCL2L1/BCL-xL compared to pre-treatment cells within the “Majority Pre Cluster” (B).

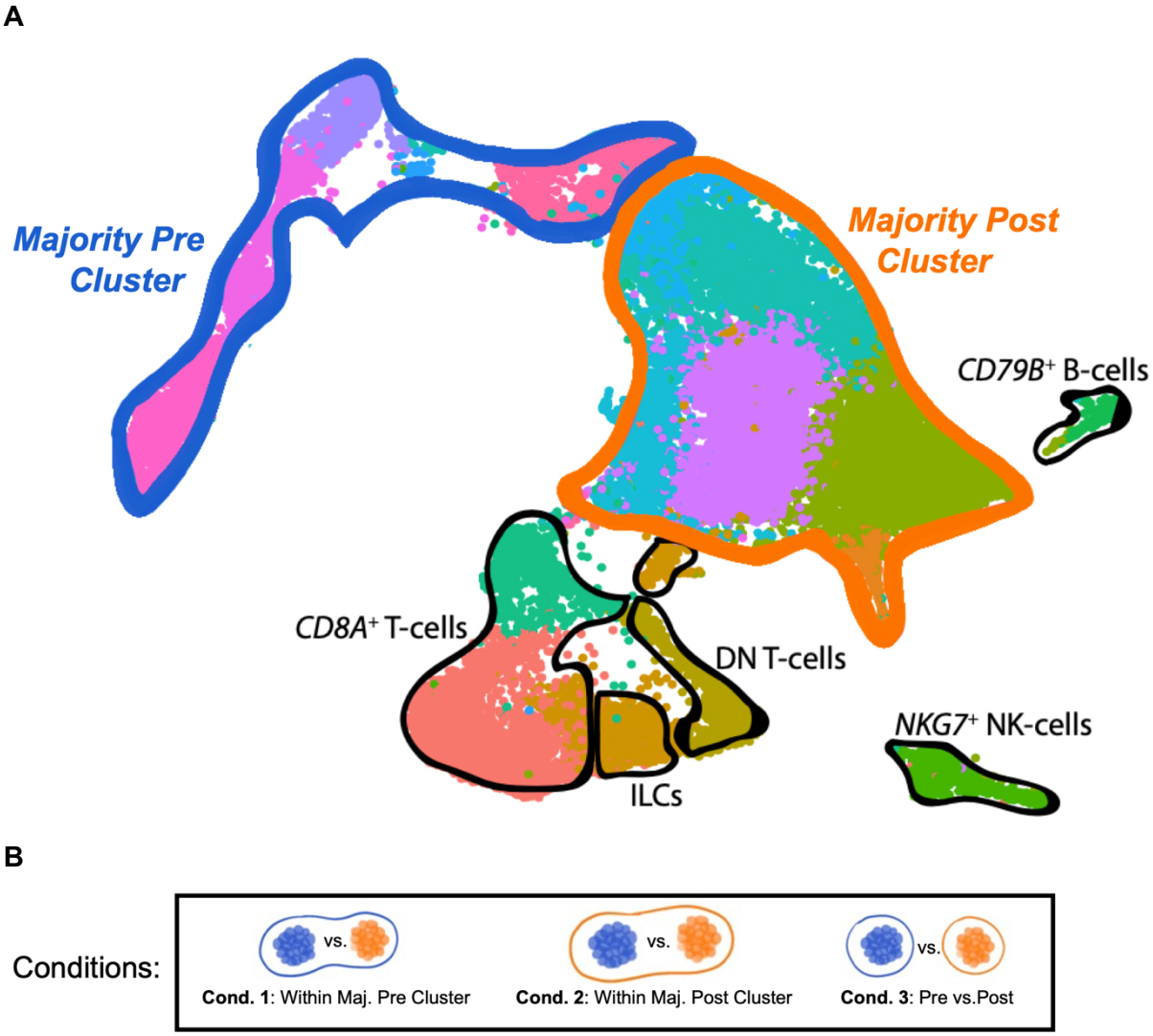

Figure 11: UMAP plot illustrating clustering of cells and analyzed conditions

Figure adapted from Dr. Stuart Blakemore

A: Clustering is based on similar expression of 2000 cell type-specific genes. The cluster outlined in blue contains the majority of pre-treatment tumor cells. The cluster outlined in orange consists of the majority of cells post-resistance tumor cells. Remaining cells outlined in black are tumor microenvironment cells (TME). **B:** Condition 1 compares pre-treatment cells (blue) with post-resistance cells (orange) within the "Majority Pre Cluster" (blue outline). Condition 2 compares pre-treatment cells (blue) with post-resistance cells (orange) within the "Majority Post Cluster" (orange outline). Condition 3 compares pre-treatment cells (blue) in the "Majority Pre Cluster" (blue outline) with post-resistance cells (orange) in the "Majority Post Cluster" (orange outline).

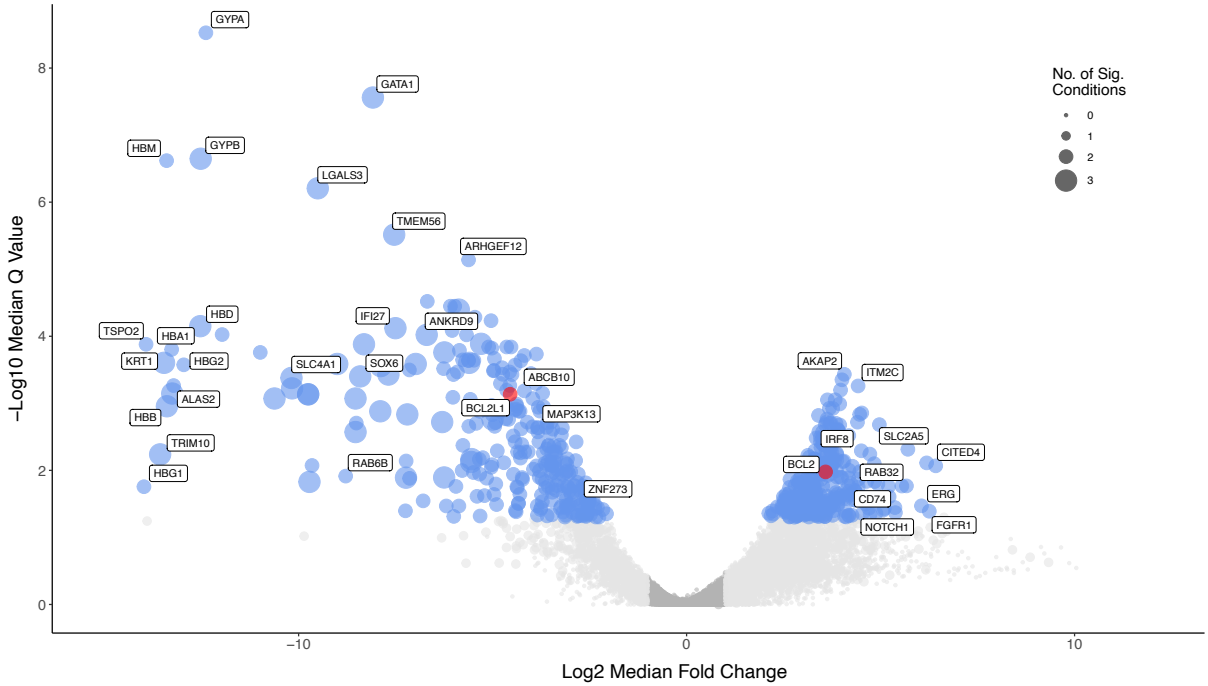

Figure 12: Volcano Plot of scRNA-seq results based on conditions 1, 2 and 3 combined highlighting deregulated Bcl-2 family members

Q Value/False Discovery Rate (FDR) on the y axis illustrates the level of significance, Log2 Fold Change on the x axis indicates changed expression level (>0 = upregulation, <0 = downregulation). Blue dots show significantly deregulated mRNA (Q Value <0.05) with a Log2 Fold Change of ≥ 1 or ≤ -1. Significantly altered expression of Bcl-2 family members expression is highlighted in red. Dot size represents the number of conditions (0, 1, 2 or 3) within which mRNA is significantly altered. For example, the largest dot stands for mRNA which was a significant finding in all three conditions.

A

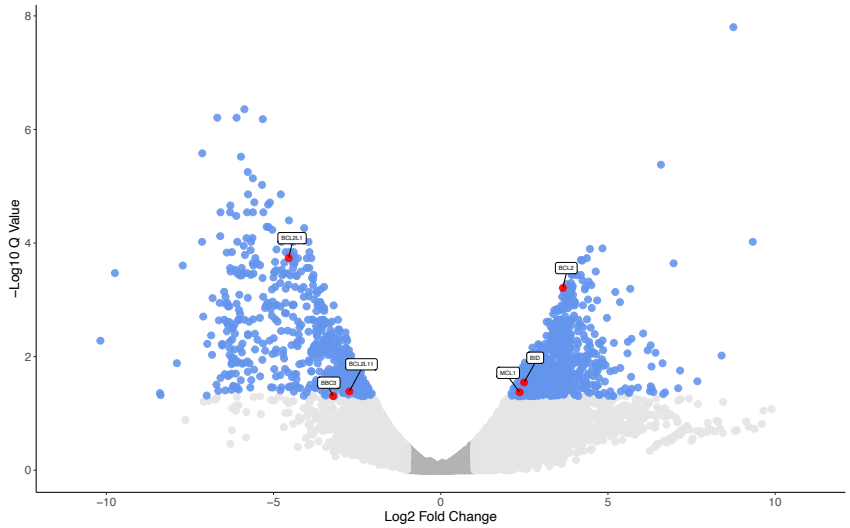

B

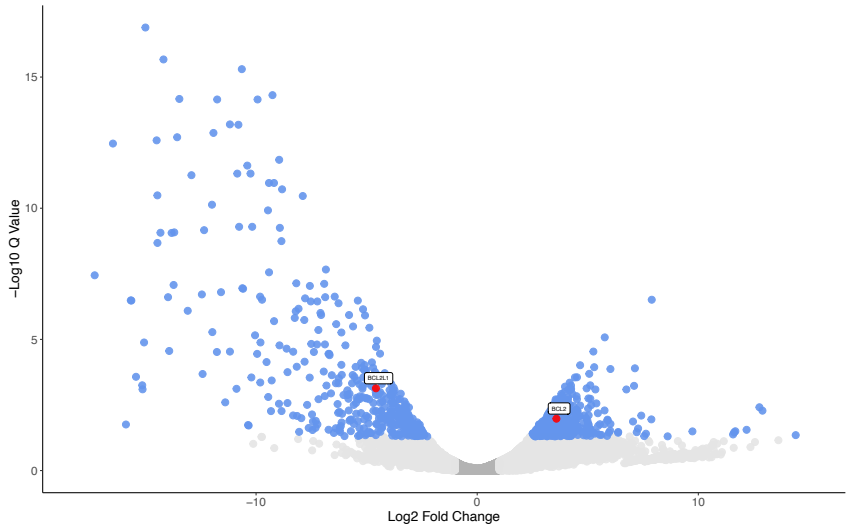

Figure 13: Volcano Plots of scRNA-seq results based on conditions 1 (A) and 3 (B) highlighting deregulated Bcl-2 family members

A: Gene expression changes between pre-resistant and post-resistant cells within the “Majority Pre Cluster” (condition 1). **B:** Gene expression changes between pre-resistant cells in the “Majority Pre Cluster” and post-resistant cells in the “Majority Post Cluster” (condition 3).

Q Value/False Discovery Rate (FDR) on the y axis illustrates the level of significance, Log2 Fold Change on the x axis quantifies the change in expression level (>0 = upregulation, <0 = downregulation). Blue dots show significantly deregulated mRNA (Q Value <0.05) with an Log2 Fold Change of ≥ 1 or ≤ -1. Significantly altered BCL2 family mRNA expression is highlighted in red.

4.6 Protein level examination of Bcl-2 family proteins

Proteins of the Bcl-2 family are commonly deregulated in cancers, including leukemic diseases, both *in vivo* and *in vitro* [229]. To add an additional method of analyzing imbalances in the homeostasis of pro- and antiapoptotic Bcl-2 family members within our 199R cell lines, we employed immunoblotting. This also allowed us to examine whether changes in mRNA level, detected via RNA sequencing, had their equivalent on protein level. Eight cell lines were tested for a total of six BCL2 family proteins, including MCL1, BCL2 and BCL-xL as antiapoptotic proteins and PUMA, BAX and BAK as proapoptotic proteins. The results are presented in Figure 14. Increased MCL1 protein expression was found in all 199R cell lines that show MCL1 expression in the parental equivalent, with significant differences in OCI AML-2, SIG-M5, MOLM-16, and NOMO-1. Only PL-21 S lacked MCL1 expression, and showed none in the 199R equivalent either. For BCL2, significant signal reduction was found after venetoclax resistance in HL-60, SIG-M5, ML-2 and KASUMI-1 compared to parental cell lines, while BCL2 signal was significantly increased in MOLM-16. Analysis of BCL-xL showed that protein expression remained similar before and after venetoclax resistance across all cell lines, as no significant differences were detected. Significant signal reduction of PUMA was found in 199R cell lines OCI AML-2, NOMO-1 and PL-21. For BAX, reduction of signal was found to be significant in 199R cell lines of OCI AML-2, and SIG-M5. Moreover, significant signal enrichment of BAK was detected in OCI AML-2, and NOMO-1.

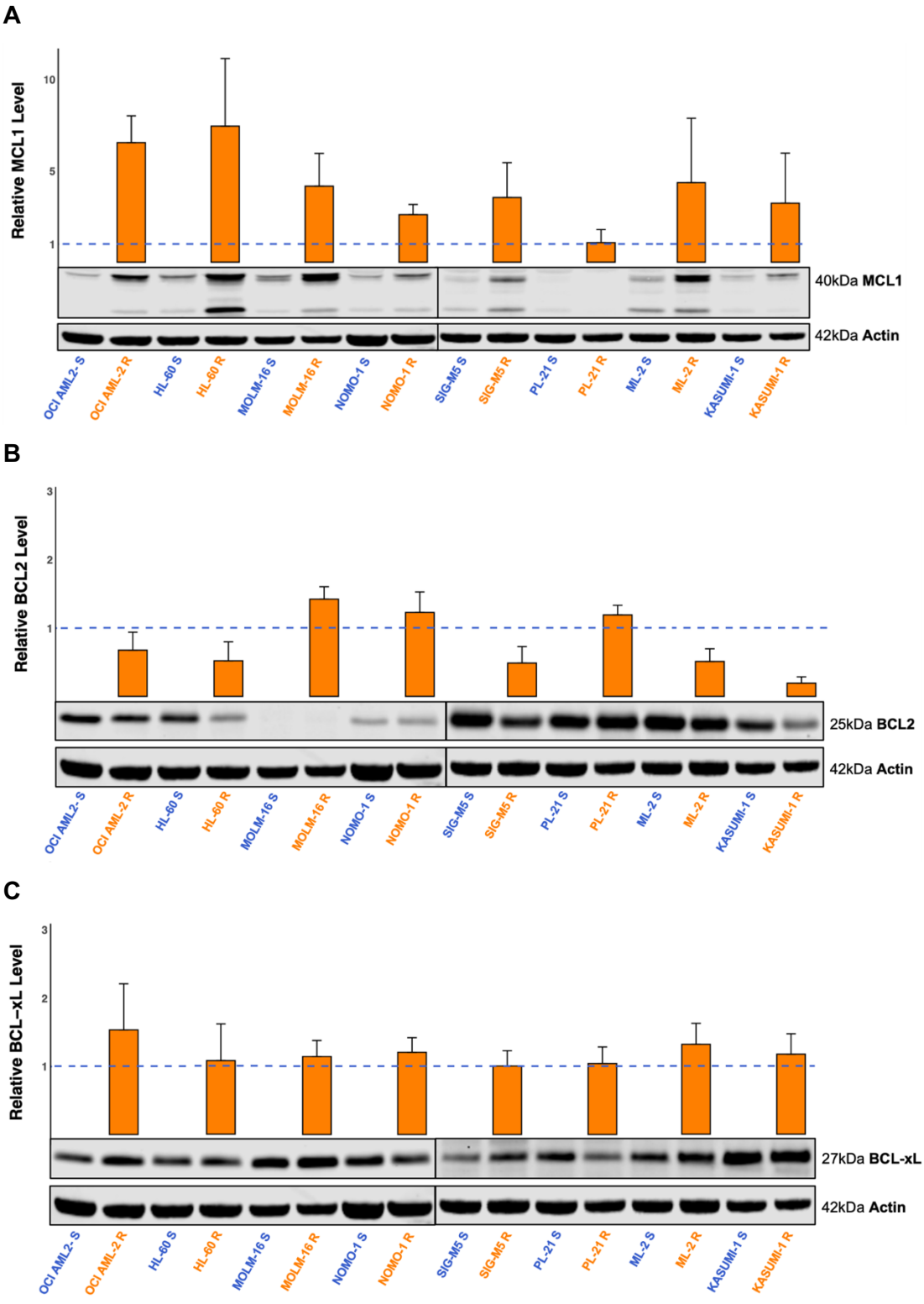
A
Relative MCL1 Level
10
5
1
40kDa MCL1
42kDa Actin
OCI AML2- S
OCI AML-2 R
HL-60 S
HL-60 R
MOLM-16 S
MOLM-16 R
NOMO-1 S
NOMO-1 R
SIG-M5 S
SIG-M5 R
PL-21 S
PL-21 R
ML-2 S
ML-2 R
KASUMI-1 S
KASUMI-1 R
B
Relative BCL2 Level
3
2
1
25kDa BCL2
42kDa Actin
C
Relative BCL-xL Level
3
2
1
27kDa BCL-xL
42kDa Actin

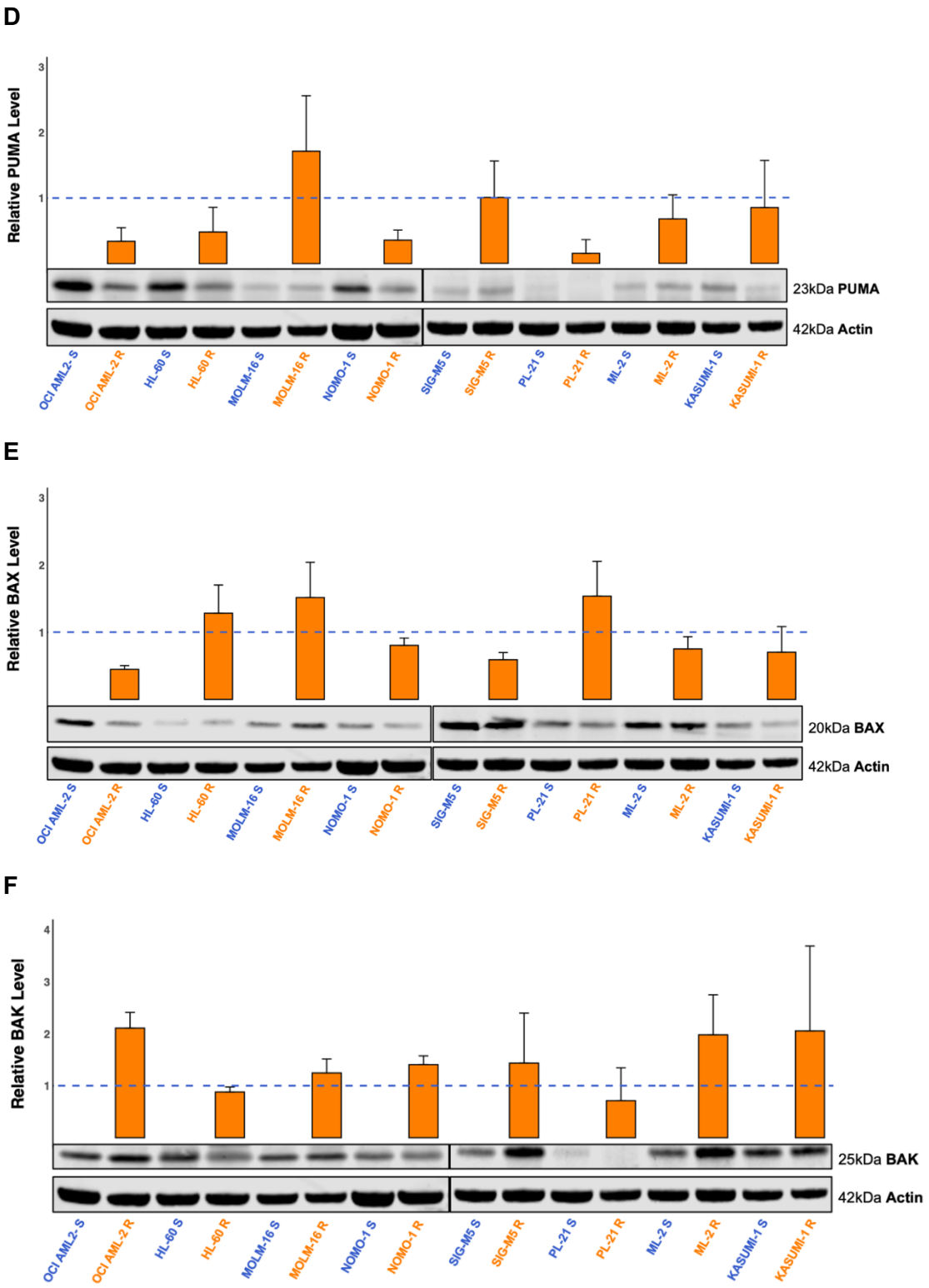

Figure 14: Western Blot analysis of anti- and proapoptotic Bcl-2 family proteins

Antiapoptotic proteins include MCL1 **(A)**, BCL2 **(B)** and BCL-xL **(C)**, proapoptotic proteins include PUMA **(D)**, BAX **(E)** and BAK **(F)**. Experimental setup: A maximum of $5x10^6$ cells was washed with PBS and lysed with 10-20µL RIPA buffer per $1x10^6$ cells. Actin was probed as a loading control. Quantification was carried out via densitometry. All blots are representative examples of three independent findings. Figures show mean and standard deviation after normalization to the respective parental cell line (dashed line).

Part III: Overcoming venetoclax resistance in 199R cell lines

4.7 The impact of PUMA downregulation

Beroukhim et al. found PUMA-encoding gene *BBC3* to be deleted in several types of cancers, implicating that loss of this proapoptotic protein could promote cell survival [149]. Moreover, our group recently found venetoclax resistance to be mediated by downregulation of PUMA expression in B-cell lymphoma cell lines [201]. Since we also observed PUMA downregulation in Western Blot analyses of all four 199R cell lines that expressed PUMA in the parental cell line (OCI AML-2, HL-60, PL-21, and NOMO-1), we concluded that the reduction of the apoptosis-promoting protein could be a major mechanism of emerging venetoclax resistance and therefore have therapeutic implications. We employed CRISPR-Cas9 on the parental AML cell line OCI AML-2 to generate a knockout of the PUMA-encoding gene *BBC3*. Single cell clones were generated via serial dilution into single cell colonies. To confirm successful knockout, we performed immunoblot analysis of different clones and used parental cells, cells transduced with the empty vector, pooled knockout clones and Puromycin selected pooled knockout clones as controls (Figure 15). Successful knockout of the *BBC3* gene was achieved in clones 1, 3, 4, 5, 6, 8, 9, 10, 11, 12 and 14, as no PUMA expression was detected. We selected clones 1, 3, 4, 5, 8, 9, 10 and 11 for subsequent experiments. Since clone 6 still expressed PUMA, but underwent the same knockout procedure as clones without PUMA expression, it was used as the main control. By running Western Blot analysis for PUMA expression on a regular basis, we ensured that PUMA was continuously absent in the knockout cell line.

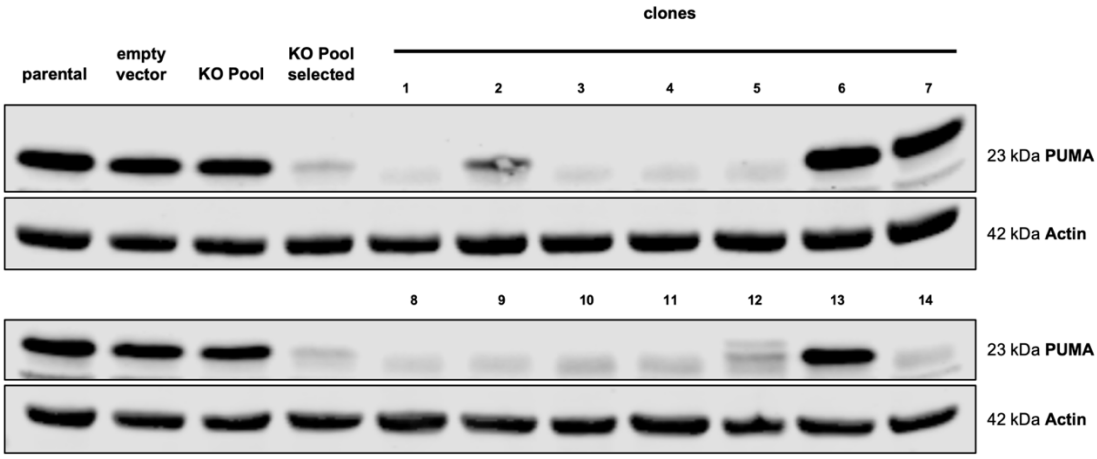

Figure 15: Western Blot analysis of PUMA expression in OCI AML-2 knockout clones

Experimental setup: A maximum of $5x10^6$ cells was retrieved from the culture flask, washed with PBS, and lysed with 10-20 µL RIPA buffer per $1x10^6$ cells. Actin was blotted as a loading control.

To investigate the impact of PUMA deletion on cell survival after venetoclax treatment, cell viability assays of selected clones and control clone 6 were performed using flow cytometry (Figure 16). As the cell line OCI AML-2 was highly susceptible to venetoclax treatment and an IC_{50} was reached at low doses (<100nM), we compared cell viability at 10nM of venetoclax. While clone 6 (control) showed 47% cell viability, all knockout clones showed slightly higher viability (cell viability ranging from 50% to 59%).

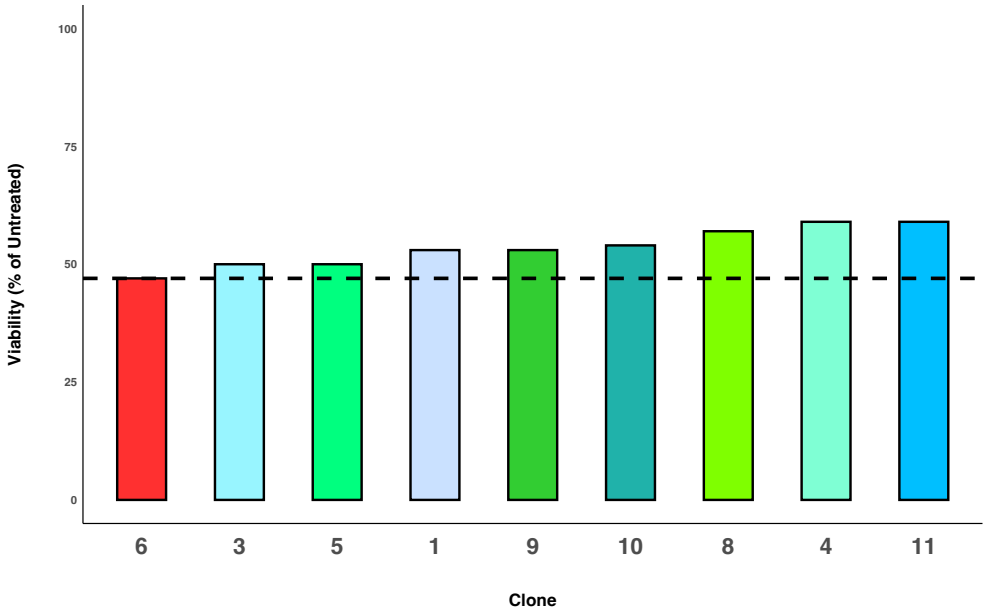

Figure 16: Cell viability of PUMA knockout clones treated with venetoclax

Experimental setup: In a 96-well plate, 1x10^5 cells per well were incubated in 100 µL medium with 10 nM venetoclax. Cells were incubated for 48 h before read-out via flow cytometric measurement of Annexin V and 7AAD. DMSO was used as a vehicle control. This experiment was carried out once.

4.8 Targeting MCL1 in 199R cell lines

As described before, MCL1 is one of the major mitochondrial players whose upregulation is involved in many cancers including tumors refractory to treatment[140,143,201]. MCL1 upregulation could also be detected following venetoclax resistance in all 199R cell lines except PL-21 via Western Blotting and in all 199R cell lines except NOMO-1 by RNA sequencing. Therefore, we examined the effect of MCL1 inhibition using the MCL1 inhibitor S63845 on venetoclax resistant cell lines. Cell viability was assessed by flow cytometry to determine the sensitivity of parental and 199R cells to MCL1 inhibition in a dose-dependent fashion. As demonstrated in Figure 17, eight out of nine 199R cell lines had a lower IC_{50} compared to the parental cell lines. Among those, seven 199R cell lines were significantly more susceptible to at least three different concentrations of the MCL1 inhibitor compared to the parental counterpart: MOLM-13, KASUMI-1, OCI AML-2, HL-60, SIG-M5, PL-21, and NOMO-1. Only for MOLM-16 and ML-2, the difference was not significant at any concentration. For most cell lines, viability decrease was especially evident at low concentrations of the inhibitor, as many 199R cell lines severely declined in cell viability at <100nM of venetoclax. In Table 22, the respective IC_{50} of each cell line can be found. Although MOLM-16 199R cells were very sensitive to MCL1 inhibition, MOLM-16 S cells were even more susceptible. Therefore, MOLM-16 was the only cell line with an IC_{50} 199R larger than IC_{50} S.

Cell Line	IC_{50} S (nM)	IC_{50} 199R (nM)
MOLM-13	103,6	<5
HL-60	1031	15,96
KASUMI-1	425,8	19,5
NOMO-1	447,7	41,65
ML-2	101,7	55,32
OCI AML-2	925,2	72,22
PL21	912	85,13
MOLM-16	61,25	131,5
SIGM-5	665,7	235,6

Table 22: IC_{50} values for MCL1 inhibitor S63845 in S and 199R AML cell lines

Cell lines are ordered by the parental cells' IC_{50}. 199R cell lines highlighted in green show greater susceptibility to MCL1 inhibition compared to the parental equivalent. 199R cell line in red shows elevated cell viability compared to the parental equivalent.

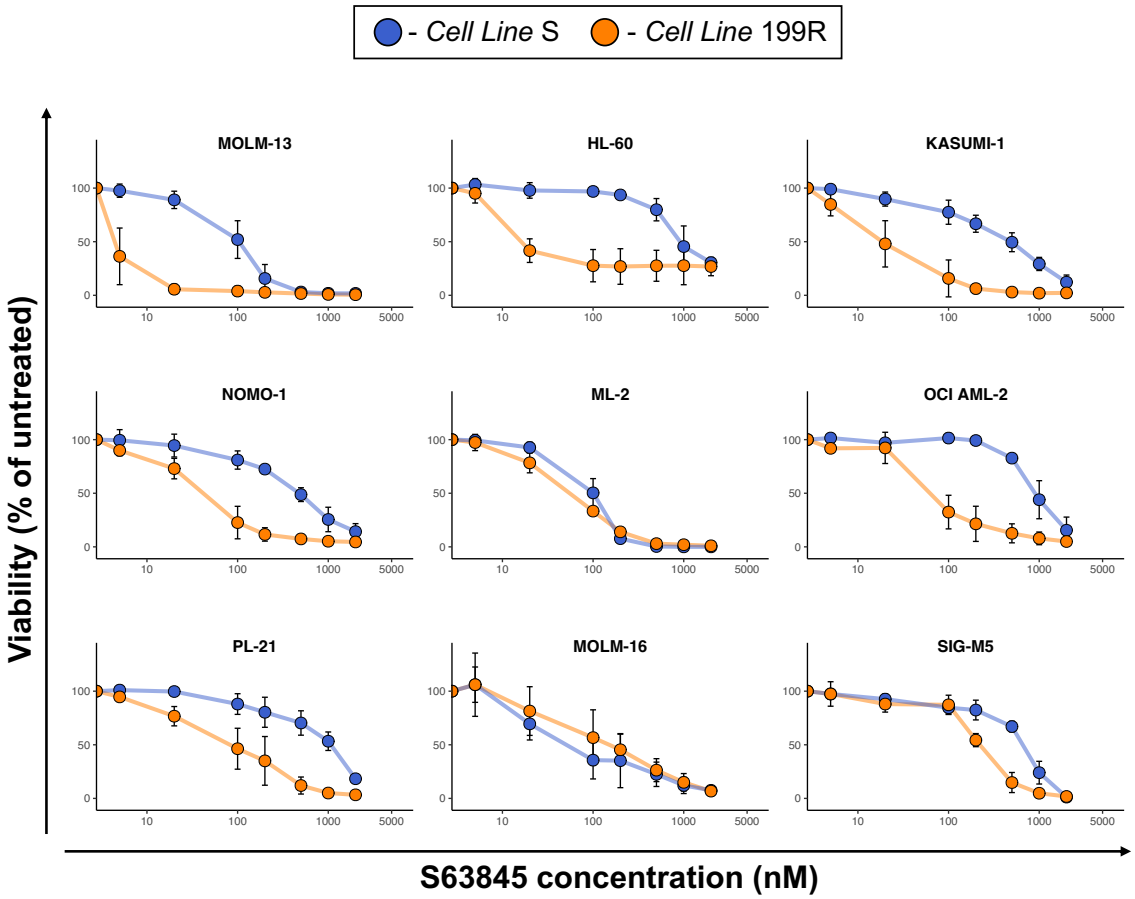

Figure 17: Cell viability of AML cell lines S and 199R treated with MCL-1 inhibitor S63845

Experimental setup: In a 96-well plate, 1x10^5 cells per well were incubated in 100 µL medium containing 0, 5, 20, 100, 200, 500, 1000, 2000 nM of S63845. The mixture was incubated for 48 h before read-out via flow cytometric measurement of Annexin V and 7AAD. DMSO was used as a vehicle control. Results show mean and standard deviation of three to four independent experiments.

4.9 Assessment of 199R cell lines treated with chemotherapy

Lastly, we aimed to investigate the impact of chemotherapeutic drugs on venetoclax resistant cell lines. In 2014, Fresquet et al. found that resistance to BCL2 inhibitors can lead to cross resistance to chemotherapeutic drugs in B cell malignancies [193]. Therefore, our final aim was to determine whether artificially established resistance to venetoclax triggered cross resistance to chemotherapeutic drugs or, on the contrary, if venetoclax resistance could be overcome by chemotherapy. We analyzed sensitivity to cytarabine, the most common chemotherapeutic drug used in AML treatment.

4.9.1 Measurement of cell viability

Cell viability of both parental and 199R AML cells after cytarabine treatment was measured in a dose-dependent manner using CTG (Figure 18). In most cell lines, higher doses of cytarabine (>1000 nM) were required to cause cell death in both parental cells and 199R cells. NOMO-1 199R, MOLM-13 199R and PL-21 199R were significantly more susceptible to higher doses of cytarabine than their parental equivalent. Significant cross resistance could be observed in AML cell line HL-60. While parental HL-60 cells showed the highest susceptibility of all AML cells, 199R cells showed no decrease in cell viability. Other than that, lack of response to cytarabine only occurred as a combined effect in both parental and 199R cells of SIG-M5, MOLM-16 and KASUMI-1. The respective IC_{50} can be found in Table 23.

Cell Line	IC_{50} S (nM)	IC_{50} 199R (nM)
HL-60	356,7	>5000
ML-2	550,7	1327
OCI AML-2	3735	3092
MOLM-13	4398	1909
PL21	>5000	2282
NOMO-1	>5000	2675
KASUMI-1	>5000	>5000
SIGM-5	>5000	>5000
MOLM-16	>5000	>5000

Table 23: IC_{50} values for cytarabine in S and 199R AML cell lines

Cell lines are ordered by the parental cells' IC_{50}. Cell lines in green are more susceptible to cytarabine upon venetoclax resistance. Cell line HL-60 in red shows decreased susceptibility to cytarabine upon venetoclax resistance.

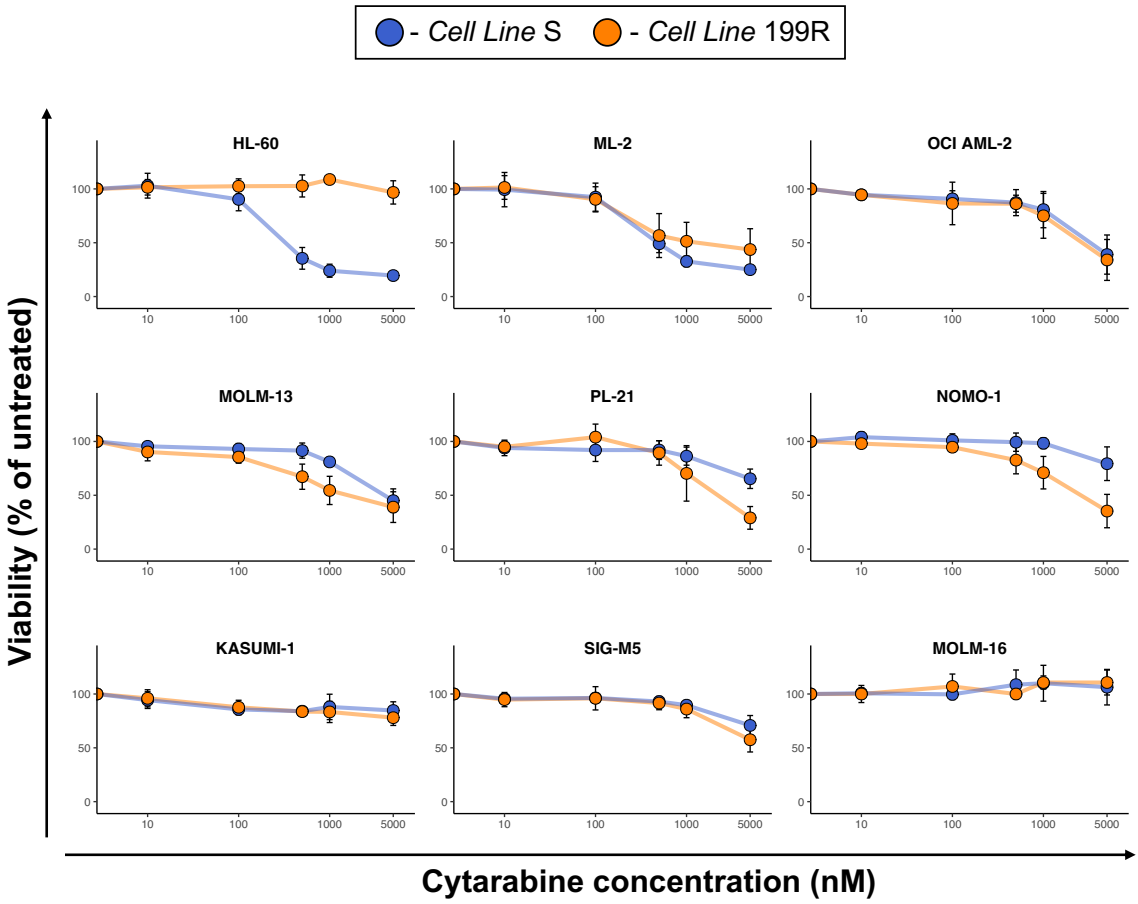

Figure 18: Cell viability of AML cell lines S and 199R treated with cytarabine

Experimental setup: In a 96-well plate, 1x10^5 cells per well were incubated in 100 µL medium containing 0, 10, 100, 500, 1000 and 5000 nM of cytarabine. The mixture was incubated for 48 h before read-out via CellTiter-Glo® Luminescent Cell Viability Assay. PBS was used as a vehicle control. Results show mean and standard deviation of three to four independent experiments.

4.9.2 Detection of cell death markers

Finally, we took a closer look at the expression of apoptosis-related proteins after cytarabine treatment. Western Blot analysis was performed on AML cell lines OCI AML-2 and HL-60. We investigated cleavage of PARP, cleavage of caspase 3 and expression of γH2A.x. Figure 19 displays that cytarabine treatment did not have a strong impact on parental OCI AML-2 cells. No definitive cleavage of PARP or caspase 3, nor increased expression of γH2A.x was detected in parental OCI AML-2 cells when exposed to cytarabine. On the other hand, strong cleavage of PARP, minor cleavage of caspase 3 and a slightly increased expression of γH2A.x could be observed in 199R cells of OCI AML-2.

However, cleavage of PARP and caspase 3 as well as increased expression of γH2A.x were indeed observed in HL-60 S cells treated with cytarabine. HL-60 199R did not express any of the marker proteins related to cell death after cytarabine treatment.

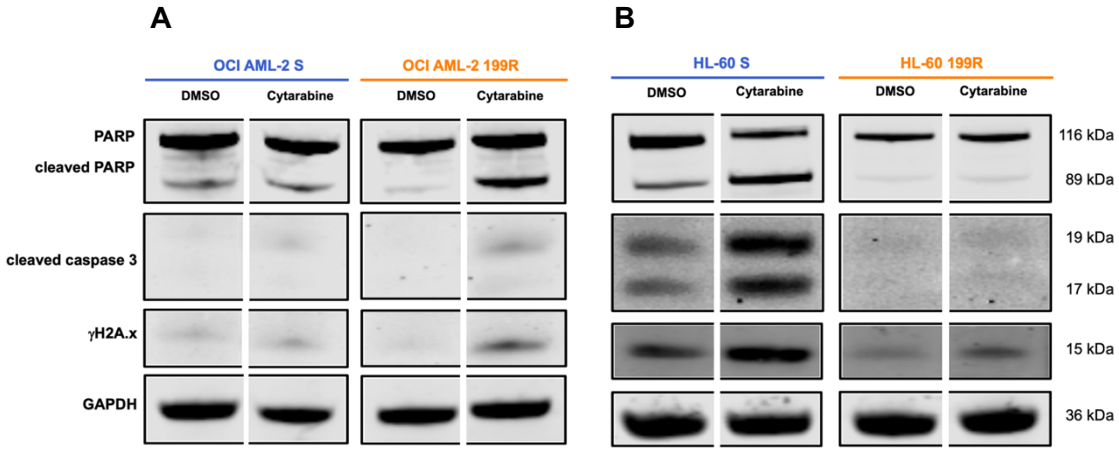

Figure 19: Western Blot analysis of cell death related proteins after cytarabine treatment

A: OCI AML-2 S and OCI AML-2 199R treated with cytarabine. **B:** HL-60 S and HL-60 199R treated with cytarabine. Experimental setup: $3x10^6$ cells were incubated with 2 µM venetoclax, 5 µM cytarabine and DMSO as a vehicle control for 4 h. GAPDH was used as loading control. This Western Blot is representative for three independent experiments.

5 Discussion

Resistance to BCL2 inhibitors in AML is a pressing issue as most patients are unfit for intensive chemotherapy and therefore reliant on potent alternatives [4]. For this reason, we aimed to enhance understanding of resistance mechanisms to BCL2 inhibitor venetoclax. Our first step was to establish a comprehensive set of venetoclax-resistant AML cell lines. The generation of drug-resistant cell lines is a powerful instrument providing insight into the evolution of tumors and has been used in cancer research since the 1970s [230,231].

We chose nine parental AML cell lines from diverse backgrounds and highly heterogeneous behavior upon venetoclax treatment, ranging from high susceptibility to primary resistance. According to the TCGA, the most commonly mutated genes in AML patients include *NPM1, KRAS, NRAS, DNMT3A, TP53, IDH2, RUNX1, MUC16, ASXL1, FLT3, KIT, PTPN11, IDH1* and *CEBPA* (data from TARGET-AML and TCGA-LAML projects) [232]. Indeed, sequencing data published at cBioPortal confirmed that many of these genes were mutated in the AML cell lines we selected. A common genetic aberration in AML, which was reported in three cell lines is rearrangement of *KMT2A* [6,7,14]. However, the common fusion genes *PML::RARA* or *CBFB::MYH11* were not detected [14]. Interestingly, 4/9 cell lines were described to harbor *TP53* mutations, which is associated with a poor prognosis [7]. On the other hand, no cell line was reported to contain mutated *NPM1*, which is among the most frequently mutated genes in AML and associated with a favorable prognosis [7,232,233]. However, it must be considered that cell lines are artificial models, which are prone to genomic instability [234]. Nonetheless, the heterogeneity of our cell line set accurately represents the complex nature of AML and treatment responses in patients, and thus enabled us to investigate venetoclax resistance in different settings.

Long-term exposure led to loss of susceptibility to venetoclax in all AML cell lines, as our results confirmed. In fact, venetoclax resistance could be established regardless of the parental cell line's genetic profile or IC_{50}. 199R cell lines exhibited no decreased cell viability up to 5µM of venetoclax, while cell lines were continuously cultivated at a maintenance dose of only 2µM. This gives proof of the robust resistance generated by our method. Cleavage of caspase 3 and PARP indicates execution phase of late apoptosis. While PARP becomes inactivated, caspase 3 becomes activated upon cleavage. Histone H2A.x serves as DNA stabilizer and is involved in DNA damage response. It is phosphorylated upon DNA double-strand breaks. Hence, expression of γH2A.x is a sign of DNA damage [235]. In parental cell lines, cleavage of PARP and caspase 3 thus demonstrate effective mitochondrial apoptosis following venetoclax treatment. Expression of γH2A.x implies occurrence of DNA double strand breaks. In 199R cell lines, however, lack of cleaved PARP and cleaved caspase 3 proves failure of intrinsic apoptosis. This finding supports our hypothesis that venetoclax resistance is based on deficient mitochondrial apoptosis.

We then sought to find cellular explanations for the emergence of venetoclax resistance in our cell lines. Therefore, we compared each pair of parental and 199R cell on DNA, RNA, and protein level in order to pinpoint potentially resistance-inducing alterations. Furthermore, we explored differences in cellular changes between intrinsically susceptible and primary resistant cell lines after the generation of venetoclax resistance.

Acquired genetic aberrations can influence drug susceptibility in many different ways and may even account for adapted resistance. Interestingly, most frequent Δ mutations revealed in our WES experiment, acquired in either three or two cell lines, are among the most common mutations across all cancers according to the TCGA database: *TTN* and *MUC16* are second and third most common genetic mutations following *TP53*, while *USH2A* ranks at position eight [228]. The exact impact of mutated *TTN*, which is usually responsible for muscle elasticity, transmembrane mucin protein *MUC16* and basement membrane-associated protein *USH2A* is not clear. However, it is suggested by a multitude of publications that all three mutations are associated with tumor mutational burden in a variety of cancers [236-241].

It is noteworthy that a large part of genes containing Δ and enriched mutations is represented by the hallmark of cancer “resisting cell death” (16 and 6 mutations, respectively). Again, this supports our hypothesis that venetoclax resistance stems from impaired mitochondrial apoptosis.

As described above, a variety of mutations in the *BCL2* gene have been found to confer resistance in patients with lymphoid malignancies undergoing long-term venetoclax treatment [194,196-198]. In our WES results, no 199R cell line harbored a *BCL2* mutation. Therefore, impaired drug binding by mutations leading to structural changes in BCL2 cannot account for adapted resistance. In fact, the only mutation found in a Bcl-2 family gene was a splice variant of *BID* in NOMO-1. To our knowledge, this mutation has not been described before, however, its relevance is questionable, as both parental and 199R cell lines exhibited this mutation and enrichment in 199R cell lines was neglectable.

Providing alternative explanations for acquired venetoclax resistance, we found that many cell lines acquired or enriched highly oncogenic mutations. It has been described that enrichment of dominant, preexisting mutations fosters venetoclax resistance in AML, rather than acquisition of new mutations like in CLL [208]. Of special interest, *FLT3* mutation, which is characteristic of AML, was enriched following venetoclax resistance in OCI AML-2. Acquisition of *FLT3* ITD has been described in patients with acquired resistance to venetoclax [209]. While internal tandem duplications of *FLT3* are more common in AML, point mutations in this gene occur as well. Usually, these affect the gene segment encoding the tyrosine kinase domain (TKD) 2. As a result, aspartate residue at 835 (D835) is substituted for tyrosine, histidine or valine [242,243]. While ITD leads to constitutive activation of FLT3 and thereby downstream

signaling of PI3K, Ras and STAT5, the exact impact of TKD mutations remains to be elucidated [244,245]. According to our results, a *FLT3* missense mutation occurs at A680V in OCI AML-2 199R. This mutation transfers to the tyrosine kinase domain 1 (TKD1). In pro-B murine Ba/F3 cells, which are usually growth-dependent on interleukin-3 (IL-3), *FLT3* A680V mutation gave rise to IL-3 independent survival and growth [246]. Molecular dynamics simulation revealed that the mutation favors a conformational shift towards a permanently active state of the kinase by destabilizing the juxtamembrane domain (JMD) [246]. Therefore, strong enrichment in our 199R cell line may indicate that this mutation promotes cell survival through constitutive oncogenic signaling.

Moreover, V600E substitution in serine/threonine kinase *BRAF* was enriched in SIG-M5 199R. V600E is the most common mutation in *BRAF* and can be detected across many types of cancer including melanoma and hairy cell leukemia [247,248]. The substitution of valine for glutamate at position 600 is located inside the activation segment and facilitates increased kinase activity, giving rise to elevated MEK/MAPK/ERK signaling [249]. A *BRAF* mutation, albeit at a different location, has been linked to clinical venetoclax resistance in a CLL patient before [191], highlighting its oncogenic potential to circumvent venetoclax treatment.

In addition, aberrations of *TP53* were acquired or enriched in several 199R cell lines. Five in six detected mutations (OCI AML-2, KASUMI-1, MOLM-16 (2), NOMO-1) affect the p53 DNA binding domain, resulting in reduced DNA binding capacity of p53 and therefore impaired protein function [250]. On the other hand, one cell line (PL-21) harbors a *TP53* deletion affecting the TAD of p53. Since the vast majority of *TP53* mutations are described to be located in the DNA binding domain, research on p53 TAD mutations is scarce. One study suggests a vital role for TAD in maintaining DNA integrity, although it is not directly involved in DNA damage repair [251]. Hence, TAD mutations could be associated with impaired protein function, just like mutations in the DNA binding domain.

In OCI AML-2 199R, *TP53* Y220C mutation was newly acquired following venetoclax resistance. This location inside the p53 DNA binding domain is among the most common *TP53* mutation sites [252], and has been described in numerous patients with hematologic malignancies, including AML [253]. Moreover, the detection of an acquired or enriched *TP53* binding domain mutation is in line with published sequencing results from AML patients relapsed under venetoclax therapy [207]. Additionally, knockout of *TP53* resulted in venetoclax resistance in AML cell lines [206]. From these results, we concluded that acquired venetoclax resistance in OCI AML-2 is likely to be mediated by this *TP53* mutation at Y220C. Surprisingly, WES revealed that parental OCI AML-2 cells harbored yet another *TP53* mutation (V274L). This mutation did not appear in the sequencing results published on cBioPortal and its clinical relevance is questionable, as there is only a negligible number of AML patients harboring this mutation [254,255]. In OCI AML-2 cells, the mutation disappeared after development of venetoclax

resistance. Consequently, the highly oncogenic potential of the newly acquired *TP53* mutation at Y220C outweighed the importance of the preexisting *TP53* mutation at V274L.

The remaining aberrations of *TP53* were found in KASUMI-1, PL-21, MOLM-16 (2) and NOMO-1. As mentioned above, these aberrations were preexistent in parental cell lines. Importantly, parental cell lines PL-21, MOLM-16 and NOMO-1 are inherently resistant to treatment with venetoclax. Therefore, we concluded that *TP53* mutation promotes not only adapted, but also primary resistance to venetoclax. Again, these results are supported by a recent publication on primary venetoclax resistance in AML patients [207]. Overall, AML patients harboring mutated *TP53* remain to have particularly poor outcomes, with similar responses to either intensive chemotherapy or combination treatment with venetoclax and HMA [256,257]. A recent study even provides evidence that in AML patients with mutated *TP53*, venetoclax in combination with HMA did not improve overall survival compared to HMA alone [258], highlighting the lack of efficacy of venetoclax in *TP53*-mutated disease. One of p53's many functions is the regulation of Bcl-2 family expression by increasing transcription of proapoptotic proteins including PUMA, NOXA, and BAK [206,259]. Therefore, lack of p53 hampers mitochondrial apoptosis via reduced expression of proapoptotic proteins. However, p53 knockout in AML cell lines has also been shown to decrease BCL2 expression [206]. As venetoclax directly binds to BCL2, reduced levels of BCL2 due to p53 inactivation may lead to reduced sensitivity to venetoclax. The exact genetic mechanisms underlying primary and secondary resistance to therapy in *TP53* mutated malignancies remain to be fully understood, but are thought to originate mainly in the association with complex karyotype and (sub-)clonal expansion [207,260,261]. In several AML patients relapsing under venetoclax treatment, *TP53* mutation expansion led to complete loss of chromosome locus 17p, while in several primary refractory AML patients, del(17p) was already present at baseline[207], suggesting that biallelic inactivation of *TP53* is a major factor in venetoclax resistance. All in all, venetoclax, as all established therapeutic options for AML, is not capable of circumventing *TP53* deficiency permanently. This highlights the need to further investigate potential treatment options, especially for high risk AML patients with *TP53* mutation or loss.

Parental KASUMI-1 cells harbor R248Q mutation, which is the second most common *TP53* mutation according to COSMIC database [252]. However, parental KASUMI-1 cells are not refractory to venetoclax. In fact, KASUMI-1 S is the second most susceptible cell line under venetoclax treatment with an IC_{50} of 44,7 nM. Consequently, mutation of *TP53* alone may not always confer intrinsic venetoclax resistance.

RNA sequencing provides valuable insights into gene expression changes which may account for venetoclax resistance. Throughout all RNA sequencing analyses of AML cell lines, the most recurrent significant finding was upregulation of antiapoptotic Bcl-2 family member MCL1. This was to be expected, as numerous publications have associated MCL1 overexpression with the

emergence of tumors in general, and BCL2 inhibitor resistance in particular [143,183,262-265]. The RNA single read counts and Western Blot results were reflective of this as well. MCL1 RNA upregulation could even be observed across all cell lines, regardless of parental cell line profile or baseline susceptibility to venetoclax treatment, including intrinsically resistant cell lines MOLM-16 and NOMO-1. Although technically no compensatory mechanism would have been necessary in those cell lines, MCL1 was upregulated in the 199R equivalent. Similar findings have been described before and indicate that reprogramming of mitochondrial apoptosis takes place [188,202]. As a result, cells no longer depend on BCL2 for survival, but shift towards MCL1. However, the exact mechanisms of MCL1 upregulation remain to be elucidated. A possible explanation is increased protein stability followed by long-term transcriptional upregulation [202]. Furthermore, downregulation of BCL2 mRNA and protein, which we detected in five cell lines (OCI AML-2, HL-60, SIG-M5, ML-2 and KASUMI-1), has been observed in cell lines before and is associated with venetoclax resistance in patients [202,265]. This mechanism may accompany compensatory upregulation of other antiapoptotic proteins like MCL1 and render BCL2 inhibition ineffective. Interestingly, BCL2 expression was almost completely absent in parental and 199R MOLM-16 cells. This finding is supported by a very low number of single read counts in our RNA sequencing analysis. While the SRC mean across all parental and 199R cell lines is 590 and 465, respectively, MOLM-16 analysis yielded 5 and 9 read counts, respectively. Likewise, immunoblotting showed very low BCL2 expression levels in parental and 199R NOMO-1 cells. Therefore, lack of BCL2 is another possible explanation for the intrinsic resistance to BCL2 inhibitor venetoclax in parental cell lines MOLM-16 and NOMO-1. BAX downregulation was detected using RNA sequencing and Western Blots in two cell lines (OCI AML-2 and SIG-M5). Loss of BAX via knockout has been described to impart venetoclax resistance in AML cell lines before [206]. By decreasing the level of this proapoptotic effector, MOMP is hampered. As a result, cytochrome c cannot be released from the mitochondrial intermembrane space and therefore activation of the execution phase of apoptosis cannot take place.

Moreover, both methods confirmed downregulation of proapoptotic mRNA/protein PUMA in OCI AML-2. PUMA is a direct target of p53 and therefore necessary for DNA damage-induced apoptosis via p53 activation. Moreover, it promotes p53-independent apoptosis upon cytotoxic stimulation. Loss of PUMA is associated with resistance to p53-dependent and independent stimuli [163,266]. However, PUMA downregulation has not been described before in venetoclax resistance. Of note, PUMA-lacking cell line OCI AML-2 acquired *TP53* mutation as a result of venetoclax resistance, as discussed earlier. Assumably, this mutation-induced lack of p53 activity resulted in diminished levels of PUMA.

Slight upregulation of BAK was detected in both RNA sequencing and Western Blot results of OCI AML-2, NOMO-1, ML-2. Single read counts indicated that even more cell lines had

upregulated levels of BAK after venetoclax resistance. As BAK is a proapoptotic member of the Bcl-2 family initiating MOMP, its upregulation upon BCL2 inhibition seems counterintuitive. However, similar observations in venetoclax resistant AML cell lines have been published before [202]. Although we cannot explain this phenomenon, the role of BAK in venetoclax resistance appears paradox.

Despite its frequently described upregulation in the context of venetoclax resistance, BCL-xL expression was not significantly altered in our 199R cell lines.

Regarding overall changes of mRNAs pan cell lines, we found upregulation of ubiquitin proteasome system (UPS) members including PSMD4, PSMB4, USP18 and UBQLN4. The UPS is responsible for proteolytic protein degradation and therefore involved in a myriad of cellular processes like gene expression, cell cycle and protein quality control [267]. Overexpression of UPS members has been described to be associated with various diseases including cancers. This pathway can be targeted by the proteasome inhibitor bortezomib, which was approved for relapsed/refractory multiple myeloma (R/R MM) nearly two decades ago [268,269]. In the past, bortezomib either alone or as combination therapy has been tested for AML treatment in both pre-clinical and clinical trials, with mixed results and frequent dose-limiting toxicity [270,271]. Moreover, combination treatment with venetoclax and bortezomib showed synergistic effects in sarcoma cell lines [272], and improved progression-free survival in R/R MM [273]. In myeloma cell lines, resistance to venetoclax did not confer increased sensitivity to bortezomib [274]. However, in venetoclax resistant MM xenografts models expressing BCL2 and MCL1, bortezomib was found to restore sensitivity to venetoclax [275]. The effect of bortezomib or other proteasome inhibitors on venetoclax resistant AML has not been studied yet, and might be a promising approach, considering our mRNA findings.

Furthermore, we detected upregulation of mitochondrial ribosomal proteins (MRPs) MRPL9 and MRPS21. MRPs not only translate mtDNA and synthesize proteins related to oxidative phosphorylation (OXPHOS), but are also reportedly involved in programmed cell death as apoptosis-inducing factors. Abnormal expression of MRPs has been found in several cancers including hematologic malignancies [276,277]. Intriguingly, Sharon et al. recently found that inhibition of mitochondrial translation with ribosome-targeting antibiotic tedizolid overcame resistance in venetoclax-resistant AML cell lines and xenograft models [204]. More studies reported that patients with intrinsic or adapted resistance to venetoclax treatment exhibited elevated OXPHOS driven by MCL1 upregulation, nicotinamide metabolism, or fatty acid metabolism, respectively [265,278,279]. This emphasizes the importance of deregulated MRPs and mitochondrial translation as a potential target for venetoclax resistant AML.

The single most upregulated mRNA in our RNA sequencing results was FOXC1. This transcription factor regulates lineage differentiation and correct embryonic development. However, its expression is also involved in stem cell regulation, and its overexpression has

been found to promote tumor progression and metastasis by fostering cancer stem cell like properties [280-282]. In AML, FOXC1 exerts its tumor-promoting potential by blocking monocytic differentiation [281].

Considering only cell lines with high intrinsic susceptibility to venetoclax (MOLM-13, KASUMI-1, OCI AML-2, ML-2), some significantly deregulated mRNAs concurred with results from all cell lines, e.g., MRPL9, MRPS21 and MCL1. However, many hits were exclusively deregulated in the venetoclax resistant counterpart of intrinsically susceptible cell lines, providing insight into the process of adapted resistance. Striking findings included upregulation of HES1, a transcription factor involved in stem cell maintenance and presumably in metastasis and multidrug resistance [283], as well as downregulation of PSTPIP2, whose absence is associated with autoinflammatory diseases [284] and SUCNR1, which regulates myeloid cell function in inflammation [285].

RNA analysis of intrinsically resistant cell lines (HL-60, SIG-M5, PL-21, MOLM-16, NOMO-1) allows detection of gene expression changes, when assumably only little or no adaption mechanisms were necessary. Elevated expression of TNFAIP8L2-SCNM1 fusion gene could be detected. Since *TNFAIP8L2* and *SCNM1* genes are neighboring on chromosome 1, fusion may occur by read-through transcription [286]. Significantly downregulated mRNA included HSPA6, which is assumed to have tumor-suppressing properties [287].

In recent years, understanding of tumor subpopulations and clonal evolution has improved massively through single cell analysis [288-291]. Here, we are able to integrate single cell RNA sequencing analysis of two patients pre-treatment and post-venetoclax resistance into our cell line-based data. Compared with RNA sequencing results from cell lines, single cell RNA sequencing results from patient samples revealed completely different gene expression changes after disease progression. Analysis of all three conditions combined yielded many interesting, upregulated mRNA hits following venetoclax resistance including NOTCH1, ERG, and FGFR1. NOTCH1 is a transmembrane protein with the ability to influence gene expression upon extracellular signals. Therefore, it is involved in a variety of signaling pathways. Activating mutations are a common feature of T-ALL, however, increased NOTCH1 expression can be found in other cancers, too [292,293]. ERG is a transcription factor necessary for development and differentiation processes like angiogenesis or hematopoiesis. Maintained expression of ERG has been linked to T-ALL, megakaryoblastic leukemias and, more recently, to prostate carcinoma [294-296]. Rearrangement of the *FGFR1* gene results in a rare, atypical myeloproliferative disorder called 8p11 myeloproliferative syndrome, which is characterized by constitutive FGFR1 kinase activation and enhanced oncogenic signaling [297].

Of note, Bcl-2 family mRNAs were found to be deregulated as well, but in a different way compared to cell lines. In fact, BCL2 was significantly upregulated following venetoclax resistance, as opposed to its downregulation in 199R cell lines, and BCL-xL (BCL2L1) was

significantly downregulated, which is contrary to published data of venetoclax resistance in AML. These phenomena cannot be explained at this point and therefore need more investigation. Since, contrary to 199R cell lines, no MCL1 upregulation was found and BCL-xL was downregulated, we inferred that no dependence shift from one antiapoptotic protein to another occurred. Instead, venetoclax resistance was accompanied by elevated BCL2 expression and upregulation of the abovementioned tumor-promoting pathways.

Individual analyses of each condition yielded similar results. Interestingly, post-resistance cells which had the same genotypic profile as tumor cells pre-treatment (condition 1), not only exhibited upregulated BCL2 and downregulated BCL-xL, but also upregulated MCL1 and BID, as well as downregulated BIM (BCL2L11) and PUMA (BBC3). These post-resistance cells are not part of the outgrown, venetoclax-resistant clone. Therefore, it is interesting to see that in condition 1, still the most Bcl-2 family members were found to be deregulated out of all conditions. Suppression of proapoptotic BIM and PUMA, concomitant with upregulation of pro-survival MCL1 suggests that deregulated mitochondrial apoptosis was associated with venetoclax resistance. Analysis of gene expression changes between cells with the genotypic profile of the venetoclax-resistant clone pre-treatment and post-resistance (condition 2) yielded no significantly altered Bcl-2 family members. As the pre-treatment cells within this group presumably had the genetic profile driving the clonal evolution during venetoclax treatment, this did not take us by surprise. No gene expression changes were needed to adapt to venetoclax treatment. Post-resistance tumor cells exhibited upregulated BCL2 and downregulated BCL-xL, compared to the majority of pre-treatment tumor cells (condition 3). This condition compares the largest number of cells (most tumor cells pre-treatment vs. most tumor cells post-resistance) and therefore represents gene expression changes upon acquired venetoclax resistance most accurately.

In summary, DNA, RNA, and protein analyses of parental and 199R cell lines provide ample information on potential mechanisms of venetoclax resistance in AML. These included the acquisition or enrichment of oncogene or tumor suppressor gene mutations, upregulation of tumor-promoting pathways and downregulation of tumor-suppressing pathways. We could confirm our first hypothesis, as we showed that defective mitochondrial apoptosis promoted venetoclax resistance via upregulation of MCL1 and downregulation of BCL2 in 199R cell lines. In patient samples, Bcl-2 family members were differently deregulated, as mainly BCL2 upregulation and BCL-xL downregulation was detectable. In addition, our data provide possible explanations for upfront resistance to venetoclax. *TP53* mutations were detected in all three primary resistant parental cell lines, and lack of BCL2 expression in one of them. Of important note, intrinsically resistant cell lines accumulated many changes on DNA, RNA, and protein level, although, technically, there was no need for adapting to venetoclax treatment.

As a final step, we sought to overcome venetoclax resistance. Targeting one proapoptotic and one antiapoptotic Bcl-2 family protein allowed us to examine the impact of deregulated mitochondrial apoptosis and possible therapeutic implications. The fact that PUMA deficiency causes resistance to p53-dependent and independent stimulation, alongside with definite downregulation of PUMA in our Western Blot and RNA sequencing results of OCI AML-2 199R, provided rationale for more detailed investigation of PUMA. Inspired by the effect of BAX knockout, which imparts venetoclax resistance in AML cell lines [206], we established a PUMA knockout in the AML cell line OCI AML-2. We showed that, upon very low doses of venetoclax, cells lacking PUMA showed slightly enhanced cell survival compared to cells expressing PUMA. This finding supports the idea that downregulation of PUMA may contribute to the emergence of venetoclax resistance.

Recent publications proved that MCL1 upregulation can be successfully targeted by multiple MCL1 inhibitors in vitro, resulting in promising phase 1 clinical trials [212,213,262,298]. We aimed to address upregulation of the antiapoptotic Bcl-2 family member MCL1 in our cell lines and determine differences in behavior to MCL1 inhibition across all cell lines. S63845 was cytotoxic in all AML cell lines with the highest IC_{50} around 1000nM. As MCL1 inhibition caused decreased cell viability compared to parental cell lines in eight of nine cell lines, we inferred that MCL1 upregulation in 199R cell lines renders cells more susceptible to MCL1 inhibition. In fact, IC_{50} of 199R cell lines ranged from <5 nM to only 235 nM, demonstrating its high efficacy in the venetoclax resistant setting. Even PL21, where hardly any MCL1 expression could be detected using Western Blot analysis, had an IC_{50} more than tenfold lower after venetoclax resistance compared to parental cells. Notably, HL-60, which according to immunoblot and RNA sequencing results showed highest enrichment of MCL1 after acquired venetoclax resistance, also had the highest IC_{50} S/IC_{50} 199R ratio (1031 nM/16 nM), suggesting that strong enrichment of MCL1 renders cells highly dependent on MCL1 and therefore highly susceptible to its inhibition. The only cell line where venetoclax resistance did not confer higher susceptibility to MCL1 inhibition was MOLM-16. We did not expect this observation, as enriched MCL1 was indeed found in Western Blot and RNA sequencing results of MOLM-16 199R, but apparently it did not render cells more susceptible to MCL1 inhibition. However, it must be considered that MCL1 was still very effective in MOLM-16 199R (IC_{50} 199R 132 nM). In short, MCL1 upregulation made cells reliable on MCL1 and thus more sensitive to MCL1 inhibition. Others have even described a synergistic effect of venetoclax and S63845 [298,299].

Finally, we evaluated the impact of the most commonly used chemotherapeutic drug in AML treatment, cytarabine, in the venetoclax-resistant setting. On the one hand, studies have shown that venetoclax resistance may trigger cross-resistance to other antineoplastic drugs [193]. On the other hand, however, combining venetoclax with chemotherapeutic drugs like daunorubicin and cytarabine has been shown to increase DNA damage and decrease MCL1

levels compared to venetoclax monotherapy [300]. Although this effect was described for combination treatment and not after established venetoclax resistance, we were eager to uncover the impact of cytarabine on our heterogeneous, venetoclax-resistant AML cell lines.
Unlike venetoclax, cytarabine in lower doses had only minor effects on cell viability in most AML cell lines. Higher doses were needed to cause cell death in both parental cells and 199R cells. Three parental cell lines showed intrinsic resistance to up to 5 µM of cytarabine, which did not change upon venetoclax resistance. With IC_{50}s usually ranging below 1000 nM according to the literature, we did not expect this phenomenon. A variety of mechanisms have been described which render AML cells resistant to cytarabine. These include upregulation of ENTPD1, which enhances mitochondrial activity, expression of the membrane transporter p-glycoprotein promoting efflux of chemotherapeutic drugs and mutations of *DCK*, a crucial kinase for incorporation of cytarabine into DNA [301-303]. However, we could not confirm any of these findings in our WES and RNA sequencing data. An improvement to this experiment would be prolonged incubation time to induce cytarabine-dependent cell death, as many published studies examined cell viability after 72 hours of treatment. Three other 199R cell lines were much more susceptible to cytarabine compared to the parental counterpart. Presumably, resistance to venetoclax sensitized these cell lines to chemotherapeutic drugs. Of important note, we could find cross resistance to cytarabine in 199R cell line HL-60. Western Blot results confirmed that cytarabine was able to induce DNA double strand breaks (γH2A.x expression) and execution phase of apoptosis (cleavage of PARP and caspase 3), while no apoptosis and only slight signs of DNA double strand breaks were visible in HL-60 199R treated with cytarabine. Our WES and RNA sequencing results did not provide conclusive explanations for this finding. However, it is notable that HL-60 cells acquired most mutations after venetoclax resistance out of all AML cell lines. Possibly, one or several mutations have led to acquired cross-resistance to cytarabine. To conclude, additional experiments would be necessary to explain differences in intrinsic susceptibility to cytarabine and the heterogeneous effect cytarabine had on 199R cell lines.
In summary, we could confirm our second hypothesis, as it is possible to circumvent venetoclax resistance in AML cell lines by targeting other Bcl-2 family proteins. Moreover, we showed that chemotherapy, which remains the backbone of AML therapy, shows heterogeneous efficacy in venetoclax-resistant cell lines.
All in all, in this study we were able to identify mechanisms of primary and acquired resistance to BCL2 inhibitor venetoclax and demonstrated approaches to overcome this resistance.

6 References

1. Dohner H, Weisdorf DJ, Bloomfield CD. Acute Myeloid Leukemia. *N Engl J Med* 2015; **373**(12): 1136-52.
2. Siegel RL, Miller KD, Fuchs HE, Jemal A. Cancer Statistics, 2021. *CA: A Cancer Journal for Clinicians* 2021; **71**(1): 7-33.
3. Visser O, Trama A, Maynadié M, et al. Incidence, survival and prevalence of myeloid malignancies in Europe. *European Journal of Cancer* 2012; **48**(17): 3257-66.
4. Cancer Research UK. Acute Myeloid Leukemia (AML) statistics. https://www.cancerresearchuk.org/health-professional/cancer-statistics/statistics-by-cancer-type/leukaemia-aml (Last accessed Feb 24, 2024)
5. National Cancer Institute. SEER Cancer Stat Facts: Acute Myeloid Leukemia. https://seer.cancer.gov/statfacts/html/amyl.html (Last accessed Feb 24, 2024).
6. Khoury JD, Solary E, Abla O, et al. The 5th edition of the World Health Organization Classification of Haematolymphoid Tumours: Myeloid and Histiocytic/Dendritic Neoplasms. *Leukemia* 2022; **36**(7): 1703-19.
7. Döhner H, Wei AH, Appelbaum FR, et al. Diagnosis and management of AML in adults: 2022 recommendations from an international expert panel on behalf of the ELN. *Blood* 2022; **140**(12): 1345-77.
8. ACKERMAN GA. MICROSCOPIC AND HISTOCHEMICAL STUDIES ON THE AUER BODIES IN LEUKEMIC CELLS. *Blood* 1950; **5**(9): 847-63.
9. Grimwade D, Walker H, Oliver F, et al. The importance of diagnostic cytogenetics on outcome in AML: analysis of 1,612 patients entered into the MRC AML 10 trial. The Medical Research Council Adult and Children's Leukaemia Working Parties. *Blood* 1998; **92**(7): 2322-33.
10. Patel JP, Gönen M, Figueroa ME, et al. Prognostic Relevance of Integrated Genetic Profiling in Acute Myeloid Leukemia. *New England Journal of Medicine* 2012; **366**(12): 1079-89.
11. Papaemmanuil E, Gerstung M, Bullinger L, et al. Genomic Classification and Prognosis in Acute Myeloid Leukemia. *New England Journal of Medicine* 2016; **374**(23): 2209-21.
12. Grimwade D, Ivey A, Huntly BJP. Molecular landscape of acute myeloid leukemia in younger adults and its clinical relevance. *Blood* 2016; **127**(1): 29-41.
13. Vakiti A, Mewawalla P. Acute Myeloid Leukemia Symptoms: StatPearls Publishing, Treasure Island (FL); 2022.
14. Cancer Genome Atlas Research N, Ley TJ, Miller C, et al. Genomic and epigenomic landscapes of adult de novo acute myeloid leukemia. *N Engl J Med* 2013; **368**(22): 2059-74.
15. Swart LE, Heidenreich O. The RUNX1/RUNX1T1 network: translating insights into therapeutic options. *Experimental Hematology* 2021; **94**: 1-10.
16. De Kouchkovsky I, Abdul-Hay M. 'Acute myeloid leukemia: a comprehensive review and 2016 update'. *Blood Cancer J* 2016; **6**(7): e441.
17. Matthews A, Pratz KW. Optimizing outcomes in secondary AML. *Hematology* 2022; **2022**(1): 23-9.
18. Houot J, Marquant F, Goujon S, et al. Residential Proximity to Heavy-Traffic Roads, Benzene Exposure, and Childhood Leukemia-The GEOCAP Study, 2002-2007 *Am J Epidemiol* 2015; **182**(8): 685-93.
19. Bizzozero OJ, Johnson KG, Ciocco A, et al. Radiation-Related Leukemia in Hiroshima and Nagasaki, 1946–1964. *New England Journal of Medicine* 1966; **274**(20): 1095-101.
20. Yi M, Li A, Zhou L, Chu Q, Song Y, Wu K. The global burden and attributable risk factor analysis of acute myeloid leukemia in 195 countries and territories from 1990 to 2017: estimates based on the global burden of disease study 2017. *Journal of Hematology & Oncology* 2020; **13**(1): 72.
21. Dohner H, Estey E, Grimwade D, et al. Diagnosis and management of AML in adults: 2017 ELN recommendations from an international expert panel. *Blood* 2017; **129**(4): 424-47.

22. Kayser S, Döhner K, Krauter J, et al. The impact of therapy-related acute myeloid leukemia (AML) on outcome in 2853 adult patients with newly diagnosed AML. *Blood* 2011; **117**(7): 2137-45.
23. Wiernik PH, Sun Z, Cripe LD, et al. Prognostic effect of gender on outcome of treatment for adults with acute myeloid leukaemia. *Br J Haematol* 2021; **194**(2): 309-18.
24. Metzeler KH, Becker H, Maharry K, et al. ASXL1 mutations identify a high-risk subgroup of older patients with primary cytogenetically normal AML within the ELN Favorable genetic category. *Blood* 2011; **118**(26): 6920-9.
25. Gaidzik VI, Teleanu V, Papaemmanuil E, et al. RUNX1 mutations in acute myeloid leukemia are associated with distinct clinico-pathologic and genetic features. *Leukemia* 2016; **30**(11): 2160-8.
26. Bowen D, Groves MJ, Burnett AK, et al. TP53 gene mutation is frequent in patients with acute myeloid leukemia and complex karyotype, and is associated with very poor prognosis. *Leukemia* 2009; **23**(1): 203-6.
27. Haferlach C, Dicker F, Herholz H, Schnittger S, Kern W, Haferlach T. Mutations of the TP53 gene in acute myeloid leukemia are strongly associated with a complex aberrant karyotype. *Leukemia* 2008; **22**(8): 1539-41.
28. Abaza Y, Kantarjian H, Garcia-Manero G, et al. Long-term outcome of acute promyelocytic leukemia treated with all-trans-retinoic acid, arsenic trioxide, and gemtuzumab. *Blood* 2017; **129**(10): 1275-83.
29. Platzbecker U, Avvisati G, Cicconi L, et al. Improved Outcomes With Retinoic Acid and Arsenic Trioxide Compared With Retinoic Acid and Chemotherapy in Non-High-Risk Acute Promyelocytic Leukemia: Final Results of the Randomized Italian-German APL0406 Trial. *J Clin Oncol* 2017; **35**(6): 605-12.
30. Sorror ML, Storer BE, Elsawy M, et al. Intensive Versus Non-Intensive Induction Therapy for Patients (Pts) with Newly Diagnosed Acute Myeloid Leukemia (AML) Using Two Different Novel Prognostic Models. *Blood* 2016; **128**(22): 216-.
31. Kantarjian H, Kadia T, DiNardo C, et al. Acute myeloid leukemia: current progress and future directions. *Blood Cancer Journal* 2021; **11**(2): 41.
32. Burnett AK, Russell NH, Hills RK, et al. Optimization of Chemotherapy for Younger Patients With Acute Myeloid Leukemia: Results of the Medical Research Council AML15 Trial. *Journal of Clinical Oncology* 2013; **31**(27): 3360-8.
33. Holowiecki J, Grosicki S, Giebel S, et al. Cladribine, But Not Fludarabine, Added to Daunorubicin and Cytarabine During Induction Prolongs Survival of Patients With Acute Myeloid Leukemia: A Multicenter, Randomized Phase III Study. *Journal of Clinical Oncology* 2012; **30**(20): 2441-8.
34. Stone RM, Mandrekar SJ, Sanford BL, et al. Midostaurin plus Chemotherapy for Acute Myeloid Leukemia with a FLT3 Mutation. *N Engl J Med* 2017; **377**(5): 454-64.
35. Wei AH, Tiong IS. Midostaurin, enasidenib, CPX-351, gemtuzumab ozogamicin, and venetoclax bring new hope to AML. *Blood* 2017; **130**(23): 2469-74.
36. Larson RA, Mandrekar SJ, Huebner LJ, et al. Midostaurin reduces relapse in FLT3-mutant acute myeloid leukemia: the Alliance CALGB 10603/RATIFY trial. *Leukemia* 2021; **35**(9): 2539-51.
37. Hills RK, Castaigne S, Appelbaum FR, et al. Addition of gemtuzumab ozogamicin to induction chemotherapy in adult patients with acute myeloid leukaemia: a meta-analysis of individual patient data from randomised controlled trials. *The Lancet Oncology* 2014; **15**(9): 986-96.
38. Kapp-Schwoerer S, Weber D, Corbacioglu A, et al. Impact of gemtuzumab ozogamicin on MRD and relapse risk in patients with NPM1-mutated AML: results from the AMLSG 09-09 trial. *Blood* 2020; **136**(26): 3041-50.
39. Lancet JE, Uy GL, Cortes JE, et al. CPX-351 (cytarabine and daunorubicin) Liposome for Injection Versus Conventional Cytarabine Plus Daunorubicin in Older Patients With Newly Diagnosed Secondary Acute Myeloid Leukemia. *Journal of Clinical Oncology* 2018; **36**(26): 2684-92.

40. Stein EM, DiNardo CD, Fathi AT, et al. Ivosidenib or enasidenib combined with intensive chemotherapy in patients with newly diagnosed AML: a phase 1 study. *Blood* 2021; **137**(13): 1792-803.
41. Dholaria B, Savani BN, Hamilton BK, et al. Hematopoietic Cell Transplantation in the Treatment of Newly Diagnosed Adult Acute Myeloid Leukemia: An Evidence-Based Review from the American Society of Transplantation and Cellular Therapy. *Transplant Cell Ther* 2021; **27**(1): 6-20.
42. Cornelissen JJ, Blaise D. Hematopoietic stem cell transplantation for patients with AML in first complete remission. *Blood* 2016; **127**(1): 62-70.
43. Sureda A, Bader P, Cesaro S, et al. Indications for allo- and auto-SCT for haematological diseases, solid tumours and immune disorders: current practice in Europe, 2015. *Bone Marrow Transplant* 2015; **50**(8): 1037-56.
44. Pelcovits A, Niroula R. Acute Myeloid Leukemia: A Review. *R I Med J (2013)* 2020; **103**(3): 38-40.
45. Elsawy M, Sorror ML. Up-to-date tools for risk assessment before allogeneic hematopoietic cell transplantation. *Bone Marrow Transplantation* 2016; **51**(10): 1283-300.
46. Sorror ML, Storb RF, Sandmaier BM, et al. Comorbidity-age index: a clinical measure of biologic age before allogeneic hematopoietic cell transplantation. *J Clin Oncol* 2014; **32**(29): 3249-56.
47. Wei AH, Döhner H, Sayar H, et al. Long-Term Overall Survival (OS) with Oral Azacitidine (Oral-AZA) in Patients with Acute Myeloid Leukemia (AML) in First Remission after Intensive Chemotherapy (IC): Updated Results from the Phase 3 QUAZAR AML-001 Trial. *Blood* 2021; **138**(Supplement 1): 871-.
48. Mamdani H, Santos CD, Konig H. Treatment of Acute Myeloid Leukemia in Elderly Patients—A Therapeutic Dilemma. *Journal of the American Medical Directors Association* 2016; **17**(7): 581-7.
49. Kantarjian H, Ravandi F, O'Brien S, et al. Intensive chemotherapy does not benefit most older patients (age 70 years or older) with acute myeloid leukemia. *Blood* 2010; **116**(22): 4422-9.
50. Burnett AK, Milligan D, Prentice AG, et al. A comparison of low-dose cytarabine and hydroxyurea with or without all-trans retinoic acid for acute myeloid leukemia and high-risk myelodysplastic syndrome in patients not considered fit for intensive treatment. *Cancer* 2007; **109**(6): 1114-24.
51. Dombret H, Seymour JF, Butrym A, et al. International phase 3 study of azacitidine vs conventional care regimens in older patients with newly diagnosed AML with >30% blasts. *Blood* 2015; **126**(3): 291-9.
52. Quintás-Cardama A, Ravandi F, Liu-Dumlao T, et al. Epigenetic therapy is associated with similar survival compared with intensive chemotherapy in older patients with newly diagnosed acute myeloid leukemia. *Blood* 2012; **120**(24): 4840-5.
53. Vachhani P, Al Yacoub R, Miller A, et al. Intensive chemotherapy vs. hypomethylating agents in older adults with newly diagnosed high-risk acute myeloid leukemia: A single center experience. *Leuk Res* 2018; **75**: 29-35.
54. Kantarjian HM, Thomas XG, Dmoszynska A, et al. Multicenter, Randomized, Open-Label, Phase III Trial of Decitabine Versus Patient Choice, With Physician Advice, of Either Supportive Care or Low-Dose Cytarabine for the Treatment of Older Patients With Newly Diagnosed Acute Myeloid Leukemia. *Journal of Clinical Oncology* 2012; **30**(21): 2670-7.
55. DiNardo CD, Jonas BA, Pullarkat V, et al. Azacitidine and Venetoclax in Previously Untreated Acute Myeloid Leukemia. *N Engl J Med* 2020; **383**(7): 617-29.
56. DiNardo CD, Pratz K, Pullarkat V, et al. Venetoclax combined with decitabine or azacitidine in treatment-naive, elderly patients with acute myeloid leukemia. *Blood* 2019; **133**(1): 7-17.
57. Pollyea DA, Pratz KW, Jonas BA, et al. Venetoclax in Combination with Hypomethylating Agents Induces Rapid, Deep, and Durable Responses in Patients with AML Ineligible for Intensive Therapy. *Blood* 2018; **132**(Supplement 1): 285-.

58. Wei AH, Montesinos P, Ivanov V, et al. Venetoclax plus LDAC for newly diagnosed AML ineligible for intensive chemotherapy: a phase 3 randomized placebo-controlled trial. *Blood* 2020; **135**(24): 2137-45.
59. Pollyea DA, Pratz K, Letai A, et al. Venetoclax with azacitidine or decitabine in patients with newly diagnosed acute myeloid leukemia: Long term follow-up from a phase 1b study. *Am J Hematol* 2021; **96**(2): 208-17.
60. Cortes JE, Heidel FH, Hellmann A, et al. Randomized comparison of low dose cytarabine with or without glasdegib in patients with newly diagnosed acute myeloid leukemia or high-risk myelodysplastic syndrome. *Leukemia* 2019; **33**(2): 379-89.
61. Montesinos P, Recher C, Vives S, et al. Ivosidenib and Azacitidine in IDH1-Mutated Acute Myeloid Leukemia. *New England Journal of Medicine* 2022; **386**(16): 1519-31.
62. Price SL, Lancet JE, George TJ, et al. Salvage chemotherapy regimens for acute myeloid leukemia: Is one better? Efficacy comparison between CLAG and MEC regimens. *Leuk Res* 2011; **35**(3): 301-4.
63. Sarkozy C, Gardin C, Gachard N, et al. Outcome of older patients with acute myeloid leukemia in first relapse. *Am J Hematol* 2013; **88**(9): 758-64.
64. Westhus J, Noppeney R, Dührsen U, Hanoun M. FLAG salvage therapy combined with idarubicin in relapsed/refractory acute myeloid leukemia. *Leuk Lymphoma* 2019; **60**(4): 1014-22.
65. Parker JE, Pagliuca A, Mijovic A, et al. Fludarabine, cytarabine, G-CSF and idarubicin (FLAG-IDA) for the treatment of poor-risk myelodysplastic syndromes and acute myeloid leukaemia. *British Journal of Haematology* 1997; **99**(4): 939-44.
66. Spadea A, Petti MC, Fazi P, et al. Mitoxantrone, etoposide and intermediate-dose Ara-C (MEC): an effective regimen for poor risk acute myeloid leukemia. *Leukemia* 1993; **7**(4): 549-52.
67. DiNardo CD, Lachowiez CA, Takahashi K, et al. Venetoclax Combined With FLAG-IDA Induction and Consolidation in Newly Diagnosed and Relapsed or Refractory Acute Myeloid Leukemia. *J Clin Oncol* 2021; **39**(25): 2768-78.
68. Perl AE, Martinelli G, Cortes JE, et al. Gilteritinib or Chemotherapy for Relapsed or Refractory FLT3-Mutated AML. *N Engl J Med* 2019; **381**(18): 1728-40.
69. Stein EM, DiNardo CD, Pollyea DA, et al. Enasidenib in mutant IDH2 relapsed or refractory acute myeloid leukemia. *Blood* 2017; **130**(6): 722-31.
70. DiNardo CD, Stein EM, de Botton S, et al. Durable Remissions with Ivosidenib in IDH1-Mutated Relapsed or Refractory AML. *N Engl J Med* 2018; **378**(25): 2386-98.
71. DiNardo CD, Maiti A, Rausch CR, et al. 10-day decitabine with venetoclax for newly diagnosed intensive chemotherapy ineligible, and relapsed or refractory acute myeloid leukaemia: a single-centre, phase 2 trial. *The Lancet Haematology* 2020; **7**(10): e724-e36.
72. Ram R, Amit O, Zuckerman T, et al. Venetoclax in patients with acute myeloid leukemia refractory to hypomethylating agents-a multicenter historical prospective study. *Ann Hematol* 2019; **98**(8): 1927-32.
73. Stahl M, Menghrajani K, Derkach A, et al. Clinical and molecular predictors of response and survival following venetoclax therapy in relapsed/refractory AML. *Blood Advances* 2021; **5**(5): 1552-64.
74. Schmid C, Schleuning M, Schwerdtfeger R, et al. Long-term survival in refractory acute myeloid leukemia after sequential treatment with chemotherapy and reduced-intensity conditioning for allogeneic stem cell transplantation. *Blood* 2006; **108**(3): 1092-9.
75. Bejanyan N, Weisdorf DJ, Logan BR, et al. Survival of patients with acute myeloid leukemia relapsing after allogeneic hematopoietic cell transplantation: a center for international blood and marrow transplant research study. *Biol Blood Marrow Transplant* 2015; **21**(3): 454-9.
76. Kerr JFR, Wyllie AH, Currie AR. Apoptosis: A Basic Biological Phenomenon with Wideranging Implications in Tissue Kinetics. *British Journal of Cancer* 1972; **26**(4): 239-57.
77. Ellis RE, Yuan J, Horvitz HR. Mechanisms and Functions of Cell Death. *Annual Review of Cell Biology* 1991; **7**(1): 663-98.
78. Nakajima K, Fujimoto K, Yaoita Y. Programmed cell death during amphibian metamorphosis. *Semin Cell Dev Biol* 2005; **16**(2): 271-80.

79. Elmore S. Apoptosis: A Review of Programmed Cell Death. *Toxicologic Pathology* 2007; **35**(4): 495-516.
80. Majno G, Joris I. Apoptosis, oncosis, and necrosis. An overview of cell death. *Am J Pathol* 1995; **146**(1): 3-15.
81. Kurosaka K, Takahashi M, Watanabe N, Kobayashi Y. Silent Cleanup of Very Early Apoptotic Cells by Macrophages. *The Journal of Immunology* 2003; **171**(9): 4672-9.
82. Cohen GM. Caspases: the executioners of apoptosis. *Biochem J* 1997; **326 (Pt 1)**: 1-16.
83. McIlwain DR, Berger T, Mak TW. Caspase functions in cell death and disease. *Cold Spring Harb Perspect Biol* 2013; **5**(4): a008656.
84. Boatright KM, Salvesen GS. Mechanisms of caspase activation. *Curr Opin Cell Biol* 2003; **15**(6): 725-31.
85. Bortner CD, Oldenburg NBE, Cidlowski JA. The role of DNA fragmentation in apoptosis. *Trends in Cell Biology* 1995; **5**(1): 21-6.
86. Fadok VA, Bratton DL, Henson PM. Phagocyte receptors for apoptotic cells: recognition, uptake, and consequences. *J Clin Invest* 2001; **108**(7): 957-62.
87. Roy S, Nicholson DW. Cross-talk in cell death signaling. *J Exp Med* 2000; **192**(8): F21-5.
88. Jin Z, El-Deiry WS. Overview of cell death signaling pathways. *Cancer Biol Ther* 2005; **4**(2): 139-63.
89. Screaton G, Xu X-N. T cell life and death signalling via TNF-receptor family members. *Current Opinion in Immunology* 2000; **12**(3): 316-22.
90. Locksley RM, Killeen N, Lenardo MJ. The TNF and TNF Receptor Superfamilies: Integrating Mammalian Biology. *Cell* 2001; **104**(4): 487-501.
91. Hsu H, Xiong J, Goeddel DV. The TNF receptor 1-associated protein TRADD signals cell death and NF-κB activation. *Cell* 1995; **81**(4): 495-504.
92. Wajant H. The Fas Signaling Pathway: More Than a Paradigm. *Science* 2002; **296**(5573): 1635-6.
93. Kischkel FC, Hellbardt S, Behrmann I, et al. Cytotoxicity-dependent APO-1 (Fas/CD95)-associated proteins form a death-inducing signaling complex (DISC) with the receptor. *The EMBO Journal* 1995; **14**(22): 5579-88.
94. Luo X, Budihardjo I, Zou H, Slaughter C, Wang X. Bid, a Bcl2 interacting protein, mediates cytochrome c release from mitochondria in response to activation of cell surface death receptors. *Cell* 1998; **94**(4): 481-90.
95. Trapani JA, Smyth MJ. Functional significance of the perforin/granzyme cell death pathway. *Nature Reviews Immunology* 2002; **2**(10): 735-47.
96. Goping IS, Barry M, Liston P, et al. Granzyme B-Induced Apoptosis Requires Both Direct Caspase Activation and Relief of Caspase Inhibition. *Immunity* 2003; **18**(3): 355-65.
97. Sakahira H, Enari M, Nagata S. Cleavage of CAD inhibitor in CAD activation and DNA degradation during apoptosis. *Nature* 1998; **391**(6662): 96-9.
98. Fan Z, Beresford PJ, Oh DY, Zhang D, Lieberman J. Tumor Suppressor NM23-H1 Is a Granzyme A-Activated DNase during CTL-Mediated Apoptosis, and the Nucleosome Assembly Protein SET Is Its Inhibitor. *Cell* 2003; **112**(5): 659-72.
99. Cory S, Adams JM. The Bcl2 family: regulators of the cellular life-or-death switch. *Nature Reviews Cancer* 2002; **2**(9): 647-56.
100. Green DR, Evan GI. A matter of life and death. *Cancer Cell* 2002; **1**(1): 19-30.
101. van Loo G, Schotte P, van Gurp M, et al. Endonuclease G: a mitochondrial protein released in apoptosis and involved in caspase-independent DNA degradation. *Cell Death Differ* 2001; **8**(12): 1136-42.
102. van Loo G, van Gurp M, Depuydt B, et al. The serine protease Omi/HtrA2 is released from mitochondria during apoptosis. Omi interacts with caspase-inhibitor XIAP and induces enhanced caspase activity. *Cell Death & Differentiation* 2002; **9**(1): 20-6.
103. Verhagen AM, Ekert PG, Pakusch M, et al. Identification of DIABLO, a mammalian protein that promotes apoptosis by binding to and antagonizing IAP proteins. *Cell* 2000; **102**(1): 43-53.

104. Goldstein JC, Waterhouse NJ, Juin P, Evan GI, Green DR. The coordinate release of cytochrome c during apoptosis is rapid, complete and kinetically invariant. *Nat Cell Biol* 2000; **2**(3): 156-62.
105. Tait SW, Green DR. Mitochondria and cell death: outer membrane permeabilization and beyond. *Nat Rev Mol Cell Biol* 2010; **11**(9): 621-32.
106. Joza N, Susin SA, Daugas E, et al. Essential role of the mitochondrial apoptosis-inducing factor in programmed cell death. *Nature* 2001; **410**(6828): 549-54.
107. Zou H, Henzel WJ, Liu X, Lutschg A, Wang X. Apaf-1, a human protein homologous to C. elegans CED-4, participates in cytochrome c-dependent activation of caspase-3. *Cell* 1997; **90**(3): 405-13.
108. Chinnaiyan AM. The Apoptosome: Heart and Soul of the Cell Death Machine. *Neoplasia* 1999; **1**(1): 5-15.
109. Slee EA, Adrain C, Martin SJ. Executioner Caspase-3, -6, and -7 Perform Distinct, Non-redundant Roles during the Demolition Phase of Apoptosis *. *Journal of Biological Chemistry* 2001; **276**(10): 7320-6.
110. D'Amours D, Sallmann FR, Dixit VM, Poirier GG. Gain-of-function of poly(ADP-ribose) polymerase-1 upon cleavage by apoptotic proteases: implications for apoptosis. *J Cell Sci* 2001; **114**(Pt 20): 3771-8.
111. Lazebnik YA, Kaufmann SH, Desnoyers S, Poirier GG, Earnshaw WC. Cleavage of poly(ADP-ribose) polymerase by a proteinase with properties like ICE. *Nature* 1994; **371**(6495): 346-7.
112. Satoh MS, Lindahl T. Role of poly(ADP-ribose) formation in DNA repair. *Nature* 1992; **356**(6367): 356-8.
113. Kaufmann SH, Desnoyers S, Ottaviano Y, Davidson NE, Poirier GG. Specific proteolytic cleavage of poly(ADP-ribose) polymerase: an early marker of chemotherapy-induced apoptosis. *Cancer Res* 1993; **53**(17): 3976-85.
114. Bratton DL, Fadok VA, Richter DA, Kailey JM, Guthrie LA, Henson PM. Appearance of Phosphatidylserine on Apoptotic Cells Requires Calcium-mediated Nonspecific Flip-Flop and Is Enhanced by Loss of the Aminophospholipid Translocase *. *Journal of Biological Chemistry* 1997; **272**(42): 26159-65.
115. van Engeland M, Nieland LJ, Ramaekers FC, Schutte B, Reutelingsperger CP. Annexin V-affinity assay: a review on an apoptosis detection system based on phosphatidylserine exposure. *Cytometry* 1998; **31**(1): 1-9.
116. Tsujimoto Y, Finger LR, Yunis J, Nowell PC, Croce CM. Cloning of the chromosome breakpoint of neoplastic B cells with the t(14;18) chromosome translocation. *Science* 1984; **226**(4678): 1097-9.
117. Tsujimoto Y, Yunis J, Onorato-Showe L, Erikson J, Nowell PC, Croce CM. Molecular Cloning of the Chromosomal Breakpoint of B-Cell Lymphomas and Leukemias with the t(11;14) Chromosome Translocation. *Science* 1984; **224**(4656): 1403-6.
118. Tsujimoto Y, Cossman J, Jaffe E, Croce CM. Involvement of the bcl-2 Gene in Human Follicular Lymphoma. *Science* 1985; **228**(4706): 1440-3.
119. Hockenbery D, Nuñez G, Milliman C, Schreiber RD, Korsmeyer SJ. Bcl-2 is an inner mitochondrial membrane protein that blocks programmed cell death. *Nature* 1990; **348**(6299): 334-6.
120. Youle RJ, Strasser A. The BCL-2 protein family: opposing activities that mediate cell death. *Nature Reviews Molecular Cell Biology* 2008; **9**(1): 47-59.
121. Yip KW, Reed JC. Bcl-2 family proteins and cancer. *Oncogene* 2008; **27**(50): 6398-406.
122. Reed JC. Proapoptotic multidomain Bcl-2/Bax-family proteins: mechanisms, physiological roles, and therapeutic opportunities. *Cell Death Differ* 2006; **13**(8): 1378-86.
123. Schinzel A, Kaufmann T, Borner C. Bcl-2 family members: integrators of survival and death signals in physiology and pathology [corrected]. *Biochim Biophys Acta* 2004; **1644**(2-3): 95-105.
124. Petros AM, Olejniczak ET, Fesik SW. Structural biology of the Bcl-2 family of proteins. *Biochim Biophys Acta* 2004; **1644**(2-3): 83-94.

125. Merino D, Bouillet P. The Bcl-2 family in autoimmune and degenerative disorders. *Apoptosis* 2009; **14**(4): 570-83.
126. Strasser A, Huang DC, Vaux DL. The role of the bcl-2/ced-9 gene family in cancer and general implications of defects in cell death control for tumourigenesis and resistance to chemotherapy. *Biochim Biophys Acta* 1997; **1333**(2): F151-78.
127. Certo M, Del Gaizo Moore V, Nishino M, et al. Mitochondria primed by death signals determine cellular addiction to antiapoptotic BCL-2 family members. *Cancer Cell* 2006; **9**(5): 351-65.
128. Motoyama N, Wang F, Roth KA, et al. Massive cell death of immature hematopoietic cells and neurons in Bcl-x-deficient mice. *Science* 1995; **267**(5203): 1506-10.
129. Opferman JT, Iwasaki H, Ong CC, et al. Obligate role of anti-apoptotic MCL-1 in the survival of hematopoietic stem cells. *Science* 2005; **307**(5712): 1101-4.
130. Vaux DL, Cory S, Adams JM. Bcl-2 gene promotes haemopoietic cell survival and cooperates with c-myc to immortalize pre-B cells. *Nature* 1988; **335**(6189): 440-2.
131. Veis DJ, Sorenson CM, Shutter JR, Korsmeyer SJ. Bcl-2-deficient mice demonstrate fulminant lymphoid apoptosis, polycystic kidneys, and hypopigmented hair. *Cell* 1993; **75**(2): 229-40.
132. Vikström IB, Slomp A, Carrington EM, et al. MCL-1 is required throughout B-cell development and its loss sensitizes specific B-cell subsets to inhibition of BCL-2 or BCL-XL. *Cell Death & Disease* 2016; **7**(8): e2345-e.
133. Hanahan D, Weinberg RA. The Hallmarks of Cancer. *Cell* 2000; **100**(1): 57-70.
134. Hanahan D. Hallmarks of Cancer: New Dimensions. *Cancer Discovery* 2022; **12**(1): 31-46.
135. Tron VA, Krajewski S, Klein-Parker H, Li G, Ho VC, Reed JC. Immunohistochemical analysis of Bcl-2 protein regulation in cutaneous melanoma. *Am J Pathol* 1995; **146**(3): 643-50.
136. Khanna KK, Wie T, Song Q, et al. Expression of p53, bcl-2, bax, bcl-x2 and c-myc in radiation-induced apoptosis in Burkitt's lymphoma cells. *Cell Death Differ* 1996; **3**(3): 315-22.
137. Yip KW, Shi W, Pintilie M, et al. Prognostic significance of the Epstein-Barr virus, p53, Bcl-2, and survivin in nasopharyngeal cancer. *Clin Cancer Res* 2006; **12**(19): 5726-32.
138. Krajewska M, Krajewski S, Epstein JI, et al. Immunohistochemical analysis of bcl-2, bax, bcl-X, and mcl-1 expression in prostate cancers. *Am J Pathol* 1996; **148**(5): 1567-76.
139. Wuillème-Toumi S, Robillard N, Gomez P, et al. Mcl-1 is overexpressed in multiple myeloma and associated with relapse and shorter survival. *Leukemia* 2005; **19**(7): 1248-52.
140. Glaser SP, Lee EF, Trounson E, et al. Anti-apoptotic Mcl-1 is essential for the development and sustained growth of acute myeloid leukemia. *Genes & Development* 2012; **26**(2): 120-5.
141. Juin P, Geneste O, Gautier F, Depil S, Campone M. Decoding and unlocking the BCL-2 dependency of cancer cells. *Nature Reviews Cancer* 2013; **13**(7): 455-65.
142. Wei G, Margolin Adam A, Haery L, et al. Chemical Genomics Identifies Small-Molecule MCL1 Repressors and BCL-xL as a Predictor of MCL1 Dependency. *Cancer Cell* 2012; **21**(4): 547-62.
143. Kaufmann SH, Karp JE, Svingen PA, et al. Elevated expression of the apoptotic regulator Mcl-1 at the time of leukemic relapse. *Blood* 1998; **91**(3): 991-1000.
144. Weiss LM, Warnke RA, Sklar J, Cleary ML. Molecular Analysis of the T(14;18) Chromosomal Translocation in Malignant Lymphomas. *New England Journal of Medicine* 1987; **317**(19): 1185-9.
145. Jacobson JO, Wilkes BM, Kwiatkowski DJ, Medeiros LJ, Aisenberg AC, Harris NL. bcl-2 Rearrangements in de novo diffuse large cell lymphoma. Association with distinctive clinical features. *Cancer* 1993; **72**(1): 231-6.
146. Yunis JJ, Frizzera G, Oken MM, McKenna J, Theologides A, Arnesen M. Multiple recurrent genomic defects in follicular lymphoma. A possible model for cancer. *N Engl J Med* 1987; **316**(2): 79-84.
147. Monni O, Joensuu H, Franssila K, Klefstrom J, Alitalo K, Knuutila S. BCL2 Overexpression Associated With Chromosomal Amplification in Diffuse Large B-Cell Lymphoma. *Blood* 1997; **90**(3): 1168-74.

148. Ikegaki N, Katsumata M, Minna J, Tsujimoto Y. Expression of bcl-2 in small cell lung carcinoma cells. *Cancer Res* 1994; **54**(1): 6-8.
149. Beroukhim R, Mermel CH, Porter D, et al. The landscape of somatic copy-number alteration across human cancers. *Nature* 2010; **463**(7283): 899-905.
150. Cerami E, Gao J, Dogrusoz U, et al. The cBio Cancer Genomics Portal: An Open Platform for Exploring Multidimensional Cancer Genomics Data. *Cancer Discovery* 2012; **2**(5): 401-4.
151. Zack TI, Schumacher SE, Carter SL, et al. Pan-cancer patterns of somatic copy number alteration. *Nature Genetics* 2013; **45**(10): 1134-40.
152. Zhou JD, Zhang TJ, Xu ZJ, et al. BCL2 overexpression: clinical implication and biological insights in acute myeloid leukemia. *Diagn Pathol* 2019; **14**(1): 68.
153. Griffiths GJ, Dubrez L, Morgan CP, et al. Cell Damage-induced Conformational Changes of the Pro-Apoptotic Protein Bak In Vivo Precede the Onset of Apoptosis. *Journal of Cell Biology* 1999; **144**(5): 903-14.
154. Nechushtan A, Smith CL, Hsu Y-T, Youle RJ. Conformation of the Bax C-terminus regulates subcellular location and cell death. *The EMBO Journal* 1999; **18**(9): 2330-41.
155. Dewson G, Ma S, Frederick P, et al. Bax dimerizes via a symmetric BH3:groove interface during apoptosis. *Cell Death & Differentiation* 2012; **19**(4): 661-70.
156. Große L, Wurm CA, Brüser C, Neumann D, Jans DC, Jakobs S. Bax assembles into large ring-like structures remodeling the mitochondrial outer membrane in apoptosis. *The EMBO Journal* 2016; **35**(4): 402-13.
157. O'Neill KL, Huang K, Zhang J, Chen Y, Luo X. Inactivation of prosurvival Bcl-2 proteins activates Bax/Bak through the outer mitochondrial membrane. *Genes & Development* 2016; **30**(8): 973-88.
158. Letai A, Bassik MC, Walensky LD, Sorcinelli MD, Weiler S, Korsmeyer SJ. Distinct BH3 domains either sensitize or activate mitochondrial apoptosis, serving as prototype cancer therapeutics. *Cancer Cell* 2002; **2**(3): 183-92.
159. Chipuk JE, Moldoveanu T, Llambi F, Parsons MJ, Green DR. The BCL-2 Family Reunion. *Molecular Cell* 2010; **37**(3): 299-310.
160. Chen L, Willis SN, Wei A, et al. Differential Targeting of Prosurvival Bcl-2 Proteins by Their BH3-Only Ligands Allows Complementary Apoptotic Function. *Molecular Cell* 2005; **17**(3): 393-403.
161. Kuwana T, Bouchier-Hayes L, Chipuk JE, et al. BH3 Domains of BH3-Only Proteins Differentially Regulate Bax-Mediated Mitochondrial Membrane Permeabilization Both Directly and Indirectly. *Molecular Cell* 2005; **17**(4): 525-35.
162. Sax JK, Fei P, Murphy ME, Bernhard E, Korsmeyer SJ, El-Deiry WS. BID regulation by p53 contributes to chemosensitivity. *Nature Cell Biology* 2002; **4**(11): 842-9.
163. Villunger A, Michalak EM, Coultas L, et al. p53- and drug-induced apoptotic responses mediated by BH3-only proteins puma and noxa. *Science* 2003; **302**(5647): 1036-8.
164. Miyashita T, Reed JC. Tumor suppressor p53 is a direct transcriptional activator of the human bax gene. *Cell* 1995; **80**(2): 293-9.
165. Li H, Zhu H, Xu C-j, Yuan J. Cleavage of BID by Caspase 8 Mediates the Mitochondrial Damage in the Fas Pathway of Apoptosis. *Cell* 1998; **94**(4): 491-501.
166. Willis SN, Chen L, Dewson G, et al. Proapoptotic Bak is sequestered by Mcl-1 and Bcl-xL, but not Bcl-2, until displaced by BH3-only proteins. *Genes & Development* 2005; **19**(11): 1294-305.
167. Edlich F, Banerjee S, Suzuki M, et al. Bcl-x(L) retrotranslocates Bax from the mitochondria into the cytosol. *Cell* 2011; **145**(1): 104-16.
168. Lindsten T, Ross AJ, King A, et al. The Combined Functions of Proapoptotic Bcl-2 Family Members Bak and Bax Are Essential for Normal Development of Multiple Tissues. *Molecular Cell* 2000; **6**(6): 1389-99.
169. Wei MC, Zong W-X, Cheng EH-Y, et al. Proapoptotic BAX and BAK: A Requisite Gateway to Mitochondrial Dysfunction and Death. *Science* 2001; **292**(5517): 727-30.

170. Rampino N, Yamamoto H, Ionov Y, et al. Somatic Frameshift Mutations in the BAX Gene in Colon Cancers of the Microsatellite Mutator Phenotype. *Science* 1997; **275**(5302): 967-9.
171. Meijerink JPP, Mensink EJBM, Wang K, et al. Hematopoietic Malignancies Demonstrate Loss-of-Function Mutations ofBAX. *Blood* 1998; **91**(8): 2991-7.
172. Konopleva M, Watt J, Contractor R, et al. Mechanisms of antileukemic activity of the novel Bcl-2 homology domain-3 mimetic GX15-070 (obatoclax). *Cancer Res* 2008; **68**(9): 3413-20.
173. Paoluzzi L, Gonen M, Gardner JR, et al. Targeting Bcl-2 family members with the BH3 mimetic AT-101 markedly enhances the therapeutic effects of chemotherapeutic agents in in vitro and in vivo models of B-cell lymphoma. *Blood* 2008; **111**(11): 5350-8.
174. Oltersdorf T, Elmore SW, Shoemaker AR, et al. An inhibitor of Bcl-2 family proteins induces regression of solid tumours. *Nature* 2005; **435**(7042): 677-81.
175. Miller LA, Goldstein NB, Johannes WU, et al. BH3 mimetic ABT-737 and a proteasome inhibitor synergistically kill melanomas through Noxa-dependent apoptosis. *J Invest Dermatol* 2009; **129**(4): 964-71.
176. Wilson WH, O'Connor OA, Czuczman MS, et al. Navitoclax, a targeted high-affinity inhibitor of BCL-2, in lymphoid malignancies: a phase 1 dose-escalation study of safety, pharmacokinetics, pharmacodynamics, and antitumour activity. *Lancet Oncol* 2010; **11**(12): 1149-59.
177. Tse C, Shoemaker AR, Adickes J, et al. ABT-263: a potent and orally bioavailable Bcl-2 family inhibitor. *Cancer Res* 2008; **68**(9): 3421-8.
178. Souers AJ, Leverson JD, Boghaert ER, et al. ABT-199, a potent and selective BCL-2 inhibitor, achieves antitumor activity while sparing platelets. *Nat Med* 2013; **19**(2): 202-8.
179. Davids MS, Roberts AW, Seymour JF, et al. Phase I First-in-Human Study of Venetoclax in Patients With Relapsed or Refractory Non-Hodgkin Lymphoma. *J Clin Oncol* 2017; **35**(8): 826-33.
180. Roberts AW, Davids MS, Pagel JM, et al. Targeting BCL2 with Venetoclax in Relapsed Chronic Lymphocytic Leukemia. *N Engl J Med* 2016; **374**(4): 311-22.
181. Stilgenbauer S, Eichhorst B, Schetelig J, et al. Venetoclax in relapsed or refractory chronic lymphocytic leukaemia with 17p deletion: a multicentre, open-label, phase 2 study. *Lancet Oncol* 2016; **17**(6): 768-78.
182. Pan R, Hogdal LJ, Benito JM, et al. Selective BCL-2 inhibition by ABT-199 causes on-target cell death in acute myeloid leukemia. *Cancer Discov* 2014; **4**(3): 362-75.
183. Konopleva M, Pollyea DA, Potluri J, et al. Efficacy and Biological Correlates of Response in a Phase II Study of Venetoclax Monotherapy in Patients with Acute Myelogenous Leukemia. *Cancer Discov* 2016; **6**(10): 1106-17.
184. DiNardo CD, Pratz KW, Letai A, et al. Safety and preliminary efficacy of venetoclax with decitabine or azacitidine in elderly patients with previously untreated acute myeloid leukaemia: a non-randomised, open-label, phase 1b study. *The Lancet Oncology* 2018; **19**(2): 216-28.
185. Wei AH, Jr SAS, Hou J-Z, et al. Venetoclax Combined With Low-Dose Cytarabine for Previously Untreated Patients With Acute Myeloid Leukemia: Results From a Phase Ib/II Study. *Journal of Clinical Oncology* 2019; **37**(15): 1277-84.
186. Kadia TM, Borthakur G, Pemmaraju N, et al. Phase II Study of Venetoclax Added to Cladribine + Low Dose AraC (LDAC) Alternating with 5-Azacytidine Demonstrates High Rates of Minimal Residual Disease (MRD) Negative Complete Remissions (CR) and Excellent Tolerability in Older Patients with Newly Diagnosed Acute Myeloid Leukemia (AML). *Blood* 2020; **136**: 17-9.
187. Zeidan AM, Garcia JS, Fenaux P, et al. Phase 3 VERONA study of venetoclax with azacitidine to assess change in complete remission and overall survival in treatment-naïve higher-risk myelodysplastic syndromes. *Journal of Clinical Oncology* 2021; **39**(15_suppl): TPS7054-TPS.
188. Guieze R, Liu VM, Rosebrock D, et al. Mitochondrial Reprogramming Underlies Resistance to BCL-2 Inhibition in Lymphoid Malignancies. *Cancer Cell* 2019; **36**(4): 369-84 e13.

189. Choudhary GS, Al-harbi S, Mazumder S, et al. MCL-1 and BCL-xL-dependent resistance to the BCL-2 inhibitor ABT-199 can be overcome by preventing PI3K/AKT/mTOR activation in lymphoid malignancies. *Cell Death & Disease* 2015; **6**(1): e1593-e.
190. Thijssen R, Roberts AW. Venetoclax in Lymphoid Malignancies: New Insights, More to Learn. *Cancer Cell* 2019; **36**(4): 341-3.
191. Herling CD, Abedpour N, Weiss J, et al. Clonal dynamics towards the development of venetoclax resistance in chronic lymphocytic leukemia. *Nature Communications* 2018; **9**(1): 727.
192. Anderson MA, Tam C, Lew TE, et al. Clinicopathological features and outcomes of progression of CLL on the BCL2 inhibitor venetoclax. *Blood* 2017; **129**(25): 3362-70.
193. Fresquet V, Rieger M, Carolis C, Garcia-Barchino MJ, Martinez-Climent JA. Acquired mutations in BCL2 family proteins conferring resistance to the BH3 mimetic ABT-199 in lymphoma. *Blood* 2014; **123**(26): 4111-9.
194. Tausch E, Close W, Dolnik A, et al. Venetoclax resistance and acquired BCL2 mutations in chronic lymphocytic leukemia. *Haematologica* 2019; **104**(9): e434-e7.
195. Lucas F, Larkin K, Gregory CT, et al. Novel BCL2 mutations in venetoclax-resistant, ibrutinib-resistant CLL patients with BTK/PLCG2 mutations. *Blood* 2020; **135**(24): 2192-5.
196. Blombery P, Anderson MA, Gong JN, et al. Acquisition of the Recurrent Gly101Val Mutation in BCL2 Confers Resistance to Venetoclax in Patients with Progressive Chronic Lymphocytic Leukemia. *Cancer Discov* 2019; **9**(3): 342-53.
197. Blombery P, Birkinshaw RW, Nguyen T, et al. Characterization of a novel venetoclax resistance mutation (BCL2 Phe104Ile) observed in follicular lymphoma. *Br J Haematol* 2019; **186**(6): e188-e91.
198. Blombery P, Thompson E, Nguyen T, et al. Detection of Multiple Recurrent Novel BCL2 Mutations Co-Occurring with BCL2 Gly101Val in Patients with Chronic Lymphocytic Leukemia on Long Term Venetoclax. *Blood* 2019; **134**(Supplement_1): 171-.
199. Chyla BJ, Popovic R, Lu C, et al. Identification of Recurrent Genomic Alterations in the Apoptotic Machinery in CLL Patients Treated with Venetoclax Monotherapy. *Blood* 2019; **134**(Supplement_1): 172-.
200. Birkinshaw RW, Gong JN, Luo CS, et al. Structures of BCL-2 in complex with venetoclax reveal the molecular basis of resistance mutations. *Nat Commun* 2019; **10**(1): 2385.
201. Thomalla D, Beckmann L, Grimm C, et al. Deregulation and epigenetic modification of BCL2-family genes cause resistance to venetoclax in hematologic malignancies. *Blood* 2022; **140**(20): 2113-26.
202. Lin KH, Winter PS, Xie A, et al. Targeting MCL-1/BCL-XL Forestalls the Acquisition of Resistance to ABT-199 in Acute Myeloid Leukemia. *Sci Rep* 2016; **6**: 27696.
203. Bhatt S, Pioso MS, Olesinski EA, et al. Reduced Mitochondrial Apoptotic Priming Drives Resistance to BH3 Mimetics in Acute Myeloid Leukemia. *Cancer Cell* 2020; **38**(6): 872-90 e6.
204. Sharon D, Cathelin S, Mirali S, et al. Inhibition of mitochondrial translation overcomes venetoclax resistance in AML through activation of the integrated stress response. *Science Translational Medicine* 2019; **11**(516): eaax2863.
205. Zhang Q, Riley-Gillis B, Han L, et al. Activation of RAS/MAPK pathway confers MCL-1 mediated acquired resistance to BCL-2 inhibitor venetoclax in acute myeloid leukemia. *Signal Transduction and Targeted Therapy* 2022; **7**(1): 51.
206. Nechiporuk T, Kurtz SE, Nikolova O, et al. The TP53 Apoptotic Network Is a Primary Mediator of Resistance to BCL2 Inhibition in AML Cells. *Cancer Discov* 2019; **9**(7): 910-25.
207. DiNardo CD, Tiong IS, Quaglieri A, et al. Molecular patterns of response and treatment failure after frontline venetoclax combinations in older patients with AML. *Blood* 2020; **135**(11): 791-803.
208. Zhang X, Qian J, Wang H, et al. Not BCL2 mutation but dominant mutation conversation contributed to acquired venetoclax resistance in acute myeloid leukemia. *Biomark Res* 2021; **9**(1): 30.

209. Chyla B, Daver N, Doyle K, et al. Genetic Biomarkers Of Sensitivity and Resistance to Venetoclax Monotherapy in Patients With Relapsed Acute Myeloid Leukemia. *Am J Hematol* 2018.
210. Prado G, Kaestner CL, Licht JD, Bennett RL. Targeting epigenetic mechanisms to overcome venetoclax resistance. *Biochim Biophys Acta Mol Cell Res* 2021; **1868**(8): 119047.
211. Chen X, Glytsou C, Zhou H, et al. Targeting Mitochondrial Structure Sensitizes Acute Myeloid Leukemia to Venetoclax Treatment. *Cancer Discov* 2019; **9**(7): 890-909.
212. Caenepeel S, Brown SP, Belmontes B, et al. AMG 176, a Selective MCL1 Inhibitor, Is Effective in Hematologic Cancer Models Alone and in Combination with Established Therapies. *Cancer Discovery* 2018; **8**(12): 1582-97.
213. Kotschy A, Szlavik Z, Murray J, et al. The MCL1 inhibitor S63845 is tolerable and effective in diverse cancer models. *Nature* 2016; **538**(7626): 477-82.
214. Ramsey HE, Fischer MA, Lee T, et al. A Novel MCL1 Inhibitor Combined with Venetoclax Rescues Venetoclax-Resistant Acute Myelogenous Leukemia. *Cancer Discov* 2018; **8**(12): 1566-81.
215. Tron AE, Belmonte MA, Adam A, et al. Discovery of Mcl-1-specific inhibitor AZD5991 and preclinical activity in multiple myeloma and acute myeloid leukemia. *Nature Communications* 2018; **9**(1): 5341.
216. Luedtke DA, Niu X, Pan Y, et al. Inhibition of Mcl-1 enhances cell death induced by the Bcl-2-selective inhibitor ABT-199 in acute myeloid leukemia cells. *Signal Transduct Target Ther* 2017; **2**: 17012.
217. Khan S, Zhang X, Lv D, et al. A selective BCL-XL PROTAC degrader achieves safe and potent antitumor activity. *Nature Medicine* 2019; **25**(12): 1938-47.
218. Pan R, Ruvolo V, Mu H, et al. Synthetic Lethality of Combined Bcl-2 Inhibition and p53 Activation in AML: Mechanisms and Superior Antileukemic Efficacy. *Cancer Cell* 2017; **32**(6): 748-60 e6.
219. Lehmann C, Friess T, Birzele F, Kiialainen A, Dangl M. Superior anti-tumor activity of the MDM2 antagonist idasanutlin and the Bcl-2 inhibitor venetoclax in p53 wild-type acute myeloid leukemia models. *Journal of Hematology & Oncology* 2016; **9**(1): 50.
220. Choi JH, Bogenberger JM, Tibes R. Targeting Apoptosis in Acute Myeloid Leukemia: Current Status and Future Directions of BCL-2 Inhibition with Venetoclax and Beyond. *Target Oncol* 2020; **15**(2): 147-62.
221. Zhan T, Rindtorff N, Betge J, Ebert MP, Boutros M. CRISPR/Cas9 for cancer research and therapy. *Seminars in Cancer Biology* 2019; **55**: 106-19.
222. Labun K, Montague TG, Krause M, Torres Cleuren YN, Tjeldnes H, Valen E. CHOPCHOP v3: expanding the CRISPR web toolbox beyond genome editing. *Nucleic Acids Research* 2019; **47**(W1): W171-W4.
223. Sanjana NE, Shalem O, Zhang F. Improved vectors and genome-wide libraries for CRISPR screening. *Nat Methods* 2014; **11**(8): 783-4.
224. Dienstmann R, Elez E, Argiles G, et al. Analysis of mutant allele fractions in driver genes in colorectal cancer - biological and clinical insights. *Mol Oncol* 2017; **11**(9): 1263-72.
225. Elez E, Chianese C, Sanz-García E, et al. Impact of circulating tumor DNA mutant allele fraction on prognosis in RAS-mutant metastatic colorectal cancer. *Mol Oncol* 2019; **13**(9): 1827-35.
226. Zhang D, Huo D, Xie H, et al. CHG: A Systematically Integrated Database of Cancer Hallmark Genes. *Frontiers in Genetics* 2020; **11**.
227. Hanahan D, Weinberg RA. Hallmarks of cancer: the next generation. *Cell* 2011; **144**(5): 646-74.
228. TCGA database. Distribution of Most Frequently Mutated Genes across all cancers. https://portal.gdc.cancer.gov/analysis_page?app=MutationFrequencyApp (Last accessed Feb 24, 2024).
229. Campbell KJ, Tait SWG. Targeting BCL-2 regulated apoptosis in cancer. *Open Biol* 2018; **8**(5).
230. Biedler JL, Riehm H. Cellular Resistance to Actinomycin D in Chinese Hamster Cells in Vitro: Cross-Resistance, Radioautographic, and Cytogenetic Studies1. *Cancer Research* 1970; **30**(4): 1174-84.

231. AMARAL MVS, DE SOUSA PORTILHO AJ, DA SILVA EL, et al. Establishment of Drug-resistant Cell Lines as a Model in Experimental Oncology: A Review. *Anticancer Research* 2019; **39**(12): 6443-55.
232. TCGA database. Distribution of Most Frequently Mutated Genes in TARGET-AML. https://portal.gdc.cancer.gov/analysis_page?app=MutationFrequencyApp (Last accessed Feb 24, 2024).
233. DiNardo CD, Cortes JE. Mutations in AML: prognostic and therapeutic implications. *Hematology Am Soc Hematol Educ Program* 2016; **2016**(1): 348-55.
234. Geraghty RJ, Capes-Davis A, Davis JM, et al. Guidelines for the use of cell lines in biomedical research. *British Journal of Cancer* 2014; **111**(6): 1021-46.
235. Sharma A, Singh K, Almasan A. Histone H2AX phosphorylation: a marker for DNA damage. *Methods Mol Biol* 2012; **920**: 613-26.
236. Oh J-H, Jang SJ, Kim J, et al. Spontaneous mutations in the single TTN gene represent high tumor mutation burden. *npj Genomic Medicine* 2020; **5**(1): 33.
237. Xie X, Tang Y, Sheng J, et al. Titin Mutation Is Associated With Tumor Mutation Burden and Promotes Antitumor Immunity in Lung Squamous Cell Carcinoma. *Front Cell Dev Biol* 2021; **9**: 761758.
238. Sun Y, Li L, Yao W, et al. USH2A Mutation is Associated With Tumor Mutation Burden and Antitumor Immunity in Patients With Colon Adenocarcinoma. *Frontiers in Genetics* 2021; **12**.
239. Wang X, Yu X, Krauthammer M, et al. The Association of MUC16 Mutation with Tumor Mutation Burden and Its Prognostic Implications in Cutaneous Melanoma. *Cancer Epidemiol Biomarkers Prev* 2020; **29**(9): 1792-9.
240. Yang Y, Zhang J, Chen Y, Xu R, Zhao Q, Guo W. MUC4, MUC16, and TTN genes mutation correlated with prognosis, and predicted tumor mutation burden and immunotherapy efficacy in gastric cancer and pan-cancer. *Clin Transl Med* 2020; **10**(4): e155.
241. Zhang F, Li X, Chen H, et al. Mutation of MUC16 Is Associated With Tumor Mutational Burden and Lymph Node Metastasis in Patients With Gastric Cancer. *Front Med (Lausanne)* 2022; **9**: 836892.
242. Mead AJ, Linch DC, Hills RK, Wheatley K, Burnett AK, Gale RE. FLT3 tyrosine kinase domain mutations are biologically distinct from and have a significantly more favorable prognosis than FLT3 internal tandem duplications in patients with acute myeloid leukemia. *Blood* 2007; **110**(4): 1262-70.
243. Yamamoto Y, Kiyoi H, Nakano Y, et al. Activating mutation of D835 within the activation loop of FLT3 in human hematologic malignancies. *Blood* 2001; **97**(8): 2434-9.
244. Daver N, Venugopal S, Ravandi F. FLT3 mutated acute myeloid leukemia: 2021 treatment algorithm. *Blood Cancer Journal* 2021; **11**(5): 104.
245. Kavanagh S, Murphy T, Law A, et al. Emerging therapies for acute myeloid leukemia: translating biology into the clinic. *JCI Insight* 2017; **2**(18).
246. Pikman Y, Tasian SK, Sulis ML, et al. Matched Targeted Therapy for Pediatric Patients with Relapsed, Refractory, or High-Risk Leukemias: A Report from the LEAP Consortium. *Cancer Discov* 2021; **11**(6): 1424-39.
247. Maldonado JL, Fridlyand J, Patel H, et al. Determinants of BRAF Mutations in Primary Melanomas. *JNCI: Journal of the National Cancer Institute* 2003; **95**(24): 1878-90.
248. Tiacci E, Trifonov V, Schiavoni G, et al. BRAF mutations in hairy-cell leukemia. *N Engl J Med* 2011; **364**(24): 2305-15.
249. Dankner M, Rose AAN, Rajkumar S, Siegel PM, Watson IR. Classifying BRAF alterations in cancer: new rational therapeutic strategies for actionable mutations. *Oncogene* 2018; **37**(24): 3183-99.
250. Baugh EH, Ke H, Levine AJ, Bonneau RA, Chan CS. Why are there hotspot mutations in the TP53 gene in human cancers? *Cell Death & Differentiation* 2018; **25**(1): 154-60.
251. Kannappan R, Mattapally S, Wagle PA, Zhang J. Transactivation domain of p53 regulates DNA repair and integrity in human iPS cells. *American Journal of Physiology-Heart and Circulatory Physiology* 2018; **315**(3): H512-H21.

252. COSMIC database. Gene TP53. https://cancer.sanger.ac.uk/cosmic/gene/analysis?ln=TP53 (Last accessed Feb 24, 2024).
253. Gener-Ricos G, Sasaki K, Loghavi S, et al. A Descriptive Analysis of TP53 Y220C Mutations in Patients with Hematologic Malignancies. *Blood* 2022; **140**(Supplement 1): 11830-2.
254. Nishida Y, Montoya RH, Morita K, et al. Clonal Expansion of Mutant p53 Clones By MDM2 Inhibition in Acute Myeloid Leukemias. *Blood* 2020; **136**: 27-8.
255. Middeke JM, Herold S, Rücker-Braun E, et al. TP53 mutation in patients with high-risk acute myeloid leukaemia treated with allogeneic haematopoietic stem cell transplantation. *Br J Haematol* 2016; **172**(6): 914-22.
256. Daver NG, Iqbal S, Renard C, et al. Treatment outcomes for newly diagnosed, treatment-naïve TP53-mutated acute myeloid leukemia: a systematic review and meta-analysis. *Journal of Hematology & Oncology* 2023; **16**(1): 19.
257. Kim K, Maiti A, Loghavi S, et al. Outcomes of TP53-mutant acute myeloid leukemia with decitabine and venetoclax. *Cancer* 2021; **127**(20): 3772-81.
258. Pollyea DA, Pratz KW, Wei AH, et al. Outcomes in Patients with Poor-Risk Cytogenetics with or without TP53 Mutations Treated with Venetoclax and Azacitidine. *Clinical Cancer Research* 2022; **28**(24): 5272-9.
259. Aubrey BJ, Kelly GL, Janic A, Herold MJ, Strasser A. How does p53 induce apoptosis and how does this relate to p53-mediated tumour suppression? *Cell Death & Differentiation* 2018; **25**(1): 104-13.
260. Chen S, Gao R, Yao C, et al. Genotoxic stresses promote clonal expansion of hematopoietic stem cells expressing mutant p53. *Leukemia* 2018; **32**(3): 850-4.
261. Katharina TP, Gudrun P, Frank GR, et al. Clinical implications of subclonal TP53 mutations in acute myeloid leukemia. *Haematologica* 2019; **104**(3): 516-23.
262. Wei AH, Roberts AW, Spencer A, et al. Targeting MCL-1 in hematologic malignancies: Rationale and progress. *Blood Rev* 2020; **44**: 100672.
263. Liu VM, Guièze R, Rosebrock D, et al. MCL-1 and PKA/AMPK Axis Fuel Venetoclax Resistance in Lymphoid Cancers. *Blood* 2019; **134**(Supplement_1): 1284-.
264. Bose P, Gandhi V, Konopleva M. Pathways and mechanisms of venetoclax resistance. *Leuk Lymphoma* 2017; **58**(9): 1-17.
265. Pei S, Pollyea DA, Gustafson A, et al. Monocytic Subclones Confer Resistance to Venetoclax-Based Therapy in Patients with Acute Myeloid Leukemia. *Cancer Discovery* 2020; **10**(4): 536-51.
266. Jeffers JR, Parganas E, Lee Y, et al. Puma is an essential mediator of p53-dependent and -independent apoptotic pathways. *Cancer Cell* 2003; **4**(4): 321-8.
267. Lecker SH, Goldberg AL, Mitch WE. Protein Degradation by the Ubiquitin–Proteasome Pathway in Normal and Disease States. *Journal of the American Society of Nephrology* 2006; **17**(7): 1807-19.
268. Park J, Cho J, Song EJ. Ubiquitin–proteasome system (UPS) as a target for anticancer treatment. *Archives of Pharmacal Research* 2020; **43**(11): 1144-61.
269. Adams J. The proteasome: a suitable antineoplastic target. *Nature Reviews Cancer* 2004; **4**(5): 349-60.
270. van Dijk AD, Hoff FW, Qiu Y, et al. Bortezomib is significantly beneficial for de novo pediatric AML patients with low phosphorylation of the NF-κB subunit RelA. *Proteomics Clin Appl* 2022; **16**(2): e2100072.
271. Csizmar CM, Kim DH, Sachs Z. The role of the proteasome in AML. *Blood Cancer J* 2016; **6**(12): e503.
272. Weller S, Toennießen A, Schaefer B, et al. The BCL-2 inhibitor ABT-199/venetoclax synergizes with proteasome inhibition via transactivation of the MCL-1 antagonist NOXA. *Cell Death Discovery* 2022; **8**(1): 215.
273. Kumar S, Harrison SJ, Cavo M, et al. Final Overall Survival Results from BELLINI, a Phase 3 Study of Venetoclax or Placebo in Combination with Bortezomib and Dexamethasone in Relapsed/Refractory Multiple Myeloma. *Blood* 2021; **138**(Supplement 1): 84-.

274. Wong KY, Chim CS. Venetoclax, bortezomib and S63845, an MCL1 inhibitor, in multiple myeloma. *J Pharm Pharmacol* 2020; **72**(5): 728-37.
275. Punnoose EA, Leverson JD, Peale F, et al. Expression Profile of BCL-2, BCL-XL, and MCL-1 Predicts Pharmacological Response to the BCL-2 Selective Antagonist Venetoclax in Multiple Myeloma Models. *Molecular Cancer Therapeutics* 2016; **15**(5): 1132-44.
276. Huang G, Li H, Zhang H. Abnormal Expression of Mitochondrial Ribosomal Proteins and Their Encoding Genes with Cell Apoptosis and Diseases. *Int J Mol Sci* 2020; **21**(22).
277. Kim HJ, Maiti P, Barrientos A. Mitochondrial ribosomes in cancer. *Semin Cancer Biol* 2017; **47**: 67-81.
278. Jones CL, Stevens BM, Pollyea DA, et al. Nicotinamide Metabolism Mediates Resistance to Venetoclax in Relapsed Acute Myeloid Leukemia Stem Cells. *Cell Stem Cell* 2020; **27**(5): 748-64.e4.
279. Stevens BM, Jones CL, Pollyea DA, et al. Fatty acid metabolism underlies venetoclax resistance in acute myeloid leukemia stem cells. *Nat Cancer* 2020; **1**(12): 1176-87.
280. Gilding LN, Somervaille TCP. The Diverse Consequences of FOXC1 Deregulation in Cancer. *Cancers (Basel)* 2019; **11**(2).
281. Somerville TD, Wiseman DH, Spencer GJ, et al. Frequent Derepression of the Mesenchymal Transcription Factor Gene FOXC1 in Acute Myeloid Leukemia. *Cancer Cell* 2015; **28**(3): 329-42.
282. Ray T, Ryusaki T, Ray PS. Therapeutically Targeting Cancers That Overexpress FOXC1: A Transcriptional Driver of Cell Plasticity, Partial EMT, and Cancer Metastasis. *Front Oncol* 2021; **11**: 721959.
283. Liu Z-H, Dai X-M, Du B. Hes1: a key role in stemness, metastasis and multidrug resistance. *Cancer Biology & Therapy* 2015; **16**(3): 353-9.
284. Xu J-J, Li H-D, Du X-S, et al. Role of the F-BAR Family Member PSTPIP2 in Autoinflammatory Diseases. *Frontiers in Immunology* 2021; **12**.
285. Krzak G, Willis CM, Smith JA, Pluchino S, Peruzzotti-Jametti L. Succinate Receptor 1: An Emerging Regulator of Myeloid Cell Function in Inflammation. *Trends Immunol* 2021; **42**(1): 45-58.
286. Prakash T, Sharma VK, Adati N, et al. Expression of conjoined genes: another mechanism for gene regulation in eukaryotes. *PLoS One* 2010; **5**(10): e13284.
287. Shen S, Wei C, Fu J. RNA-Sequencing Reveals Heat Shock 70-kDa Protein 6 (HSPA6) as a Novel Thymoquinone-Upregulated Gene That Inhibits Growth, Migration, and Invasion of Triple-Negative Breast Cancer Cells. *Frontiers in oncology* 2021; **11**: 667995-.
288. Chen J, Facchinetti F, Braye F, et al. Single-cell DNA-seq depicts clonal evolution of multiple driver alterations in osimertinib-resistant patients. *Annals of Oncology* 2022; **33**(4): 434-44.
289. Li C, Xu J, Wang X, et al. Whole exome and transcriptome sequencing reveal clonal evolution and exhibit immune-related features in metastatic colorectal tumors. *Cell Death Discovery* 2021; **7**(1): 222.
290. Morita K, Wang F, Jahn K, et al. Clonal evolution of acute myeloid leukemia revealed by high-throughput single-cell genomics. *Nature Communications* 2020; **11**(1): 5327.
291. Kwok M, Wu CJ. Clonal Evolution of High-Risk Chronic Lymphocytic Leukemia: A Contemporary Perspective. *Frontiers in Oncology* 2021; **11**.
292. Gharaibeh L, Elmadany N, Alwosaibai K, Alshaer W. Notch1 in Cancer Therapy: Possible Clinical Implications and Challenges. *Molecular Pharmacology* 2020; **98**(5): 559-76.
293. Weng AP, Ferrando AA, Lee W, et al. Activating mutations of NOTCH1 in human T cell acute lymphoblastic leukemia. *Science* 2004; **306**(5694): 269-71.
294. Thoms JAI, Birger Y, Foster S, et al. ERG promotes T-acute lymphoblastic leukemia and is transcriptionally regulated in leukemic cells by a stem cell enhancer. *Blood* 2011; **117**(26): 7079-89.
295. Rainis L, Toki T, Pimanda JE, et al. The Proto-Oncogene ERG in Megakaryoblastic Leukemias. *Cancer Research* 2005; **65**(17): 7596-602.
296. Adamo P, Ladomery MR. The oncogene ERG: a key factor in prostate cancer. *Oncogene* 2016; **35**(4): 403-14.

297. Cowell JK, Hu T. Mechanisms of resistance to FGFR1 inhibitors in FGFR1-driven leukemias and lymphomas: implications for optimized treatment. *Cancer Drug Resist* 2021; **4**(3): 607-19.
298. Ramsey HE, Fischer MA, Lee T, et al. A Novel MCL1 Inhibitor Combined with Venetoclax Rescues Venetoclax-Resistant Acute Myelogenous Leukemia. *Cancer Discovery* 2018; **8**(12): 1566-81.
299. Hormi M, Birsen R, Belhadj M, et al. Pairing MCL-1 inhibition with venetoclax improves therapeutic efficiency of BH3-mimetics in AML. *Eur J Haematol* 2020; **105**(5): 588-96.
300. Niu X, Zhao J, Ma J, et al. Binding of Released Bim to Mcl-1 is a Mechanism of Intrinsic Resistance to ABT-199 which can be Overcome by Combination with Daunorubicin or Cytarabine in AML Cells. *Clinical Cancer Research* 2016; **22**(17): 4440-51.
301. Pallis M, Turzanski J, Higashi Y, Russell N. P-glycoprotein in Acute Myeloid Leukaemia: Therapeutic Implications of its Association With Both a Multidrug-resistant and an Apoptosis-resistant Phenotype. *Leukemia & Lymphoma* 2002; **43**(6): 1221-8.
302. Aroua N, Boet E, Ghisi M, et al. Extracellular ATP and CD39 Activate cAMP-Mediated Mitochondrial Stress Response to Promote Cytarabine Resistance in Acute Myeloid Leukemia. *Cancer Discov* 2020; **10**(10): 1544-65.
303. Wu B, Mao ZJ, Wang Z, et al. Deoxycytidine Kinase (DCK) Mutations in Human Acute Myeloid Leukemia Resistant to Cytarabine. *Acta Haematol* 2021; **144**(5): 534-41.

7 Appendix

7.1 Table of figures

7.2 Table of tables